GULP regulates TGF-β responses in ovarian surface epithelial cells

Ji-Hyun Chung
Master of Science

Faculty of Medicine
Department of Biochemistry
McGill University
Montreal, Quebec, Canada

This thesis is submitted to McGill University in partial fulfillment of the requirements for the degree of Master of Science.

August 2018

Table of Contents

List of Tables and Figures

Abstract

Transforming growth factor beta (TGF-β), is a cytokine which regulates cell proliferation and programmed cell death or apoptosis. Despite its invaluable role in tumour-suppression, TGF-β signaling have been shown to promote cancer. Previously, engulfment protein (GULP), a specific adapter protein of low density lipoprotein receptor-related protein 1 (LRP1), was shown to be decreased among epithelial ovarian cancers. We identified the correlation between GULP's expression and Suppressor of Mothers Against Decapentaplegic 3 (Smad3) phosphorylation, which was further associated with sensitivity towards TGF-β associated growth inhibition or cell migration. To best recapitulate aberrations in intracellular signaling events in ovarian cancers, primary ovarian surface epithelial (OSE) cells were isolated and cultured from human normal or cancerous ovary tissues. Growth and 3-(4,5-Dimethylthiazol-2-Yl)-2,5-Diphenyltetrazolium Bromide (MTT) assays showed cells with high levels of GULP were growth inhibited by TGF-β, whereas low levels of GULP resulted in resistance to growth inhibition and increased cell proliferation. By knocking out GULP expression in SKOV3 ovarian adenocarcinoma cell line, decreased levels of GULP showed decreased growth inhibition and increased cell proliferation. In addition, despite reduced level of GULP, migration was increased in GULP-knocked out SKOV3 cells. Thus, GULP may primarily regulated tumour-suppressive TGF-β responses, which may function as the 'molecular switch', dictating the utilization of TGF-β signaling components, including regulatory Smads.

Résumé

Le facteur de croissance transformant Beta (TGF-β) est une cytokine dont la fonction est de réguler la prolifération cellulaire et la mort cellulaire programmée ou apoptose. Malgré ses rôles inestimables dans la suppression des tumeurs, il a été démontré que la signalisation du TGF-ß favorise les cancers. La protéine adaptatrice « enGULfment Protein » (GULP), une protéine adaptatrice spécifique de la protéine-récepteur membranaire de type 1 apparentée au récepteur des lipoprotéines de faible densité (LRP1), s'est avérée être diminuée dans les cancers épithéliaux de l'ovaire. Nous avons identifié une corrélation entre l'expression de GULP et la phosphorylation de « Suppressor of Mothers Against Decapentaplegic 3 » ou Smad3, qui était en outre associée à une sensibilité à l'inhibition de la croissance associée au TGF-β ou migration cellulaire. Pour mieux répliquer les aberrations relevées lors des événements de signalisation intracellulaire dans les cancers ovariens, des cellules primaires épithéliales de surface ovarienne (OSE) ont été isolées et cultivées à partir de tissus ovariens humains normaux ou cancéreux. Des essais de prolifération cellulaire au bromure de 3- (4,5-diméthylthiazol-2-yl)-2,5-diphényltétrazolium (MTT) ont montré que la croissance des cellules contenant des niveaux élevés de GULP était inhibée par le TGF-β, alors que les faibles niveaux cellulaires de GULP entraînaient une résistance contre l'inhibition de la croissance menant à une augmentation de la prolifération cellulaire. En désactivant l'expression de GULP dans la lignée cellulaire d'adénocarcinome ovarien SKOV3, les diminutions des niveaux de GULP ont montré un gain de résistance contre l'inhibition de la croissance et une tendance accrue à la prolifération cellulaire. De plus, malgré les niveaux réduits de GULP, la migration était augmentée dans les cellules SKOV3 dont l'expression du GULP avait été désactivée. Ainsi, la protéine GULP semble principalement réguler les réponses de suppresseur de tumeurs de TGF-ß, qui pourraient fonctionner comme un « interrupteur moléculaire » dictant l'utilisation des composants de signalisation du TGF-ß, incluant les régulateurs Smads.

Acknowledgements

In helping me to achieve my goals, I would like to specifically thank all my family members including my maternal grandmother who was always available to listen to my concerns and fears throughout my Master's duration. Moreover, I would like to thank my girlfriend for supporting me throughout my struggles and cheering me up when I felt depressed and overwhelmed from various technical difficulties encountered throughout experiments.

My appreciation continues to Dr. Hong, Choi and Dr. Isabelle Ruel from the laboratory of Dr. Jacques Genest for giving me advices and guiding me through difficulties encountered throughout experiments. Moreover, I would like to thank Mr. Julien Boudreault from the laboratory of Dr. Jean-Jacques Lebrun for continuous advice and special technical support in generating GULP CRISPR/Cas9 knockout ovarian cancer cell lines and helping me to optimize TGF-β treatment in cells.

With regards of obtaining valuable primary human ovarian tissue samples, I would like to convey my appreciation to Royal Victoria Hospital Anesthesiology team. More specifically, I would like to thank Dr. Thomas Schricker, Dr. Ralph Lattermann, and Dr. Albert Moore. Moreover, I would like to thank Dr. Ziggy Xeng who was involved in surgery of patients and further providing me with specimens throughout my studies. In relevance, I would like to thank McGill's Pathology team for prompt sample diagnosis and professional sample handling, which were crucial for the isolation of viable population of ovarian surface epithelial cells.

Lastly, I would like to thank Dr. Robert Scott Kiss who have been my supervisor and provided the most amount of guidance in terms of knowledge and technical difficulties. In addition, I would like to specially thank members of my research advisory committee including Dr. Jason Young, Dr. Jean-Jacques Lebrun, and Dr. Giuseppina Ursini-Siegel in giving me valuable advices so I could prioritize my goals to get to the finish line.

Contribution of Authors

Experiments were designed and optimized with advice from Dr. Robert Scott Kiss and my research advisory committee members, including Dr. Jason Young, Dr. Jean-Jacques Lebrun, and Dr. Giuseppina Ursini-Siegel.

All experiments have been executed and optimized by myself and I acquired all images for the scratch/wound-healing assay.

Mr. Julien Boudreault generated SKOV3 GULP knockout cells using CRISPR-Cas9 system. However, downstream experiments including Western blot, growth assay, MTT assay, and scratch assay were performed by myself.

Finally, illustration 3, 5, 6, and 7 were created by myself.

1. Introduction

Ovarian cancer: An overview

With rapid industrialization and the emergence of poor lifestyle choices, the number of individuals diagnosed with different forms of cancer is increasing annually (1). Compared to breast cancer, which receives significant attention, ovarian cancer has been overlooked for the past two decades (2,3). While it is true that ovarian cancer does not easily metastasize to secondary organs (4), overall survival of ovarian cancer patients is considerably low (~29%) (2), due to the asymptomatic nature of ovarian cancer, which is associated with late-stage diagnosis (5). In fact, for the past 40 years, five-year survival rates have only marginally increased, to 46% for early-stage diagnosis and 29% for advanced-stage diagnosis (2,3,6). The National Cancer Registration Analysis Service stated in 2012 that while the number of individuals diagnosed with ovarian cancer has remained relatively static in developed countries such as the United Kingdom (7), the number is continuing to increase in developing countries, including China (2). Additionally, although Reid, *et al.* state that ovarian cancer has a low incidence rate affecting approximately 4.1 individuals out of 100,000 in China, China's large population means that more than 52,100 new ovarian cancer cases are diagnosed there each year (8).

Current standards of care for ovarian cancer include surgical removal of a tumour via hysterectomy (oophorectomy) followed by platinum-based chemotherapy (9). With advances in technology, multiple drug administration methods have been advised, involving an active development of drug carriers (10,11). Despite this effort, however, cancer relapse is commonly seen within five years of front-line treatment, and more importantly, recurrent patients rapidly gain resistance to chemotherapy (12).

Ovarian cancer: Conventional risk factors

The best method to reduce incidence of ovarian cancer is to identify risk factors, allowing for earlier diagnosis. Currently, it is well accepted that both reproductive and hormonal factors contribute to the onset of ovarian cancer (13,14). In support of this claim, two main hypotheses

have been suggested: ‘incessant ovulation’ (13) and the ‘gonadotropin hypothesis’ (14). ‘Incessant ovulation’ associates the number of an ovulatory cycle with increased spontaneous mutation (13). Indeed, the repair of surface epithelium after each ovulation is accompanied by increased cellular division (13). Alternatively, the ‘gonadotropin hypothesis’ links gonadotropins (luteinizing hormone and follicle-stimulating hormones) to risk (15). Alternatively, the ‘gonadotropin hypothesis’ links gonadotropins (luteinizing hormone and follicle-stimulating hormones) to risk (15). Although the associations between ovarian cancer risk and age, parity, and lactation have been extensively examined, increases in unhealthy lifestyles around the globe require considering additional factors such as physical activity, obesity, diet, and smoking.

Unfortunately, controversies concerning each risk factor continues as a recent meta-analysis has failed to prove the literature but instead showed an overall inverse relationship between the age at menarche and ovarian cancer risk (16). On the other hand, while Nurses’ Health Study reported a positive correlation between the menopausal age and ovarian cancer risk for endometrioid subtypes (17), it remains unclear if an association exists between the age of menopause onset and ovarian cancer (18-20). However, estrogen or estrogen/progestin (collectively known as hormone replacement therapy) has been used for more than 50 years to alleviate menopausal symptoms in women (21), including ‘hot flashes’, a sudden sensation of warmness and more rapid heartbeat, and urogenital atrophy (22). Interestingly, while progestin has been hypothesized to promote apoptosis (as estrogen has been shown to promote the growth of ovarian epithelial cells (23)), long-term estrogen treatment in postmenopausal women might be detrimental to their health. Supporting this concern, a recent meta-analysis involving 14 different populations demonstrates an association between estrogen therapy and a 22% increase in ovarian cancer risk (24). Contrastingly, co-administration of progestin was associated with only a 10% risk increase, supporting the notion that progestin may mitigate the detrimental effect of estrogen (24). Furthermore, a cohort study in 2007 reported significantly elevated risk among individuals who have used hormone replacement therapy for at least five years (25). Despite several reports describing side effects and even potentially serious health concerns (26), a considerable number of women (>12%) still use hormone replacement therapy for menopausal symptoms (27,28). Therefore, more than 6 million women are currently at increased risk for ovarian cancer in the United States and United Kingdom alone (29).

In women, pregnancy induces anovulation and suppresses the secretion of pituitary gonadotropin (2), which may lower ovarian cancer risk (13,14). Indeed, while the extent of protection ranges between 50-70% among subtypes (17,30,31), 'parous' women have been proposed to have lower risk than 'nulliparous' women (~30-60% reduction), with each additional full-term pregnancy reducing the risk by an additional 15% (32,33). The literature generally agrees that infertility in nulliparous women poses the greatest risk (18,32). However, multiple factors – including fertility drug exposure, personal history of endometriosis, and polycystic ovarian syndrome, which may influence infertility (34,35) – complicate the assessment of infertility as a risk factor for ovarian cancer. Although there may be several reasons behind pregnancy's protection against ovarian cancer, most relevant studies indicate breastfeeding provides protective effects against epithelial ovarian cancer (32,36), with long-term breastfeeding (>12 months) most significantly reducing risk (37).

Ovarian cancer: Emerging risk factors

With an increasing proportion of women working outside the home worldwide, sedentary lifestyles are rapidly increasing among women, placing them at higher risk for health concerns. Long-term sitting may lead to elevated ovarian cancer risk (38,39). By contrast, a meta-analysis from 2007 proposes increased physical activity lowers ovarian cancer risk by 20% (40). Additionally, physical activity has been proposed to provide protective effects against epithelial ovarian cancer irrespective of histological subtypes (39), while high body mass index (indicative of obesity) has been shown to elevate risk for non-serous and low-grade serous ovarian cancer subtypes (41,42). Of concern here, adipose tissue may aromatize androgens (43), functioning as the predominant source of circulating levels of estrogen in postmenopausal women (43); thus, the ovarian cancer incidence rate may rise in future with increases in the proportion of the population that is obese (44).

As the result of unhealthy lifestyles and the cultural tendency toward group-activity, women in East Asian countries (South Korea in particular) are more prone to irregular diet patterns, increased consumption of fast food and alcohol, and indirect exposure to smoking. Although ovarian cancer incidence rate has remained steady for more than two decades (7), a significant number of individuals currently may be at risk. In fact, a meta-analysis involving 430,476 women

with 1,522 incidents of ovarian cancer cases found regular intake of saturated fats and dietary nitrate, often found in processed meats, was associated with elevated risk of ovarian cancer (45,46). Interestingly, while alcohol consumption may increase the risk of breast cancer (47), beer consumption among younger individuals (20 to 30 years old) only moderately elevated the risk for serous subtypes (48). On the other hand, smokers were shown to have a more than 50% increase in risk for invasive, mucinous subtypes and more than a two-fold increase in borderline mucinous subtypes (49).

Hereditary ovarian cancer: Ovarian cancer susceptibility genes

While cancers result from the accumulation of genetic mutations, certain individuals may be at an increased risk of cancer. For example, a rare form of eye cancer, known as retinoblastoma, which typically affects young children, was first discovered to be associated with genetic mutations in the *RB1* gene (50). The possibility of increased cancer risk alongside genetic mutations subsequently led to extensive assessment of whether an individual can inherit targeted mutations in several genes, increasing their risk of cancer onset. Indeed, family history of a disease is one of the most significant risk factors for ovarian cancer (51). Furthermore, with advances in genetic sequencing, more than 16 ovarian cancer susceptibility genes have been identified (52), with more than 20% of ovarian cancers estimated to be hereditarily associated (53). Following its description in the mid-1960s, Lynch syndrome – an autosomal-dominant hereditary syndrome predisposing young individuals to colorectal cancer (54) – was shown to elevate the risk of extra-colorectal cancers such as carcinomas in the endometrium, ovary, ureter, and breast (55,56). Lynch syndrome accounts for 10-15% of hereditary ovarian cancer (57), and it involves one allele inheriting germline mutations in mismatch repair genes (MLH1, MSH2/6, and PMS2) (58). Subsequently, the second allele becomes impaired somatically with mutation, methylation, or both (59). Additionally, Li-Fraumeni syndrome, an autosomal-dominant cancer syndrome linked to heterozygous germline mutations in the *p53* tumour suppressor gene, significantly accelerates tumour onset (60). In fact, the median age for Li-Fraumeni syndrome patients is 39.5 years, compared to 64.3 years for sporadic ovarian cancer (61).

With a better understanding of genes, ovarian cancers can be divided into type I and type II tumours (62,63). While type I tumours are relatively stable with frequent mutations seen in

KRAS, BRAF, ERBB2, PTEN, PI3KCA, ARID1A, and PPP2R1A, type II ovarian tumours are advanced and aggressive, with severe genomic instability (62,63). Interestingly, the mutation in *p53* accounts for more than 95% of type II tumours (62,63). Owing to uncontrolled cell proliferation, which leads to genomic instability, DNA repair mechanisms are frequently affected by ovarian cancer, exacerbating genomic instability (64,65). For example, while nucleic acid exchange repair, base excision repair, or mismatch repair restore singe-strand DNA breaks, homologous recombination or nonhomologous end joining repairs the double-strand breaks (64). Homologous recombination involves critical players such as BRCA1/2, ATM, CHEK2, RAD51, BRIP1, and PALB2 (65), and it functions in error-proof repair using sister chromatids as a template (66). By contrast, when homologous recombination is defective, double-strand breaks are repaired by nonhomologous end joining, an error-prone mechanism (65,66).

Researchers have found that germline mutations in BRCA genes account for the majority (65-85%) of hereditary ovarian cancer (67). Additionally, BRCA mutations leading to defects in homologous recombination predispose BRCA mutation carriers to significantly increased lifetime risk for ovarian cancer – for example, up to 54% (68) in Ashkenazi Jews, the population with the highest frequency of founder mutations in BRCA genes (69). Interestingly, several reports of BRCA-negative tumours with defects in homologous recombination showing similar characteristics to BRCA-related cancers (64) support the hypothesis that not only BRCA genes but also genes coding for interacting partners of BRCA1/2 may be susceptible to targeted mutations (70).

Ovarian cancer: Current limitations and difficulties

In addition to its asymptomatic nature, leading to late-stage diagnosis (5), several factors restrict effective treatment of ovarian cancer. First, compared to other cancer types – including breast, which is currently classified into four major molecular subtypes (71) – ovarian cancer may arise from epithelial, granulosa-theca (sex cord-stromal), or germ cells (2). Epithelial cells account for approximately 90% of ovarian cancer cases, granulosa-theca (sex cord-stromal) for 5-6%, and germ cells for 2-3% (72). Furthermore, as shown in Illustration I, epithelial ovarian cancer can be further classified based on histological characteristics as high-grade serous (~70% of cases), endometrioid (~10%), clear cell (10%), mucinous (3%), and low-grade serous (<5%) (73). Of

concern here, however, the subtypes of epithelial ovarian cancer are essentially different, with different aberrations (62,63). Additionally, initiation of epithelial ovarian cancer remains controversial (74); although it was thought to initiate and progress from the ovarian surface epithelium (OSE) (74), some evidence has led to an alternative theory that epithelial ovarian cancer may begin in different pelvic organs and only secondarily spread to ovaries as cancer advances (74).

Limited understanding and current standards of care have also prevented patients from maximizing therapeutic benefits. While hysterectomy may be sufficient for some patients (9), contrary to popular belief, it may not be adequate on its own in all cases. In fact, despite surgical removal of a primary tumour, relapse occurs in more than 80% of epithelial ovarian cancer patients (12). More importantly, while risks are low for young women (20 to 30 years of age), they can still develop ovarian cancer (75); a less radical, ovarian conservation therapy is in needed to maintain the ability of women to procreate, giving rise to societal and ethical concerns. Finally, notorious heterogeneity and ambiguous classification of ovarian cancer makes the active development of therapeutics exceptionally difficult, despite the identification of 16 ovarian cancer susceptibility genes (52). Thus, an ideal alternative would be the discovery of compromised signaling pathways or those for which normal function is hijacked by different types of ovarian cancer.

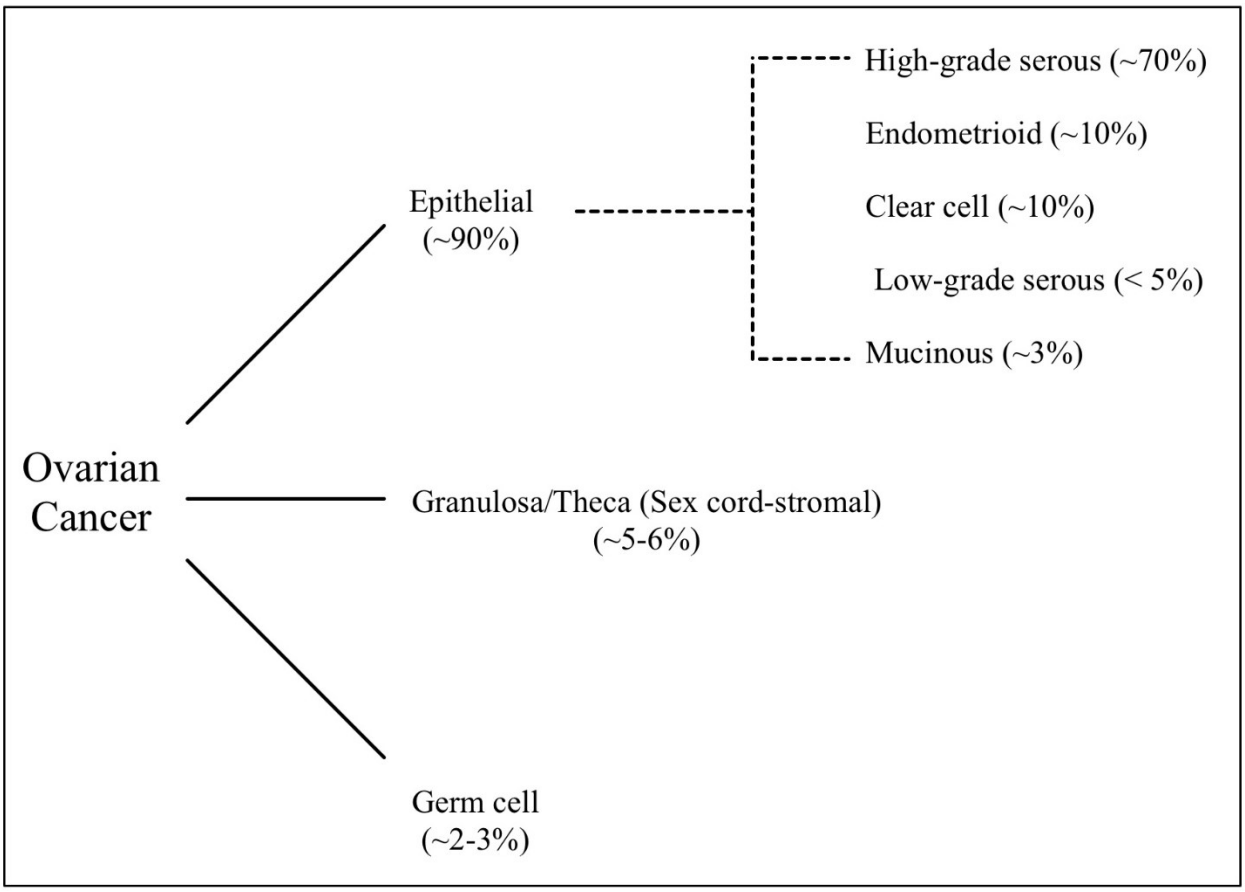

Illustration 1. Cellular origins of ovarian cancer

Ovarian cancer may arise from different cellular origins, including epithelial, sex cord-stromal, or germ cells (2). Nevertheless, ovarian cancer originating from epithelial cells accounts for the majority of cases of ovarian cancers diagnosed. Epithelial ovarian cancer can be further classified based on histological characteristics as high-grade serous, endometrioid, clear cell, low-grade serous, or mucinous (73).

Transforming growth factor-beta (TGF-β) Signaling: Overview

Cancer is not the result of aberration of a single gene, but instead of defects in regulatory mechanisms that orchestrate cell growth and death (62-65). Among numerous pathways, the transforming growth factor-beta (TGF-β) signaling pathway has been extensively studied (74). TGF-β is secreted as inactive, homodimeric polypeptides, which have three isoforms: TGF-β1, TGF-β2, and TGF-β3 (76). Although the function of each isoform is not yet fully understood, they share signaling components (76,77). Conventionally, secreted TGF-β ligand is recognized and bound by TGF-β receptor type II (TGF-βRII) (77), which then heterodimerizes with TGF-β receptor type I (TGF-βRI) and phosphorylates the cytosolic domain for full activation (77). An active form of the receptor complex signals through Smad2/3 (suppressor of mothers against decapentaplegic 2/3), also known as regulatory Smads, upon phosphorylation of the carboxy-terminal serine residue (78). Nevertheless, oligomerization with 'co-Smad', 'Smad4, is essential to transport active regulatory Smad complex into the nucleus (79), where Smad complex activates or represses transcriptional activities of several genes. For instance, cyclin-dependent kinase inhibitors such as p21cip1 or p15ink4b, which are responsible for TGF-β-mediated growth inhibition (77), are transcribed. On the contrary, Smad6 and -7 – also known as inhibitory Smads – compete with regulatory Smads for co-Smad interaction (77) and inhibit TGF-β signaling by preventing the nuclear transport of regulatory Smads (77).

Surprisingly, activated, heterotetrameric TGF-β receptors may signal in a Smad-independent manner (80). Indeed, activated TGF-β receptors have been demonstrated to 'non-canonically' activate several pathways commonly affected in carcinomas, including PI3K-AKT-mTOR, RHOA, and MAPK pathways (80).

TGF-β signaling response: A dual-edged sword

Nowadays, TGF-β is known as a 'dual-edged sword' that is tumour-suppressive at early stages but tumour-promoting (oncogenic) in the late stages of cancer (81,82). For several decades, there were disputes about the role of the cytokine TGF-β in tumorigenesis (77,80,82,83). Via 'canonical', Smad-dependent signaling, TGF-β transcriptionally represses *Myc* and *cyclin-dependent kinase 4* (*CDK4*), strengthening cytostatic effects (77,81). Additionally, TGF-β induces

programmed cell death or apoptosis by producing Kruppel-like factor 10 (TIEG1), death-associated protein kinase 1 (DAPK1), and pro-apoptotic protein, BCL-2 interacting mediator of cell death (BIM) (84). Nonetheless, Bottinger, *et al.* reported loss of TGF-β signaling components associated with cancer progression (83). By contrast, TGF-β signaling may be tumour-promoting (80,82). For example, Huber, *et al.* showed that inhibitor of DNA binding 1 (ID1) was inhibited by TGF-β, associated with decreased expression of epithelial markers Cadherin 1 (*E-cadherin*) and zona occludens 1 (*ZO1*) (82). Instead, TGF-β induced the expression of snail family zinc finger 1/2 (*SNA1/2*), zinc finger E-box binding homeobox 1/2 (*ZEB1/2*), and lymphoid enhancer-binding factor 1 (*LEF1*); these are associated with epithelial to mesenchymal transition, which is crucial for the migration of cells and thus allows further cancer metastasis (82).

Recently, however, evidence has further supported the pro-oncogenic roles of TGF-β (80,82). First, TGF-β-mediated, non-canonical activation of RHO-ROCK signaling has been demonstrated as essential for promoting cell migration and invasion (80). Moreover, non-canonical activation of PI3K-AKT signaling may allow for the evasion of apoptosis, advancing cancer progression (80.85). Most importantly, TGF-β has been shown to activate metazoan target of rapamycin (mTOR), the master regulator of nutrient sensing in eukaryotic cells that is capable of regulating cell growth, anabolism, and autophagy (80,85). Due to its versatility and importance, the mTOR pathway is commonly affected (in ~80% of cases) in cancer (80,85). Thus, components of TGF-β responses may be an ideal therapeutic target.

TGF-β responses in ovarian cancer

The literature has investigated the dual-edged role of TGF-β primarily in breast cancer (80). However, since genetic aberrations associated with different forms of cancer may vastly differ (62,63), it is unclear if TGF-β signaling affects ovarian cancer. The first evidence of this effect came from the finding that TGF-β isoforms (β1, β2, and β3) are expressed in normal ovary epithelium (74,86). Moreover, high levels of active Smad2 could be detected in normal Fallopian tube epithelium, indispensable for normal follicle development and oocyte maturation (87). Considering TGF-β responses' importance in normal ovaries, it could be inferred that they may be affected in ovarian cancer. High levels of active Smad2 (phosphorylated and nuclear-localized) were seen in high-grade serous ovarian cancer, and these high levels were negatively correlated

with patients' overall survival (87). Nevertheless, the tumour-suppressive roles of TGF-β in ovarian cancer remain controversial, with cell cycle arrest at the G1/S phase induced only in OVCCRI cells, but not in IGROVI ovarian cancer cells (88). Moreover, the cytostatic effects of TGF-β could not be seen in primary human ovarian cancer (89).

As previously mentioned, TGF-β signaling may be tumour-suppressive or oncogenic, depending on the developmental stage of cancer (81,82). In 2010, Do, *et al.* found that the knockdown of Smad3 significantly reduced the invasive potential of ovarian cancer cells, which was accompanied by decreased expression of matrix metalloproteinase 2/9 (MMP2/9) (90). Following Smad3 knockdown, induction of matrix metalloproteinases – which digest extracellular matrix, advocating extravasation of disseminated tumour cells in response to TGF-β – decreased (90). Most importantly, high levels of Smad3 were associated with poor patient outcomes (90).

LRP1's potential function as TGF-β receptor in ovarian cells

Low-density lipoprotein receptor-related protein-1 (LRP1) is a type I transmembrane protein processed in the *tran*s-Golgi to generate a mature 515-kDa α-chain and a 85-kDa β-chain (91). Interestingly, LRP1's α-chain, which is entirely extracellular, includes four clusters of complement-like repeats (CCRs), with CCR2 and CCR4 being responsible for most of LRP1's ligand binding (91,92). The β-chain – which forms strong noncovalent interactions with the α-chain – consists of YxxL and dileucine motifs serving as principal endocytosis signals and two NPxY motifs functioning as the binding site for various adapter proteins (93,94).

In 1989, apolipoprotein E-containing β-VLDL was the first identified LRP1 ligand (95). LRP1, serving as the receptor for activated α_2-macroglobulin, was subsequently identified (96). However, LRP1 is not a receptor for a small family of ligands. Indeed, currently identified LRP1 ligands include proteases, extracellular matrix proteins, and growth factors (91). Furthermore, 'interactive pathway analysis by ingenuity' has identified LRP1's possible interactions with the plasma membrane, effects on protein phosphorylation, and effects on cellular localization (91), signifying LRP1's various function *in vivo*. Interestingly, although LRP1 may transiently localize to lipid rafts, it becomes internalized by clathrin-coat mediated endocytosis and efficiently recycled (97,98). In comparison, upon internalization, LRP1-associated ligands are dissociated in mature (late) endosomes (97,98).

Supporting LRP1's diverse roles, mass spectrometry analysis has revealed identical protein sequences for LRP1 and TGF-β RV (99). Although this suggests LRP1 might function as the TGF-β receptor, it is unclear whether it genuinely mediates TGF-β responses *in vivo*. Nonetheless, in Chinese hamster ovary (CHO) cells, LRP1 has been documented as the primary receptor mediating TGF-β's growth inhibitory effects (100). Furthermore, cell cycle arrest was found to be absent in LRP1-deficient CHO cells (101). In addition to Dab2 and AP2, which mediate ligand-bound LRP1's lateral diffusion across the plasma membrane or clathrin-coat mediated endocytosis (101), a highly specific adapter protein for LRP1 known as 'GULP' was identified in 2002 (102).

GULP: Mechanism of function

'GULP' stands for 'engulfment protein' and is also known as 'CED-6'. It includes an N-terminal (phosphotyrosine binding) domain, a leucine zipper domain, and a C-terminal region of 100 amino acids without an obvious domain (102,103). LRP1 was associated historically with the engulfment of apoptotic bodies and cellular lipid homeostasis (102); however, since LRP1 may function as the TGF-β receptor in the ovary (100), researchers began to examine GULP's role in TGF-β responses. According to Ma, *et al.*, TGF-β was trapped inside the early endosome complex in CHO cells transfected with full-length GULP (FL-GULP) (101). Degradation of TGF-β increased in CHO cells expressing low levels of GULP, whereas TGF-β increased with high levels of GULP, suggesting that GULP stabilizes early endosomes and thus may enhance TGF-β signalling (101). In 2007, Ma, *et al.* reported a novel interaction between the PTB (phosphotyrosine binding) domain containing GULP and a small GTPase, Arf6, which mediates endocytosis and phagocytosis (103). However, GULP did not bind other small GTPases such as Rac1, RhoG, and Cdc42 in its GDP- or GTP-bound form (103). Accordingly, GULP's role as a mechanism governing TGF-β responses in the ovary was proposed (101).

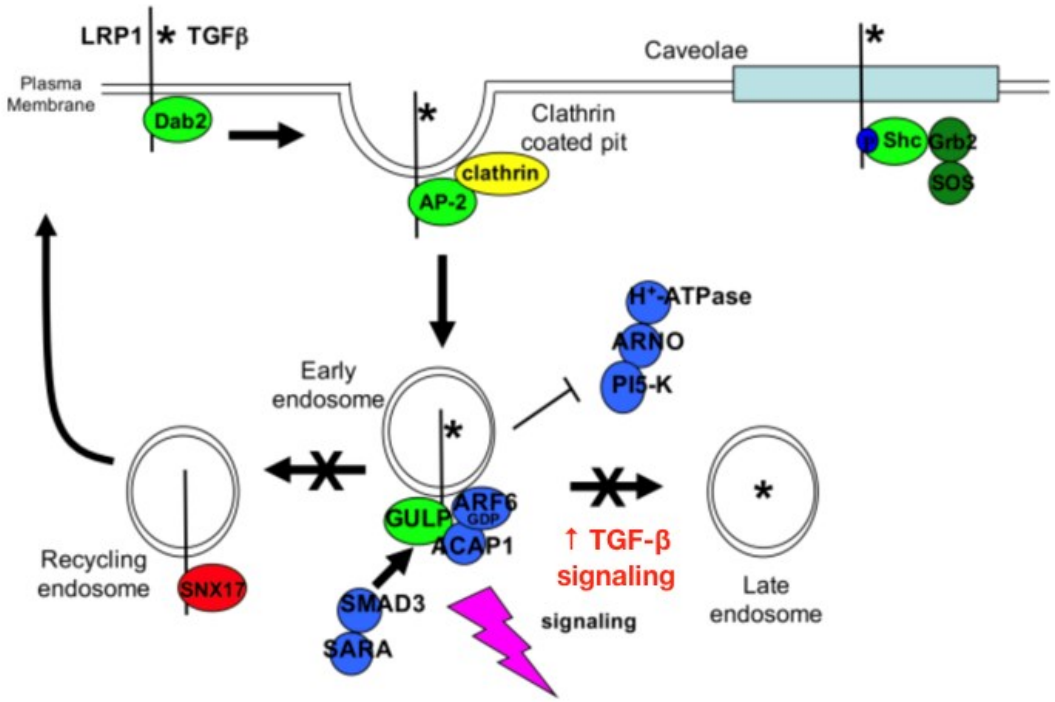

Illustration 2. Schematic diagram illustrating GULP's mechanism (101)

First, TGF-β binds to LRP1's cytosolic domain and then LRP1 can be bound by an adapter protein, Dab2, which preferentially binds clathrin. This leads to the ligand-bound LRP1's lateral diffusion across the plasma membrane towards a clathrin-coated pit. At this point, the cytosolic domain of LRP1 can be bound by another adapter protein, AP2, leading to clathrin-coat mediated endocytosis, forming an 'early endosome'. In the absence of GULP, Arf6 binds LRP1 on the early endosome. Subsequently, by interacting with 'ARNO', a GEF (guanine nucleotide exchange factor) specific for Arf6, an inactive, GDP-bound Arf6 can be activated (GTP-bound). Then, ARNO recruits the vacuolar H^+-ATPase and PI-5 (Phosphoinositide-5)-kinase, crucial for the late endosome formation, where TGF-β dissociates and gets degraded. On the other hand, when GULP is present, it leads to the favorable interaction between the GDP-bound form of Arf6 and 'ACAP1', a GAP (GTPase-activating protein) specific for Arf6, leading to the failure of interaction between Arf6 and ARNO, further preventing early endosome maturation. Most importantly, increased longevity of TGF-β responses may originate from signaling competent early endosomes, in which TGF-β bound LRP1's interaction with the Smad anchor for receptor activation protein (SARA), a FYVE domain-containing protein helps to recruit and activate Smads.

Rationale of the study

Current therapeutic options and limitations

For the past two decades, there has not been active development of therapeutics targeting ovarian cancer with the exception of olaparib and bevacizumab (9). Previous research has focused mainly on identifying genetic aberrations within cancer cells (9). By contrast, awareness of the importance of tumour microenvironment (which includes tumour-infiltrating immune cells and fibroblasts) in cancer progression continues to grow (9,104). Interestingly, although tumour microenvironment may be benign, heterotypic interaction between cancer and stromal cells has been reported; this interaction is essential for angiogenesis and stromal invasion/metastasis (105), the two hallmarks of cancer (106). For cells to sustain growth, they require a sufficient supply of oxygen and nutrients, and cells need to be within 100 μm of the capillary (9). Therefore, angiogenesis is essential for aggressive tumour progression (107). Vascular endothelial growth factor (VEGF), first identified by Ferrara *et al.*, in 1999, is a primary regulator of angiogenesis, which consists of seven family members: VEGF-A to -E and placental growth factors 1 and 2 (9,108). Moreover, VEGF signals through the VEGF receptor (VEGFR), with VEGFR-2 governing angiogenic effects (108).

Observation of higher levels of VEGF expression in the serous or clear cell subtypes of ovarian cancer has provided preliminary evidence for the therapeutic potential of interrupting angiogenic pathways in ovarian cancer (9). Accordingly, small molecule tyrosine kinase inhibitors against VEGFR were invented to terminate downstream signaling (9). Although numerous tyrosine kinase inhibitors – including sunitinib, sorafenib, and cediranib – have been tested, only modest activity has been found in recurrent ovarian cancer despite substantial toxicity (109,110). By contrast, bevacizumab, a recombinant, humanized monoclonal IgG antibody targeting VEGF-A, recently showed statistically significant improvement in progression-free survival in phase III trials (9). Furthermore, bevacizumab may enhance the delivery of chemotherapeutic agents by normalizing the vasculature (9), although its inclusion in standard chemotherapy has been found to be cost-ineffective (111).

Among ovarian cancer patients with mutations in BRCA genes, the homologous recombination DNA repair system is defective, leaving them more dependent on alternatives

(64,66,67). Thus, inhibition of poly (ADP-ribose) polymerase (PARP) - dependent, base excision repair (112) instead leads to the accumulation of single-strand DNA breaks. The accumulation of DNA damage, in turn, results in replication-associated double-strand breaks, which can only be repaired by error-prone non-homologous end joining (63,66) in BRCA mutation carriers. Ultimately, prolonged accumulation of DNA damage results in selective tumour cell death, known as synthetic lethality (112,113). According to Kaufman, *et al.* the use of PARP inhibitors (e.g. olaparib) in 193 ovarian cancer patients (chemotherapy-resistant) resulted in progression-free survival (>8 weeks) in more than 40% of patients and a 31% tumour response rate (114). Despite its strength, however, it is questionable whether PARP inhibitors can significantly, or universally, benefit ovarian cancer patients irrespective of subtype. Since the efforts and cost required for drug development is tremendous, an alternative therapy that may universally benefit ovarian cancer patients is critically needed.

GULP expression's downregulation in ovarian cancer

Although GULP's role in TGF-β signaling has been examined using CHO, SKOV3, and HEY ovarian cells (101), several concerns remained unaddressed. First of all, the classification of ovarian cancer cell lines is ambiguous or unknown (115). Furthermore, CHO cells, which were established from the ovary of a Chinese hamster in the 1950s (116), rapidly became favoured in the research (117). Unfortunately, CHO cells initially had a fibroblast-like morphology, which gradually became more epithelial-like (116,118), depending on growth conditions (i.e. nutrient ingredients). All of this means that CHO cells do not represent a strong physiological model of ovarian cells. Besides, since ovarian cancers are vastly heterogeneous (62,63), misclassification further complicates useful therapeutic guidance for each ovarian cancer patient across subtypes. Despite the existing limitations, shown in illustration 3, GULP's expression in different types of cancer was generally decreased, including breast and ovarian cancer. More importantly, decreased expression of GULP was found (Illustration 4) irrespective of ovarian cancer subtype (101).

Disease Summary for GULP1

Analysis Type by Cancer	Cancer vs. Normal	
Bladder Cancer		2
Brain and CNS Cancer	1	4
Breast Cancer		7
Cervical Cancer		3
Colorectal Cancer		3
Esophageal Cancer		2
Gastric Cancer		1
Head and Neck Cancer		7
Kidney Cancer	1	4
Leukemia		
Liver Cancer		
Lung Cancer		
Lymphoma		
Melanoma		
Myeloma		
Other Cancer		3
Ovarian Cancer		3
Pancreatic Cancer		1
Prostate Cancer		
Sarcoma	1	
Significant Unique Analyses	3	40
Total Unique Analyses	418	

Illustration 3. GULP expression's decrease in numerous types of cancer

Based on microarray dataset from ONCOMINE, GULP's expression is significantly decreased in different types of cancer, including the breast and ovary. Although GULP's expression increased in brain and central nervous system cancer, kidney cancer, and sarcoma, incidences were significantly lower compared to total analysis (3 significant analysis out of 418 total analysis).

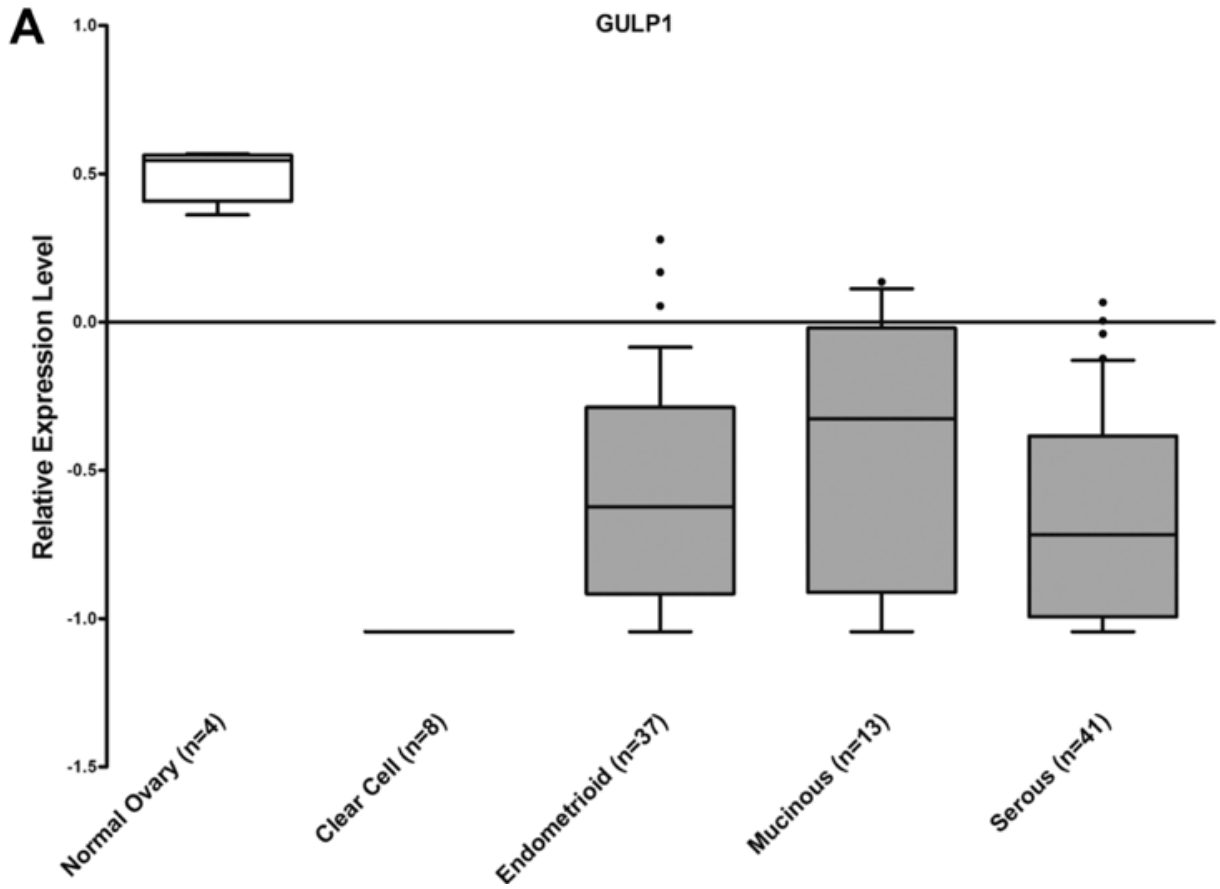

Illustration 4. GULP expression level's decrease in ovarian adenocarcinoma (101)

Among different subtypes of epithelial ovarian cancer, GULP's expression is significantly decreased compared to a normal, healthy ovary, according to tissue microarrays. Most importantly, GULP's expression is universally reduced in cancerous cells, which may be used as a reliable prognostic factor for ovarian cancer.

Importance of the project and hypothesis

Cell lines can only partially recapitulate the phenotype of ovarian cancer. Therefore, this study involves obtaining primary human ovarian tissue samples (normal and cancerous), where OSE cells are established, as the most physiologically relevant cell model.

Since research has demonstrated that GULP's expression universally decreases in ovarian cancer compared to normal, healthy ovaries (101), this study seeks to demonstrate that reduced

GULP expression is associated with ovarian cancer progression *in vivo*, which has not previously been shown. In agreement with Ma, *et al.*, who reported that low levels of GULP is associated with decreased TGF-β responses in ovarian cancer cell lines (101), this study hypothesizes that GULP is involved in TGF-β responses in the human ovarian surface epithelium. Furthermore, it hypothesizes that reduced levels of GULP in ovarian cancer allows cancer cells' evasion of TGF-β's tumour-suppressive effects (77,81).

To precisely understand the functional consequences of reduced expression of GULP for ovarian cancer risk, GULP's expression is knocked out in SKOV3 ovarian cancer cells initially having high levels of GULP. Thus, a loss of GULP is hypothesized to increase the proliferation of ovarian cancer cells and that decreased levels of GULP might restrict oncogenic effects (e.g. cell migration) of TGF-β (80.82,85).

2. Materials and Methods

2.1 Materials

Cell culture medium and associated reagents were warmed in the metal bath from *VWR®* (Radnor, PA). T25 tissue culture flasks and 6-well plates were purchased from *Sarstedt* (Nümbrecht, Germany). 12, 24, and 96-well plates were purchased from *Corning* (New York, USA). Glass Pasteur pipettes were purchased from *Fisher Scientific* (Quebec, CA) and sterilized by autoclaving for cell culture. For the estimation of a cell population, hemocytometer purchased from *Fisher Scientific* (Quebec, CA) was used. For downstream experiments, cells were collected and diluted to desired density in 15 or 50 mL Falcon tubes purchased from *Sarstedt* (Nümbrecht, Germany). Sterile, surgical-grade blades purchased from *Fisher Scientific* (Quebec, CA) were used to gently scrape the ovarian surface epithelium (smooth surface of the ovary) of primary human ovary samples for mechanical isolation of OSE cells. To sterile filter solutions for cell culture, 0.2 µm syringe filters from *Sarstedt* (Nümbrecht, Germany) were used. For general inspection of cell culture, an inverted contrasting microscope for living cell applications from *Leica Microsystems* (Wetzlar, Germany) was used. Throughout experiments, cells were maintained in a 37°C incubator with 5% CO_2, from *PharmaMedSci* (Quebec, CA).

For cell seeding and liquid handling during MTT assay, 100 µL multi-channel pipette from *Eppendorf* (Hamburg, Germany) was used. For liquid handling with multi-channel pipettes, Corning™ Costar™ Sterile Disposable Reagent Reservoirs from *Corning* (New York, USA) were used. For solubilization of MTT crystals, a 30-300 µL Finnpipette™ Novus electronic multichannel pipette and a 5-50 µL Finnpipette™ multichannel pipette from *Thermo Fisher Scientific* (Massachusetts, USA) were used. For gentle agitation of microplates, The Belly Dancer® orbital shaker from *IBI Scientific* (Iowa, USA) was used. For MTT assay and protein concentration measurement using modified Lowry's method, absorbance was measured using M200 Infinite microplate reader from *Tecan* (Männedorf. Switzerland).

For cell lysis, cell scrapers purchased from *Corning* (New York, USA) were used to collect lysates into 1.5 mL Eppendorf tubes from *Sarstedt* (Nümbrecht, Germany) and supernatants were further collected into 1.5 mL screw-top tubes from *Sarstedt* (Nümbrecht, Germany).

During Western blot analysis, a mini-PROTEAN® Tetra Cell system purchased from *Bio-Rad* (Ontario, CA), was used to hand-cast mini-gels. Glass plates were cleaned thoroughly by rinsing with a Milli-Q® integral water purification system for ultrapure water from *EMD Millipore Corporation* (California, USA) and dried using grade 3mm Chr cellulose chromatography papers from GE Healthcare (Quebec, CA). 4 and 15% Gel solutions were vortexed using the vortex genie from *Scientific Industries, Inc* (New York, USA). Protein samples for Western blot analysis were heated using Accublock digital dry bath from *Montreal Biotech Inc.* (Quebec, CA) and subsequently centrifuged for 30 seconds at room temperature using a table-top microcentrifuge from *Fisher Scientific* (Quebec, CA). A power supply from *Amersham Biosciences Corp.* (Buckinghamshire, UK) was used to resolve gels at a constant voltage in conjunction with magnetic stir plate from *Fisher Scientific* (Quebec, CA) to evenly distribute ions. Trans-Blot® SD Semi-Dry Transfer Cell system purchased from *Bio-Rad* (Ontario, CA) was used to transfer resolved gels to an Immobilon-P PVDF membrane purchased from *EMD Millipore Corporation* (California, USA). Chemiluminescent images were acquired using ImageQUANT LAS 4000 system from GE Healthcare (Quebec, CA).

Lastly, the wounded area from the scratch assay at T_0 and T_{24} time points were acquired using an EVOS™ XL Core Imaging System from *Thermo Fisher Scientific* (Massachusetts, USA).

2.2 Reagents and antibodies

Reagents

Acrylamide/Bis-Acrylamide, 30% solution 29:1, glycerol, sodium fluoride and sodium orthovanadate were purchased from *BioShop* (Ontario, Canada). D-(+)-glucose solution (45%), Dispase II protease, 6N-HCl, NaCl, Na_2HPO_4, KH_2PO_4, $MgCl_2$, Tween 20, poly-L-Lysine, and bovine serum albumin were purchased from *Sigma-Aldrich* (Ontario, Canada). DMSO, guanidine hydrochloride, glycine, $CaCl_2$, KCl, and methanol were purchased from *Fisher Scientific* (Quebec, Canada). Insulin, human recombinant (yeast), SDS, Tris base, and cOmplete™, EDTA-free Protease Inhibitor Cocktail Tablets were purchased from *Roche Ltd* (Laval, Quebec, Canada). SuperSignal® West Pico Plus Chemiluminescent Substrate and puromycin dihydrochloride was purchased from *Thermo Fisher Scientific* (Massachusetts, USA). 2-mercaptoethanol, Precision Plus Protein™ All Blue Standards, TEMED, and Bio-Rad DC Protein Assay were purchased from

Bio-Rad (Ontario, Canada). DMEM, M199, MCDB-105, FBS, 100X penicillin-streptomycin solution, 0.25% trypsin/2.21 mM EDTA, 0.05% trypsin/0.53 mM EDTA were purchased from *Wisent* (Quebec, Canada). RPMI-1640 medium without L-glutamine, 10X MEM Nonessential Amino Acids, 200 mM L-alanyl-L-glutamine, and 100 mM sodium pyruvate were purchased from *Corning* (New York, USA). Lastly, recombinant Human TGF-β1 (HEK293 derived) was purchased from *Peprotech* (New Jersey, USA) and prepared as instructed by the manufacturer as 50 nM stock.

Antibodies

For Western blot analysis, the rabbit polyclonal antibody to phospho-Smad3 was purchased from *Cell Signaling* (Massachusetts, USA). The rabbit polyclonal antibody against Smad3 and β-tubulin were purchased from *Santa Cruz Biotechnology* (Texas, USA). The rabbit polyclonal antibody against GULP was purchased from *Thermo Fisher Scientific* (Massachusetts, USA). The rabbit polyclonal antibody against GAPDH was purchased from *Sigma-Aldrich* (Ontario, Canada). Lastly, goat-anti-rabbit, HRP-conjugated secondary antibody was purchased from *Jackson ImmunoResearch* (Pennsylvania, USA).

2.3 Cell culture

Cell culture of ovarian cancer cell lines

HEY ovarian cancer cells were originally obtained from ATCC (Manassas, VA). HEY cells were cultured in DMEM supplemented with 10% FBS and 1% penicillin and streptomycin (P/S). HEY cells were subcultured at a subculture ratio of 1:5 (v/v) in a T25 tissue culture flaks to 80-90% confluence. For passaging, the existing medium was carefully aspirated using a sterile Pasteur pipette. Subsequently, the cells were gently washed with free DMEM without any supplements. For trypsinization, 0.25% trypsin/2.21mM EDTA solution was used. After gentle shaking to evenly spread trypsin solution in a tissue culture flask, the trypsin solution was aspirated and then the tissue culture flasks were left in 37 ℃ for 5 minutes to allow the detachment of cells. The detachment of cells was further monitored under an inverted light microscope, followed by gentle tapping along the sides of the T25 tissue culture flask.

SKOV3 and PEO-14 cells were kind gifts from Dr. Carlos Telleria (McGill University). SKOV3 cells were cultured in RPMI-1640 medium without L-glutamine supplemented with 0.45% D-(+)-glucose, 10µg/mL human insulin, 1X non-essential amino acid, 4 mM L-alanyl-L-glutamine, 1 mM sodium pyruvate, 10% FBS, and 1% P/S. Similarly, PEO-14 cells were cultured in RPMI-1640 medium without L-glutamine supplemented with 10µg/mL human insulin, 4 mM L-alanyl-L-glutamine, 1 mM sodium pyruvate, 10% FBS, and 1% P/S. Both ovarian adenocarcinoma cells were subcultured in the same manner as HEY cells, excepting, T25 flasks were left for a longer period (5-10 minutes) to ensure complete detachment of cells.

Cell culture of GULP-knockout cell line

Both SKOV3 knockout-control (scrambled) SKOV3 GULP knockout (SKOV3 GULP-KO) cells were cultured in medium matching that of parental SKOV3 cells except for the further inclusion of puromycin dihydrochloride at a final concentration of 1µg/mL. Both Scrambled and GULP-knocked out SKOV3 cells were subcultured in the same manner as HEY cells.

Cell culture of primary ovarian surface epithelial cells

Primary human ovarian surface epithelial cells (OSE) (normal and cancerous) were isolated from human ovary tissue samples obtained from patients undergoing surgery who signed the consent for the research purposes. The OSE cells were cultured in 1:1 (v/v) mixture of M199 and MCDB-105 containing 10% FBS, 1% P/S. Upon initial isolation, the primary OSE cells were trypsin-digested using 0.05% trypsin/0.53mM EDTA solution to stimulate growth when they were grown to 30~40% confluence.

2.4 Generation of GULP knockout cell lines

GULP1 and scrambled single-guide sequence annealing and molecular cloning

For CRISPR-Cas9 gene knockout in SKOV3 cells, LentiCRISPRv2, a new vector capable of producing higher-titer virus (~10 fold improvement over) developed by Sanjana, *et al.* in 2014 was utilized (119). LentiCRISPRv2 (Addgene, #52961) was digested and dephosphorylated using Esp3I restriction enzyme (*Thermo Fisher Scientific*, #ER0451) and FastAP (*Thermo Fisher*

Scientific, #EF0654), respectively. Then, the plasmid was agarose gel purified and extracted using QIAquick Gel Extraction Kit (QIAGEN, #28704).

Each single-guide primer sequences below (5'-3') were phosphorylated using T4 PNK (NEB, #M0201S), annealed by slow cooling from 65°C to room temperature in T4 ligation buffer (NEB, #B0202S) and ligated in Esp3I digested and gel purified, lentiCRISPRv2 plasmid using Quick Ligase (NEB, #M2200S). Each sgRNA ligated plasmid was transformed in STBL3 chemically competent *E. coli* (*Thermo Fisher Scientific*, #A10469) and collected from an amplified single bacterial colony using QIAprep Spin Miniprep Kit (QIAGEN, #27104).

	Sequences
GULP sg1F	CACCGAAGCATTTGACCTGGCATAC
GULP sg1R	AAACGTATGCCAGGTCAAATGCTTC
GULP sg2F	CACCGCTAGAAATTTCCTGTATGCC
GULP sg2R	AAACGGCATACAGGAAATTTCTAGC
GULP sg3F	CACCGTTTCATTCCCTATAATGCAA
GULP sg3R	AAACTTGCATTATAGGGAATGAAAC
SCR sg1F	CACCGACGGAGGCTAAGCGTCGCAA
SCR sg1R	AAACTTGCGACGCTTAGCCTCCGTC
SCR sg2F	CACCGCGCTTCCGCGGCCCGTTCAA
SCR sg2R	AAACTTGAACGGGCCGCGGAAGCGC
SCR sg3F	AAACTTGCGACGCTTAGCCTCCGTC
SCR sg3R	AAACCGCCGTTAAGCGGAAACGATC

Table 1. Sequences of GULP1 and scrambled single-guide primers.

Lentiviral infection

HEK293T cells were transfected with scrambled sgRNA or GULP1 sgRNA and packaging plasmids pMD2.G (Addgene, #12259) and psPAX2 (Addgene, #12260). After 48hours post-transfection, cell supernatants containing sgRNA lentiviruses were collected. Ovarian cancer cells (PEO-14, SKOV3) were infected with lentiviral sgRNAs in the presence of 8μg/mL polybrene

(*Sigma Aldrich*, #107689) and selected for 7-10 days in the presence of 1µg/mL puromycin (*Thermo Fisher Scientific*, #A1113803).

2.5 Isolation and culture of OSE cells from human ovary tissue samples

An original method by Shepherd, *et al.* in 2006 (120) for the isolation of human ovarian surface epithelial cells was adopted in this study (Illustration 5).

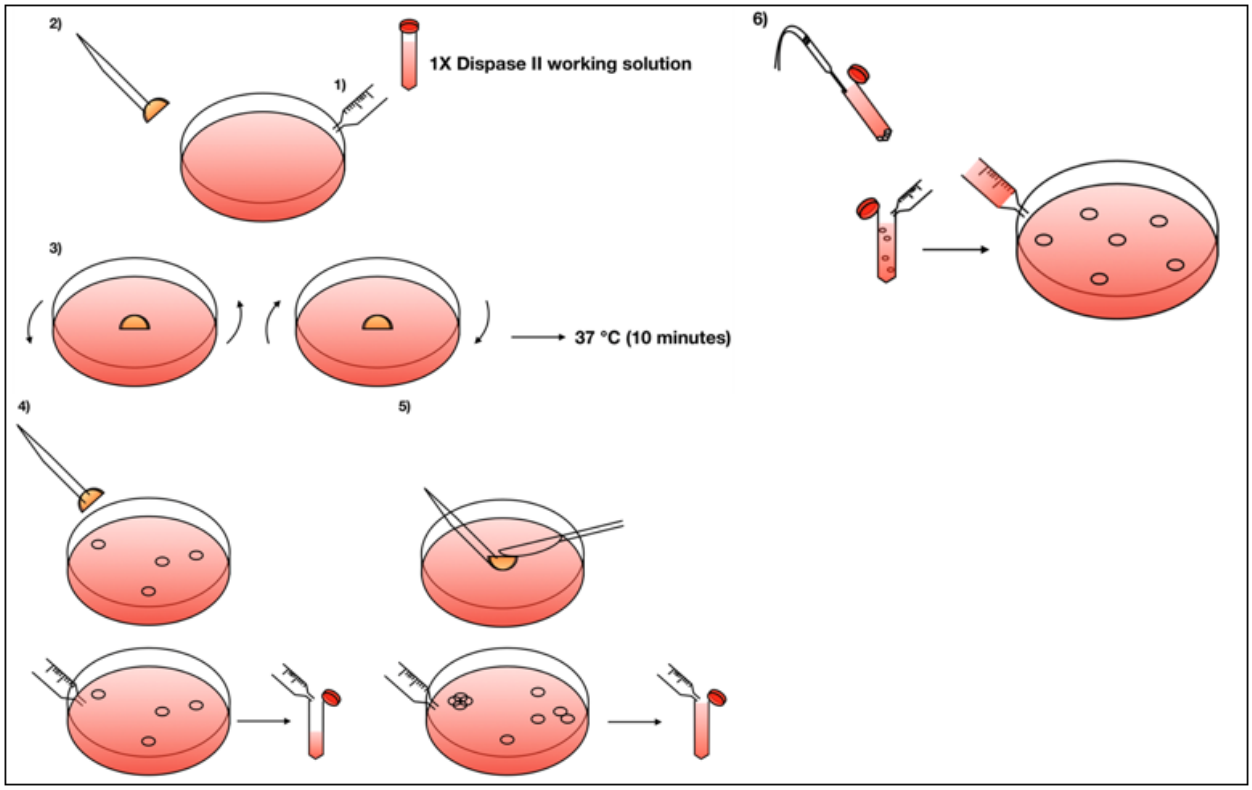

Illustration 5. Illustration of primary OSE cell isolation from the ovary tissue

Primary human ovary tissue samples from patients (normal or cancerous) packaged in sterile specimen containers were received from surgical staffs inside the operating room at Royal Victoria Hospital. Subsequently, samples were promptly transported to a tissue culture hood and washed with free cell culture medium (MCDB105/M199 supplemented with only antibiotics) for three times to remove contaminating microorganisms and red blood cells. Before processing of samples, cell culture medium and Dispase II stock solution (5X) were warmed to 37 ℃ for 30

minutes in a metal bath. Working Dispase II solutions were prepared by diluting the stock at a ratio of 1:5 (v/v) with complete cell culture medium and sterile-filtering using a 0.2 μm syringe filter. 2 mL of working solution was dispensed to a single well of a 6-well cell-culture plate (Step 1) with the ovary surface epithelium-side (smooth surface) facing the solution (Step 2). The ovary tissues were carefully handled with sterile forceps. A 6-well plate was swirled for 60 times total in counter and clockwise manner and left inside the 37 ℃ incubator for 10 minutes for further enzymatic digestion (Step 3). This step was repeated for 2 more times. Afterwards, 2 mL of complete cell culture medium was dispensed to an adjacent well, and the digested surface of the ovary (smooth surface) was gently scraped off using a sterile surgical blade. Following the mechanical isolation, the medium from each well was collected in a sterile 15mL Falcon tube (Steps 4-5). Each well was further washed with fresh medium to collect remaining cells. Then, volumes were brought up to the full capacity. The tube was centrifuged at 100 x *g* at 4 ℃ for 10 minutes. Afterwards, the medium was aspirated with a sterile Pasteur glass pipette using vacuum suction while leaving ~ 0.5 mL of volume to ensure minimal loss of OSE cells. The sediment pellet was resuspended in 2 mL of fresh culture medium and dispensed to a new well of a 6-well plate (Step 6).

Upon initial isolation, 'grape fruit' shaped clusters of epithelial cells could be observed under the light microscope. The plate was further left inside the incubator for 3~4 days until clear attachment of epithelial cells and typical 'cobblestone' morphologies could be observed (120). At that point, the medium was changed to remove non-attached contaminants, including red blood cells.

2.6 Enrichment of ovarian surface epithelial cells

Upon initial isolation, OSE clusters were left to be propagated until 30~40% confluence was reached. At that point, to maximize the purity of epithelial cells, partial trypsinization described by Dairkee, *et al.* (121) was performed using 0.05% trypsin/0.53 mM EDTA solution (Illustration 6). Additionally, the property of fibroblasts, which allows rapid attachment to tissue culture flasks, was utilized (Illustration 6) to remove contaminating fibroblasts preferably (122).

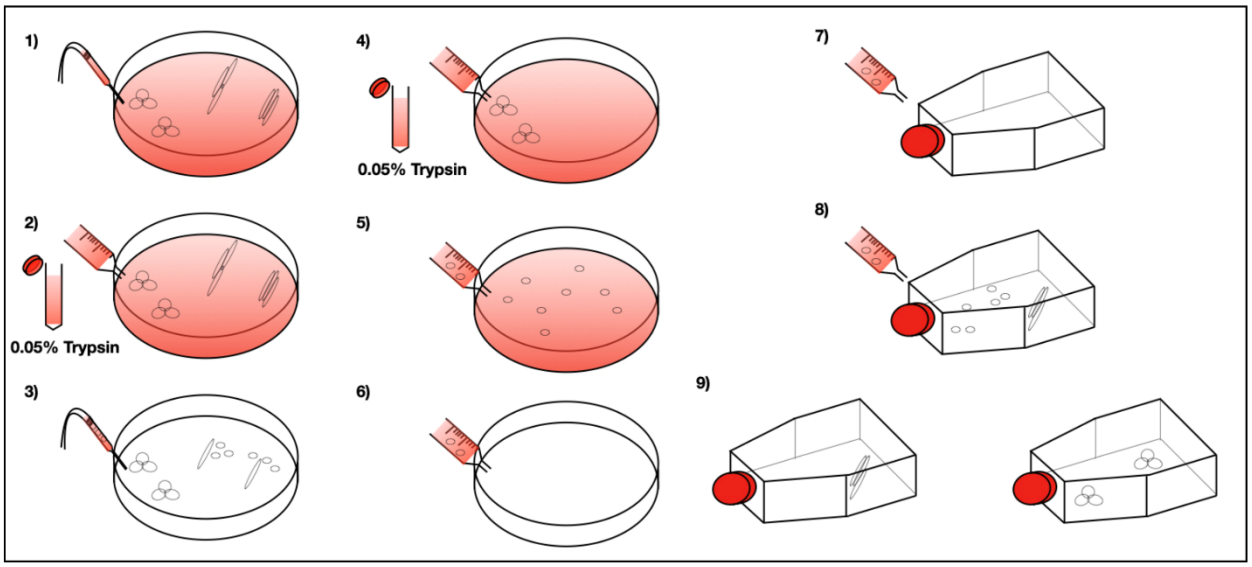

Illustration 6. Illustration of the enrichment of ovarian surface epithelial cells

floral shapes are representative of 'cobble-stone' morphology of OSE clusters. Long and thin oval shapes are representative of contaminating fibroblasts. Round, individual circles are representative of trypsinzed/detached cells.

The wells in a 6-well plate containing OSE cells were rinsed with warm, free culture medium and then washed briefly with the trypsin/EDTA solution for 1~2 minutes (Steps 1-2). The plate was monitored under an inverted light microscope until rounding and detachment of the first cell could be observed. Then, the trypsin/EDTA solution was gently aspirated and this step was repeated for additional time before epithelial cells were retrieved (Step 3). The cells were then resuspended in the original well and left to be propagated until 80~90% confluence was reached.

When confluence was reached in an individual well of 6-well plate, OSE cells were trypsinized and resuspended in 5 mL of complete medium (Steps 5-6). This cell-containing medium was transferred to T25 tissue culture flask and left at 37 ℃ incubator for 15 minutes to allow removal of fibroblastic or contaminating stromal cells (Steps 7-8). After 15 minutes, medium (supernatant) was retrieved and transferred to a fresh T25 tissue culture flask and cultured until confluence was reached (Step 9; right). Simultaneously, T25 flask with contaminating cell population was cultured to ensure minimal loss of epithelial population from this method (Step 9; left). Due to the limited dividing potential of primary OSE cells, downstream experiments were performed by the third passage.

2.7 Growth Assay

Cells were seeded to 3, 12-well plates in quadruplicate. Each well of a 12-well tissue-culture plate was coated with poly-D-lysine for 15 minutes at 37℃. Subsequently, each well was washed using free culture medium without any supplements of respective cell lines (Free DMEM or RPMI-1640). Afterwards, HEY, SKOV3, SKOV3 Scrambled, SKOV3 GULP-KO, and PEO-14 cells were trypsinized in a manner described previously and collected in 15mL Falcon tubes using supplemented culture medium. After repetitive pipetting to ensure even distribution of cells, 10μL of cell suspension from each 15 mL tube was loaded into the groove of a hemocytometer. Cells in four quadrants on corners were counted for the estimation of the total number of cells per mL. Dilution of each cell line to the desired cell density (70,000 cells/mL) was achieved using complete culture medium of respective cell line.

Following overnight incubation of cells, existing medium in each well of a 12-well plate was carefully aspirated and washed with 0.5mL of free culture medium. After gentle rocking of the 12-well plate, the medium was aspirated, and 0.5mL of culture medium containing all supplements except serum was dispensed to each well for 24-hour serum starvation. After starvation, starvation medium in each well was replaced by 0.5mL of respective culture medium with 1% serum. Then, the cells were further incubated with or without 0.2 nM TGF-β1 (served as a control) in a 37℃ incubator. Additionally, just after starvation for 24 hours, cells were harvested (plate #1) and the number of cells was counted. Similarly, after 48 and 72 hours, cells in second and third 12-well plates were harvested and counted. Total cell numbers were estimated by multiplying estimated cell density from each well (cells/mL) by the volume used to resuspend trypsin-digested cells in each well (0.5 mL).

2.8 MTT Assay

Cells were seeded to 3, 96-well tissue culture plates in sextuplicate. Sterile, disposable reagent reservoirs were used for liquid handling with multichannel pipettes, throughout the assay. Each well of a 96-well plate was coated with 40μL poly-D-lysine using a 100μL multichannel pipette for 15 minutes at 37℃. Subsequently, each well was washed with a free culture medium. To minimize differential evaporation of outermost wells, the wells were filled with 200μL of CMF-PBS. Ovarian cancer cells or primary OSE cells were trypsinized and seeded at a density of 10,000 cells/mL or 1,000 cells/well (HEY/SKOV3 and HEY/PEO-14) and 20,000 cells/mL or 2,000

cells/well (SKOV3 Scrambled/GULP-KO, and primary OSE cells) and 100µL was dispensed in each well. While seeding, gentle, repetitive pipetting (5~6 times) was done each time to ensure even distribution of cells per well. Following overnight incubation, the medium was carefully removed using a multichannel pipette. Subsequently, the cells were serum starved for 24 hours in 100 µL of the respective starvation medium. To minimize the loss of cells, after 24 hours, additional 100 µL of media with 2% serum was dispensed to each well with or without 0.4 nM TGF-β1 to achieve a final concentration of 0.2 nM in 200 µL instead. Additionally, adjacent row filled with PBS was aspirated, and 200 µL of media with 1% serum was dispensed (cell-free control). Following starvation, one of the plates was further treated with MTT solution by adding 25 µL to each well. MTT solution was prepared by dissolving MTT powder in CMF-PBS to yield a final concentration of 5mg/mL. After complete dissolution, the MTT solution was filtered and stored at 4 ℃ for no more than 1 week after covering with aluminum foil to protect against light. The plate was incubated at 37 ℃ for 2 hours until dark/purple crystals could be observed under a light microscope. Then, each well was carefully and slowly aspirated using a Pasteur pipette and then 200 µL of DMSO was dispensed to each well. Also, 25 µL of Sorensen's glycine buffer (0.1 M Glycine, 0.1 M NaCl, pH 10.5), an extra inclusion described by Plumb, *et al.* (123) was dispensed and the plates were wrapped in aluminum foil to protect against light. Lastly, the plates were left in gentle agitation for 15 minutes and absorbance was measured at 570 nm (signal) and 690 nm (reference). The absorbances were similarly measured after 24 and 48 hours.

In a similar manner stated above, SKOV3, PEO-14, and scrambled or GULP knocked-out SKOV3 cells were treated with torin-1 alone or together with 0.2 nM of TGF-β for 24 hours. Torin-1 was prepared as 1 mM stock solution dissolved in DMSO according to manufacturer's instruction. For cell culture treatment, 1,000 times fold dilution in each cell line's respective culture medium was done to prepare 1 µM working solution. Subsequently, final treatment solution was prepared to include 250 nM of torin-1 and 0.4 nM of TGF-β1, which were diluted by half (final concentration 125 nM torin-1, 0.2 nM TGF-β) by adding on top of 100µL of the starvation medium in each well. For comparison of each compound's effect, cells were also treated with TGF-β (0.2 nM) or torin-1 (125 nM) alone. After 24 hours, MTT solution was added, and absorbance was measured.

2.9 Scratch/Wound-healing Assay

Cells were seeded to 24-well tissue culture plates in triplicate or sextuplicate. 24-well tissue culture plates were similarly prepared as previously described for the growth assay. HEY, SKOV3 and PEO-14 cells were seeded at a density of 150,000 cells/mL, 70,000 cells/mL, and 120,000 cells/mL, respectively. Similarly, SKOV3 Scrambled and SKOV3 GULP-KO cells were seeded at a density of 100,000 cells/mL. The seeding density was optimized to yield a confluent monolayer (70~80%) of cells following overnight incubation at 37 ℃. Subsequently, the cells were serum starved for 24 hours following thorough washing of individual wells using free culture medium. After 24 hours, each well was scratched using a sterile P200 pipette tip and thoroughly washed twice with a starvation medium to remove cellular debris. Then, 0.5 mL of serum starvation medium was dispensed to each well and further treated with or without 0.2 nM TGF-β1. After the initial scratch, a photograph was taken (T_0). The plates were further incubated at 37 ℃ for 24 hours and then the same field of view was photographed for comparison (T_{24}).

The wounded area was measured by an image analysis software imageJ from the National Institutes of Health and outlines of the wound were drawn with a polygonal selection tool. The extent of cellular migration represented as the percentage (%) of wound-healed by migrating cells was computed in the following manner: [(average wound area at T_{24} - average wound area at T_0)/(average wound area at T_0)]. Then, cell migration in response to TGF-β was graphed by subtracting the percentage of migration of respective, non-treated cells.

2.10 Western blot analysis

Preparation of acrylamide gels for SDS-PAGE

A day before each Western blot analysis, two 4-15% gradient acrylamide gels were casted. Both short and 1.5 mm-spacing tall plates for Biorad® Mini-PROTEAN Tetra Cell system were cleaned with double-distilled water and carefully dried. Glass plates were casted and initially checked for leakage using distilled water. The assembly was left for 15 minutes to ensure the absence of any leakage. After 15 minutes, water between glass plates was drained, and casting stand was left at an angle to collect remaining water, which was dried using filter papers.

For casting gradient resolving gels, 4% and 15% gels were prepared separately. Each gel solution was mixed thoroughly by inversion and vortexing. Subsequently, 500 µL of 15% gel

solution was slowly poured using a P1000 micropipette. Afterwards, 3 mL of 4% and 3 mL of 15% of gel solutions were taken using 5 mL serological pipette and a single bubble was introduced and allowed to travel upwards along the pipette to allow mixing of two solutions. Mixed gel solutions were then slowly dispensed in between glass plates, and 500 µL of 4% gel solution was dispensed on top followed by 500 µL of isopropanol solution to block the contact with open air. The gradient resolving gels were allowed to be polymerized for 1 hour at room temperature. Each leftover gel solution was kept at room temperature to monitor polymerization. Upon complete polymerization, overlaid isopropanol was drained and the gels were cleaned with distilled water for five times. The casting stand was left at an angle to drain water in between glass plates before stacking gels were poured.

4% Stacking gel solution was thoroughly mixed and carefully poured to the top of the glass plate using serological pipettes. A 1.5 mm 15-well comb was inserted, and the gels were left to be polymerized for 30 minutes. Upon completion, glass plates were removed from casting frames and wrapped with paper towels wetted with distilled water for overnight storage at 4 ℃.

Preparation of cell lysates for TGF-β response analysis

For Western blot analysis, cells were seeded at the density of 100,000 cells/mL into a 24-well tissue culture plate and left overnight in a 37 ℃ incubator. On the following day, the culture medium in each well was aspirated and washed twice with culture medium deprived of serum for ovarian cancer cell lines (HEY, SKOV3, PEO-14, SKOV3 Scrambled, and SKOV3 GULP-KO) or culture medium with reduced serum (1%) for primary OSE cells. Following 24 hours of starvation, existing medium was aspirated and refreshed with the medium containing 1% serum. Cells were further treated with or without 0.2 nM TGF-β1. Each cell line or primary OSE cells (normal or cancerous) were treated with TGF-β1 for variable periods: 30 min, 1 hour, 6 hour, and 24 hours. Afterwards, medium with or without TGF-β was aspirated from each well and subsequently washed with 1X-PBS twice. Then, 50 µL of RIPA lysis buffer (50 mM Tris-HCl, pH7.6; 150 mM NaCl; 1% NP-40; 0.5% sodium deoxycholate; 0.1% SDS; 1 mM EDTA) supplemented with phosphatase inhibitors, sodium fluoride (50 nM) and sodium orthovanadate (1 nM) as well as protease inhibitor cocktail (50X) was dispensed to each well and 24-well plate was left on ice for 10 minutes following gentle rocking. Lysis was monitored under the inverted light microscope, and cell scraper was used to scrape off cells. Resulting crude lysates were then

collected into pre-labelled, pre-chilled 1.5 mL Eppendorf tubes and further incubated on ice for 30 minutes. After 30 minutes, crude lysates were centrifuged at 13,000 rpm for 10 minutes to remove cellular debris and to collect only supernatants.

Sample preparation for Western blot analysis

Cell lysates were stored at a -80 ℃ fridge following initial lysis. Protein concentration was measured using modified-Lowry's method using Bio-rad DC protein assay. The lysates were diluted at a ratio of 1:5 (v/v) using a RIPA-lysis buffer to the total volume of 5 µL. Protein concentration was measured in duplicates at 750nm, and average absorbances were used. BSA protein standards from 0 mg/mL to 1.2 mg/mL in RIPA-lysis buffer were prepared. After addition of reagents, samples were left for 15 minutes following gentle tapping alongside a 96-well plate and left in the dark for development of blue shades. Absorbance at 570 nm was measured. Ten to fifteen µg of cell lysates were used following the addition of a 4X Laemmli sample preparation buffer (250 mM Tris-HCl pH 6.8, 10% SDS, 0.008% Bromophenol Blue, 40% Glycerol) supplemented with β-mercaptoethanol (355 mM final concentration). Lastly, distilled water was used to match the volume of each sample.

Resolving gels

For Western blot analysis, gels were assembled in Mini-PROTEAN® Tetra electrode assembly (Bio-rad) and fitted into the buffer tank. Subsequently, 1X running buffer was prepared from the 10X stock solution (250 mM Tris-base, 1.92 M Glycine, 1% SDS). 15-well combs were carefully removed, and wells were thoroughly cleaned with 1X running buffer for five times. Then, the electrode assembly chamber was filled with 1X running buffer, and gels were allowed to be equilibrated. Meanwhile, samples were heated at 70 ℃ for 10 minutes. During this incubation, non-sample loaded wells were filled with matching volumes of 1X sample preparation buffer supplemented with β-mercaptoethanol. In addition, 5 µL of molecular weight markers were loaded to each gel. After incubation, samples were centrifuged for 30 seconds at 12,000 x *g* using table-top microcentrifuge and loaded using a P20 micropipette attached to gel-loading tips.

Gels were initially resolved at constant voltage (80V) until clear separation of protein standards could be observed. Afterwards, gels were resolved at 100V until the dye front reached the end of the gel. Throughout the gel resolution, buffer tank was left on top of magnetic stir plate

to distribute ions evenly. Upon completion of resolution, glass plates were carefully lifted using a gel releaser. Stacking layer was cut using a gel releaser and discarded, whereas resolving layer was transferred to the plastic container filled with 15 mL of cathode buffer (25 mM Tris, 40 mM Glycine, pH 9.4). Before transfer, gels were washed for 15 minutes for equilibration and removal of excess SDS.

Transfer

For semi-dry protein transfer, discontinuous transfer with anode buffer I (300 mM Tris, pH 10.4), II (25 mM Tris, pH 10.4), and cathode buffer (25 mM Tris, 40 mM Glycine, pH 9.4) were used (124). PVDF membranes were pre-cut, matching the size of the mini gel (5 cm × 8.3 cm) and were activated in 100% methanol for 1 minute and briefly rinsed with distilled water. Subsequently, membranes were further equilibrated by soaking them in anode buffer II. After 15 minutes of equilibration, transfer sandwich setup was prepared by laying two filter papers soaked in anode buffer I, one filter paper and PVDF membrane soaked in anode buffer II. Subsequently, gels were carefully laid on top. Lastly, three filter papers soaked in cathode buffer were laid. Upon laying each layer, a plastic roller was used to gently, yet thoroughly roll-off air bubbles trapped underneath. Gels were transferred for 45 minutes under constant current (0.1A).

Antibody incubation and detection for chemiluminescence

For antibody incubation, Western blot protocol proposed by Cell Signaling Technology® (125) was adopted. After 45 minutes, a successful transfer was monitored via Ponceau-S staining. Subsequently, 15 mL of 5% skim milk in TBS-T was used for blocking of nonspecific sites for 1 hour at room temperature with gentle agitation. Afterwards, 15 mL of TBS-T was used for three times membrane washing for 5 minutes. For the analysis of phosphorylated Smad3, technical modifications, suggested initially by Sharma, *et al.* in 2002, were made (126). More specifically, TBS-T supplemented with 50 mM sodium fluoride and 5 mM sodium orthovanadate was used throughout the experiment to prevent non-desirable dephosphorylation from contaminating phosphatase activities, which was associated with up to 6-fold increase in the signal (126). Primary antibodies were prepared at 1:1,000 dilutions (v/v) for p-Smad3, Smad3, GULP, Beta-tubulin, and GAPDH in 5% BSA in TBS-T. Membranes were incubated with primary antibodies overnight at

4 ℃ with gentle agitation. Next day, primary antibodies were recovered and then membranes were washed for three times for 5 minutes using TBS-T as described above. Secondary antibodies were diluted at 1:10,000 (v/v) in 5% skimmed-milk in TBS-T and membranes were incubated for 1 hour at room temperature with gentle shaking. After 1 hour, membranes were washed three times for 5 minutes with TBS-T and developed for chemiluminescence.

2.11 Membrane stripping

An original method described by Yeung *et al.* (2009) was utilised to strip antibodies bound to PVDF membranes effectively (127). Following initial detection for phospho-Smad3 and GULP, each PVDF membrane was briefly rinsed with distilled water. Subsequently, 10 mL of guanidine hydrochloride stripping solution (6 M guanidine HCl; 0.2% NP40; 20 mM Tris-HCl) was added to each membrane in a plastic container. 70 µL of β-mercaptoethanol (0.1 M final concentration) was added to guanidine hydrochloride stripping solution just before 5 minute incubation of membranes with gentle shaking at room temperature. After 5 minutes, the solutions were discarded and the membranes were further stripped for 5 minutes with a fresh stripping solution. Then, the membranes were washed with 1X TBS-N (TBS-NP40) 4 times for 3 minutes with gentle shaking. After the last wash, the membranes were blocked using 5% skimmed milk in TBS-T for 1 hour and incubated overnight with Smad3, GAPDH, or β-tubulin primary antibodies.

3. Results

Early evidence demonstrated the importance of TGF-β signaling in normal ovary development and function. In association with TGF-β signaling's importance, aberrations in this signaling and its components was observed in ovarian cancer, including in regulatory Smads (87,90). More importantly, although GULP has been shown to regulate TGF-β responses in CHO cells (100), due to its controversial origins and resemblance to fibroblasts (116,118), it is difficult to understand how differences in the expression of GULP in humans affect TGF-β responses *in vivo*.

Despite several drawbacks, GULP expression was universally and significantly downregulated among different subtypes of ovarian cancers (101), which necessitated deeper understanding of the functional consequences in humans caused by differences in GULP level. Thus, to address previous limitations, the correlation between GULP expression and the intensity of Smad3 phosphorylation (which was used to infer the activity of canonical TGF-β signaling) was first assessed in ovarian adenocarcinoma cells, including HEY, SKOV3 (Fig. 1A), and PEO-14 (Fig. 1B). Cells were treated with TGF-β1 (0.2 nM) for a varying duration, with significant Smad3 phosphorylation seen after as little as 30 minutes. For Western blot analyses, fifteen μg of each lysate was used, and GAPDH was used as a loading control.

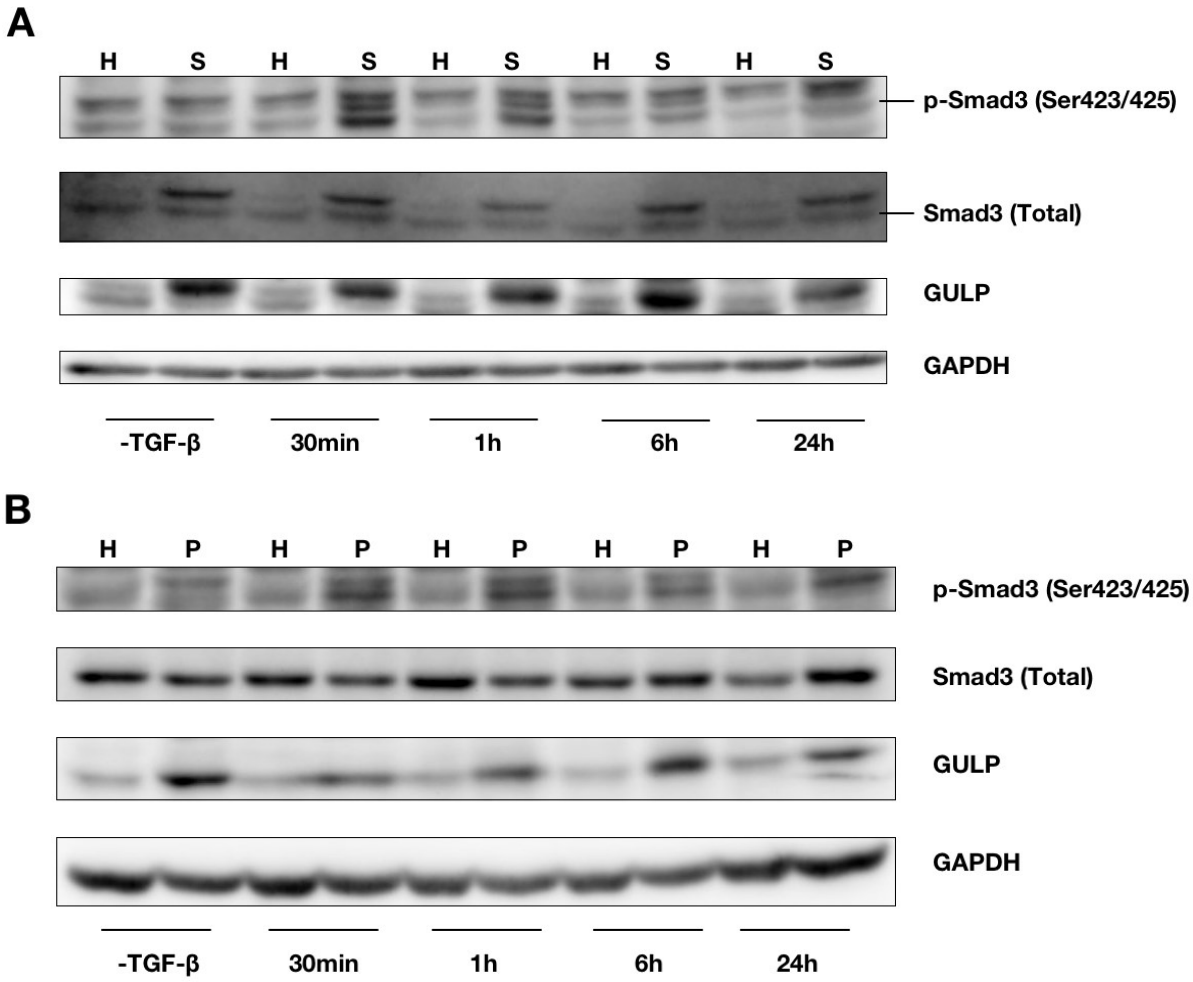

Figure 1. Association between high level of GULP and increased Smad3 phosphorylation

A. *Western blot analysis of Smad3 phosphorylation in HEY and SKOV3 ovarian adenocarcinoma cells.* GULP was expressed in high levels in SKOV3, whereas GULP was weakly expressed in HEY cells. Moreover, Smad3 phosphorylation was not significantly induced in HEY cells. (*H: HEY, S: SKOV3*)

B. *Western blot analysis of Smad3 phosphorylation in HEY and PEO-14 cells.* Significant Smad3 phosphorylation was induced only in PEO-14 cells, which expressed GULP at high levels. Fifteen μg of each lysate was used. (*H: HEY, P: PEO-14*)

According to the Western blot analysis, GULP was weakly expressed in HEY ovarian cancer cells, whereas its expression was strong in SKOV3 (Fig. 1A) and PEO-14 cells (Fig. 1B) for varying durations of TGF-β1 treatment. Based on these findings, HEY cells were used in subsequent phases of this study to represent ovarian cancers with low levels of GULP. Alternatively, SKOV3 and PEO-14 cells were representative of ovarian cancers with high levels of GULP. Interestingly, while GULP expression remained relatively stable for up to 24 hours of TGF-β treatment, the intensity of p-Smad3 rapidly increased after 30 minutes of incubation with TGF-β1. Although its intensity continued to decrease over long durations, p-Smad3's intensity was noticeably higher in SKOV3 (Fig. 1A) and PEO-14 ovarian cancer cells (Fig. 1B) compared to non-treated cells even at 24 hours of treatment. However, in HEY cells with low levels of GULP, Smad3 phosphorylation barely increased, and its intensity remained relatively unchanged compared to non-treated cells (Fig. 1A, B), indicating HEY cells were unresponsive to TGF-β1.

Effect of differences in GULP expression on TGF-β-associated growth inhibition

The Western blot analysis demonstrated the positive correlation between GULP expression and the intensity and longevity of Smad3 phosphorylation. However, increased TGF-β signaling responses may not only be tumour-suppressive but also tumour-promotive and oncogenic (80,82). Therefore, to address the functional consequences of increased Smad3-dependent TGF-β signaling in human cells, a growth assay was performed by monitoring changes in cell number for up to 72 hours of treating or not treating cells with TGF-β1 (0.2 nM) to assess changes in cellular proliferation or cell death (Fig. 2). Cells were seeded at 70,000/mL in triplicate. After overnight incubation at 37 °C, cells were serum-starved for 24 hours to deprive them of the effects of residual TGF-β present in FBS. Cells were counted after starvation (T_0), which was used for the normalization, and then incubated with or without TGF-β1 (0.2 nM) in a growth medium supplemented with 1% serum for 48 or 72 hours.

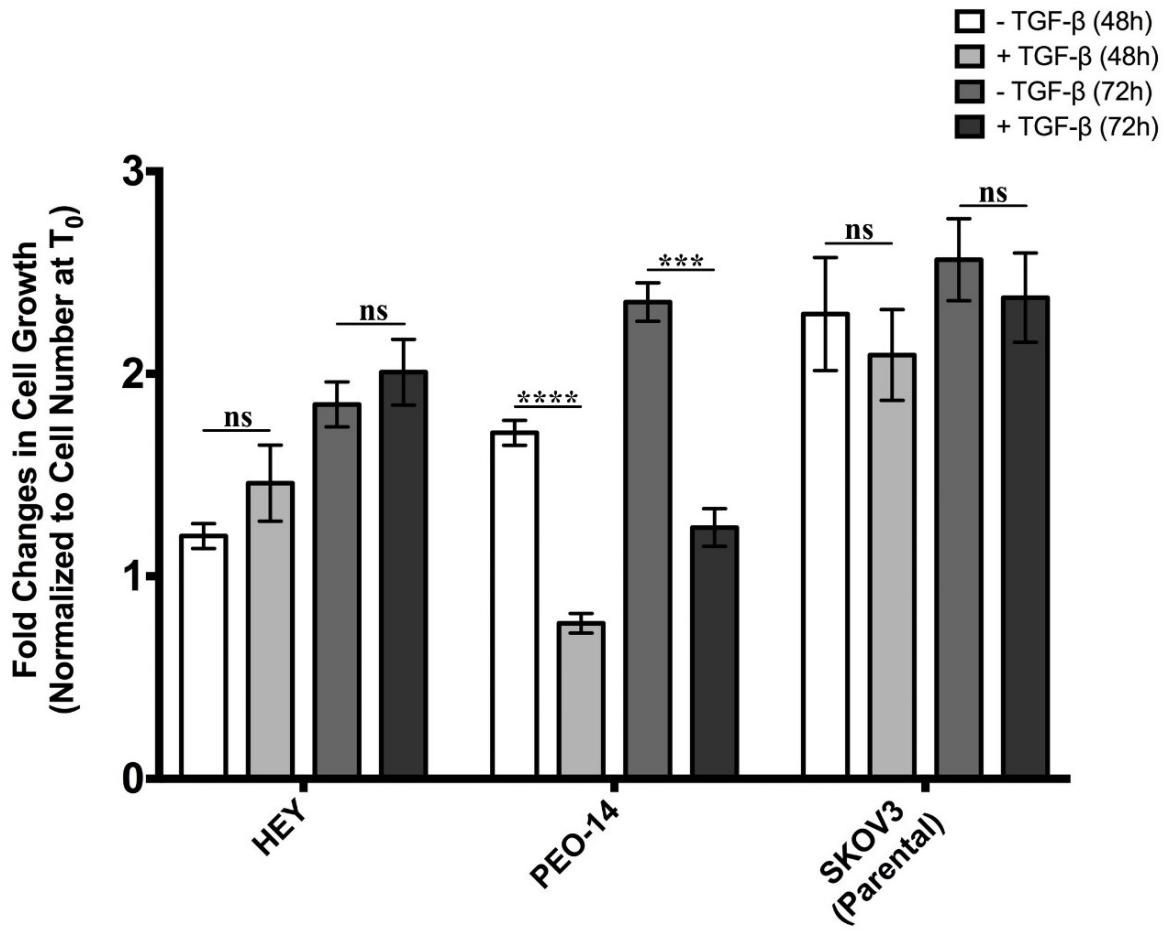

Figure 2. Association between difference in p-Smad3 levels and functional consequences.

Fold changes in cell growth were calculated as: (Average Cell Number at T_{48} or T_{72})/(Average Cell Number at T_0). Despite TGF-β, HEY cells showed increased proliferation at 48 and 72 hours (*t*-test 95% confidence, p = 0.0843, 0.2337). By contrast, PEO-14 and SKOV3 cells, with high levels of GULP were growth inhibited. However, PEO-14 cells were significantly growth inhibited, by nearly 50% (*t*-test 95% confidence, p < 0.0001, p = 0.0001), whereas SKOV3 cells only showed slightly decreased proliferation (*t*-test 95% confidence, p = 0.3844, 0.3386).

Based on the growth assay, for which cell numbers were counted for up to 72 hours with or without the treatment of TGF-β1 (0.2 nM), sensitivity towards TGF-β-associated growth inhibition differed among ovarian cancer cells. HEY cells with low levels of GULP lacking rapid induction of Smad3 phosphorylation (Fig. 1) were not only resistant to growth inhibition but also showed increased proliferation at 48 and 72 hours (Fig. 2). By contrast, PEO-14 ovarian adenocarcinoma cells were significantly growth-inhibited by TGF-β1 at 48 and 72 hours (Fig. 2). Although their growth was significantly impacted, TGF-β1-treated PEO-14 cells still proliferated at 72 hours (Fig. 2). Interestingly, SKOV3 cells with similarly high levels of GULP (Fig. 1) were associated with weak growth inhibition in response to TGF-β1 (Fig. 2). Nevertheless, similar to PEO-14 cells, SKOV3 cells continued to proliferate in the presence of TGF-β1 (Fig. 2). Despite differences among cell lines, growth inhibition was associated with high levels of GULP, indicative of its tumour-suppressive role.

Lack of effect of TGF-ß on the proliferation of ovarian cancer cells with low levels of GULP

Although assessing changes in cell number could provide information about different cell lines' responsiveness to TGF-β's tumour-suppressive roles, including the regulation of cell proliferation and the promotion of programmed cell death (apoptosis), it was difficult to determine whether changes in cell number were due to changes in cellular proliferation or to viability. MTT assay was used to better understand how TGF-β affected each ovarian cancer cell line (Fig. 3 A-C), with MTT reagents only reduced by active mitochondria in living and proliferating cells, forming formazan crystals. Upon solubilization of formazan crystals, purple colouration developed and actively proliferated cells were associated with higher absorbance (darker shades of purple).

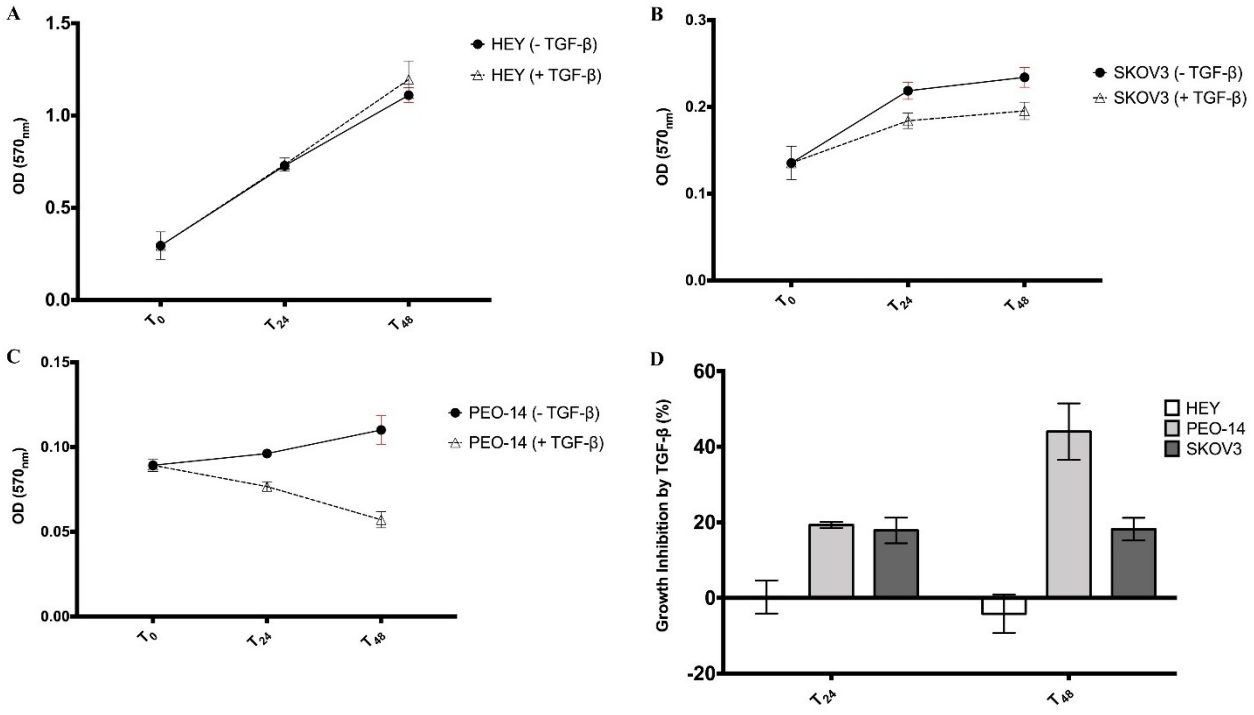

Figure 3. High levels of GULP is associated with increased growth inhibition.

A-C. *Average absorbance.* Average absorbance measured at 570 nm upon solubilization of formazan crystals after 2 hours of incubation at 37 ℃ with 25 µL of MTT solution (5mg/mL) in HEY (Panel A), SKOV3 (Panel B), and PEO-14 cells (Panel C). MTT assay was performed in replicates of six for each condition. Solid lines indicate the average absorbance of cells without TGF-β1, and dashed lines indicate absorbance of cells treated with TGF-β1.

D. *Comparison of average percentage of growth inhibition by TGF-β.* HEY cells were not only unresponsive but continued to proliferate under the presence of TGF-β1 (0.2 nM). SKOV3 cells were moderately growth inhibited (~20%) at 24 and 48 hours, whereas PEO-14 cells were significantly growth inhibited (> 40%) upon 48 hours of treatment.

In agreement with the growth assay (Fig. 2), the absorbance of TGF-β-treated HEY cells continued to increase at 24 and 48 hours of treatment (Panel A). Similarly, absorbance of TGF-β-treated SKOV3 and PEO-14 cells was lower than non-treated control cells (Panel B, C), indicating decreased cell proliferation. In addition, despite high levels of GULP, the absorbance of TGF-β-treated SKOV3 cells continued to increase for up to 48 hours, whereas absorbance continued to decrease in PEO-14 cells. In alignment with the growth assay (Fig. 2), SKOV3 cells were only moderately growth-inhibited by TGF-β (~20%), whereas PEO-14 cells were significantly growth-inhibited at 48 hours (>40%) (Panel D). Nevertheless, in further support of GULP's role as a tumour-suppressor, HEY cells with low levels of GULP were not only unresponsive towards TGF-β-mediated growth inhibition but also grew uncontrollably with long-term exposure to TGF-β1 (48 hours).

GULP's potential to enhance cancer progression via the induction of migration

Growth and MTT assays were used to assess changes in sensitivity towards TGF-β's tumour-suppressive effects in different ovarian cancer cells. These assays found reduced levels of GULP were negatively correlated with cell proliferation, which would benefit cancer progression. Moreover, while SKOV3 cells with high levels of GULP were moderately growth-inhibited by TGF-β1 (~20%), their sensitivity was rather weak and cells were capable of growth, albeit at a decreased rate.

For cancer metastasis, which accounts for the majority of cancer-associated deaths (1), increased cell migration conferred by the induction of epithelial to mesenchymal transition is critical (82). More importantly, EMT is significantly associated with peritoneal metastasis, further exacerbating ovarian cancer progression (128). Furthermore, ovarian cancers that overexpress EMT-inducing transcription factors are associated with poor prognosis (129). However, for this event to occur, TGF-β responses are necessary; this led the study to further consider whether reduced levels of GULP during early stages of carcinogenesis might hamper effective cancer progression at an advanced stage. Furthermore, despite high levels of GULP, SKOV3 cells indicated a build-up of resistance, or 'molecular switching', of TGF-β responses toward its oncogenic roles. To address whether high levels of GULP could accelerate cancer progression at late stages, a scratch assay was performed to assess changes in cell migration (Fig. 4A-C).

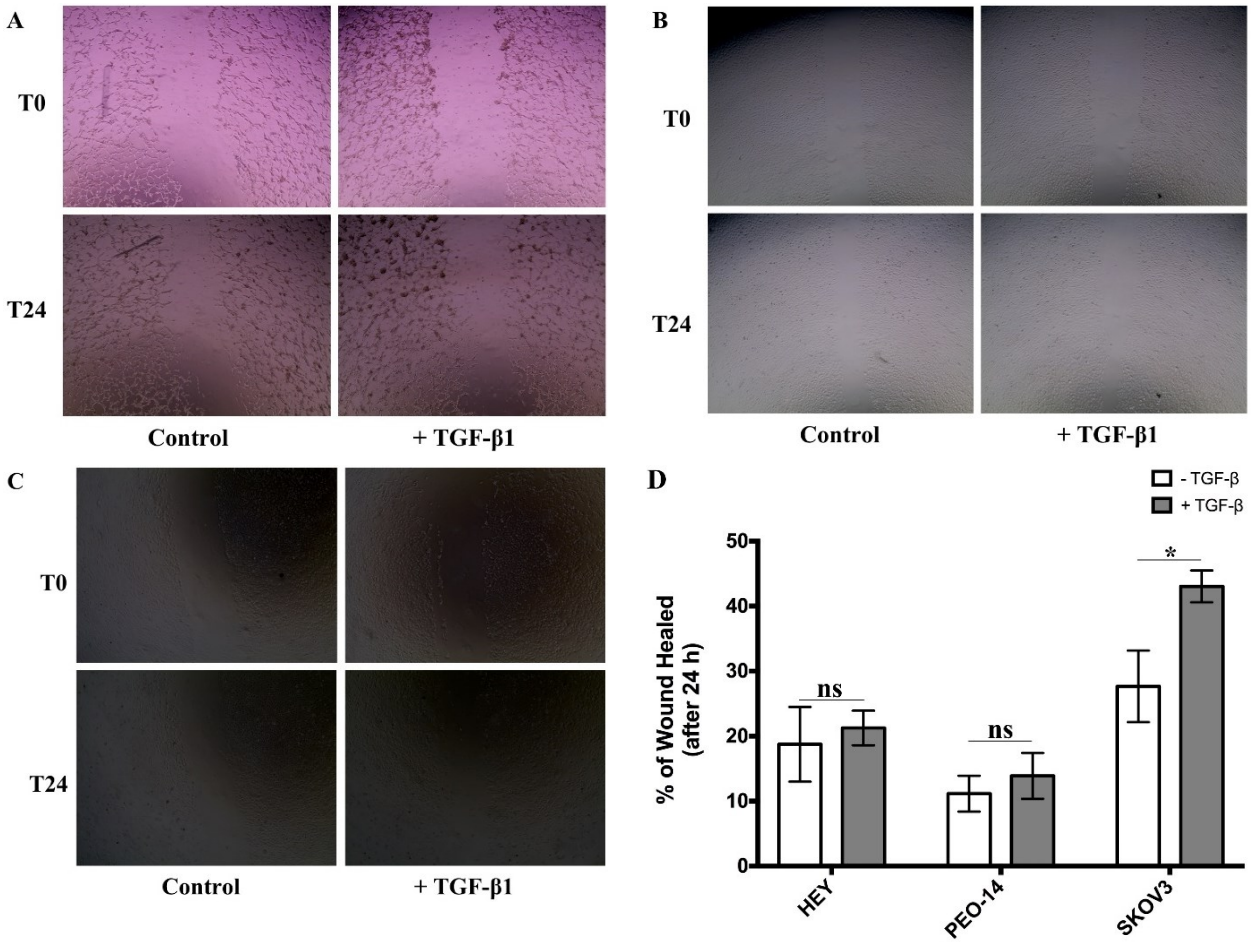

(Figure legend continues on the next page.)

Figure 4. Association between high levels of GULP and increased cell migration

A. *Representative images acquired immediately after 'scratching' of the monolayer or 24 hours of treatment with or without TGF-β1 (0.2 nM), performed in triplicate.* Each well was washed carefully three times using a serum-free medium after scratching to remove cell debris. HEY cells were moderately migratory after 24 hours, but there was no significant induction of migration in response to TGF-β1 (two-tailed *t*-test 95% confidence, p = 0.4583).

B. *Representative images of scratched SKOV3 cell monolayer upon 'scratching' or after 24 hours of treatment with or without TGF-β1 (0.2 nM), performed in triplicate.* A noticeable degree of migration was seen in the control (left panels), which was enhanced by TGF-β (two-tailed *t*-test 95% confidence, p = 0.0116).

C. *Representative images of scratched PEO-14 cell monolayer upon 'scratching' or after 24 hours of treatment with or without TGF-β1 (0.2 nM), performed in triplicate.* There was no noticeable degree of migration, which was not affected by TGF-β (two-tailed *t*-test 95% confidence, $p = 0.3511$).

D. *Comparison of average % of wound healed, indicative of cell migration.* HEY and PEO-14 cells were only moderately migratory regardless of TGF-β1 (~10-20%), whereas SKOV3 cells were noticeably migratory (~30%), which was further induced by TGF-β1 (> 40%).

In support of GULP's essential role in TGF-β signaling (101), migration of SKOV3 ovarian adenocarcinoma cells significantly increased in response to TGF-β. By contrast, HEY cells with low levels of GULP, which lacked short-term or long-term induction of Smad3 phosphorylation in response to TGF-β (Fig. 1), were unresponsive toward TGF-β and were only weakly migratory (Panel D). Although differences in wound-healing seemed to correlate with the expression level of GULP, PEO-14 cells were mostly unresponsive towards TGF-β-mediated induction of cell migration despite high levels of GULP, which resulted in ineffective wound closure (wound-healing).

GULP's positive correlation with Smad3 phosphorylation in normal OSE cells

While valuable information was obtained from established ovarian cancer cells, it was unclear whether each cell line was representative of human physiology. More importantly, various currently used ovarian cancer cell lines have ambiguous classification and origins (115); however, these classifications were crucial for this study to assess changes in GULP's expression and its functional consequences, which may be used in therapeutic interventions or as a prognostic factor allowing for earlier diagnosis. Thus, to address current limitations, primary OSE cells isolated from human ovary tissue samples (normal and cancerous) were established and cultured for experiments.

Despite previous observations in ovarian cancer cell lines, their limitations in the resemblance of human physiology made it unclear whether GULP expression is affected in primary human ovarian cancer. Thus, whether GULP expression correlates with Smad3 phosphorylation in primary OSE cells was addressed first in this study (Fig. 5). Primary, normal OSE cells were cultured to 70~80% confluence before incubation or not with TGF-β1 (0.2 nM) for durations ranging from 30 minutes to 24 hours. Ten μg of each lysate was separated for the Western blot analysis.

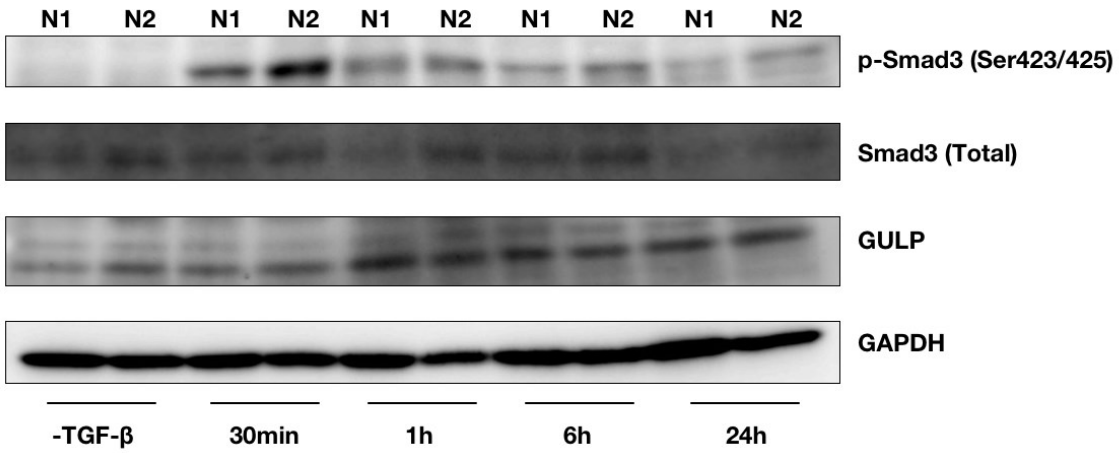

Figure 5. GULP's high level of expression in normal ovarian surface epithelium

Comparison of Smad3 phosphorylation between normal OSE cells. Despite similarities in GULP's level (high) and induction of Smad3 phosphorylation, the intensity of Smad3 phosphorylation differed noticeably in response to TGF-β between the short term (30 minutes) and long term (six hours, 24 hours). (*N1: Normal OSE sample #1, N2: Normal OSE sample #2*)

Supporting the literature (101), GULP was highly expressed among normal primary OSE cells and its level remained relatively stable regardless of the duration of TGF-β treatment. More importantly, in further agreement with the literature (74,86,87), high levels of Smad3 activity inferred from its phosphorylation could be seen. In fact, similar to SKOV3 and PEO-14 cells with high levels of GULP, rapid and significant induction of Smad3 phosphorylation could be seen. But despite similarities in GULP levels among pathologically classified normal OSE cells, the intensity of p-Smad3 was higher in normal sample 2 (N2) upon short-term signaling (30 minutes) and long-term signaling (six or 24 hours). This further suggests the importance of GULP in the ovary surface epithelium and its role as a tumour-suppressor, whose level is decreased among different subtypes of EOCs.

GULP expression differentially affected in cancerous OSE cells

This study found that the correlation between GULP level and both the intensity and longevity of Smad3 phosphorylation was functionally associated with TGF- signaling's tumour-suppressive aspects, which orchestrate normal development and maturation of the ovary (87). Therefore, it was hypothesized that GULP expression would be reduced in primary cancerous OSE cells, which would be associated with decreased Smad3 phosphorylation, allowing uncontrolled cellular proliferation for tumourigenesis. However, literature indicated regulatory Smads association with cancer progression. For instance, high levels of Smad2 activity were associated with cancer cell proliferation (87), and knockdown of Smad3 was associated with the decreased invasive potential (i.e., reduced production of MMP2/9) of ovarian cancer cells (90). To address this contradiction, cancerous primary OSE cells were cultured and first assessed for changes in GULP's expression and the intensity of phosphorylated Smad3 (Fig. 6). Primary OSE cells were grown to 70~80% confluence and treated with or without TGF-β1 (0.2 nM) for 30 minutes before lysis. GULP was expressed at high levels in normal OSE samples (N1, N2), which was correlated with significant induction of Smad3 phosphorylation within 30 minutes. For the Western blot analysis, Ten μg of each lysate was loaded, and GAPDH was used as a loading control.

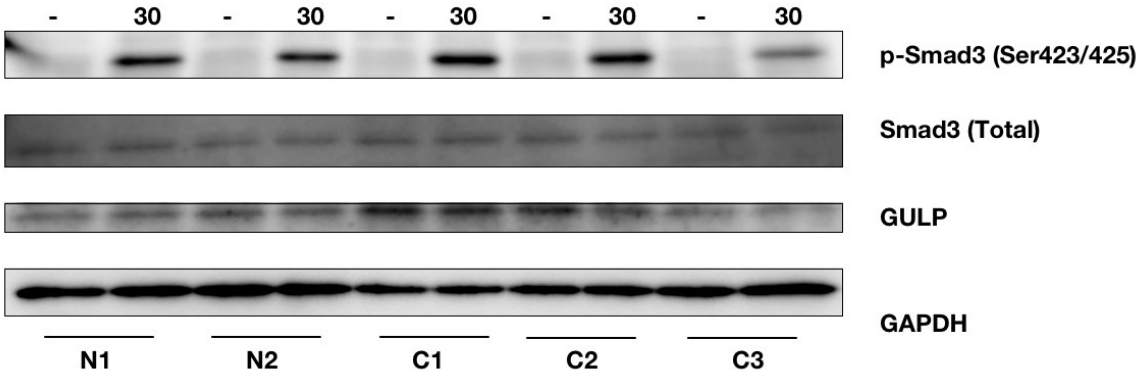

Figure 6. Association between Lower levels of GULP and reduced Smad3 phosphorylation.

Western blot analysis of Smad3 phosphorylation in normal and cancerous primary OSE cells. GULP level differed among cancerous OSE cells, with high levels of GULP associated with significant Smad3 phosphorylation (C1, C2). By contrast, when GULP expression was low, there was a noticeable reduction in Smad3 phosphorylation within 30 minutes (C3). *(-: untreated; 30: treated with 0.2 nM of TGF-β1; N: Normal OSE; C: Cancerous OSE)*

As with ovarian cancer cell lines or normal OSE cells, while differences in GULP level were associated with the longevity of Smad3 phosphorylation, the consequences were strongest during the induction of Smad3 phosphorylation as a short-term response or the activation of TGF-β signaling. Based on this, normal or cancerous OSE cells were treated or not with TGF-β1 (0.2 nM) for 30 minutes, with the levels of GULP and phosphorylated Smad3 compared via Western blot. Unexpectedly, while GULP was expressed at high levels in normal OSE cells, it was also strongly expressed in cancerous OSE cells (C1 and C2). Moreover, as with normal OSE cells, high levels of GULP in cancerous OSE cells were associated with increased and prolonged Smad3 phosphorylation in response to TGF-β. By contrast, another sample of cancerous OSE cells (C3) demonstrated decreased GULP expression, which was associated with significantly decreased levels of phosphorylated Smad3 similar to that observed in HEY cells (Fig. 1). Despite differences among cancerous samples, a correlation was conserved between GULP level and Smad3 phosphorylation in primary OSE cells.

Growth inhibition by TGF-β of primary OSE cells with high levels of GULP

Since increased levels of regulatory Smads (Smad2/3) have been associated with cancer progression (80,82), the high levels of GULP associated with significant increases in Smad3 phosphorylation in cancerous OSE cells led to the question of whether this increase was associated with enhanced cancer progression. More specifically, GULP's expression differed among cancerous primary OSE cells and its decrease was associated with a significant decline in Smad3 phosphorylation (Fig. 6), in support of the tumour-suppressive role of TGF-β signaling; thus, an MTT assay was performed to assess whether, compared to normal OSE cells (Fig. 7 A-B), cancerous OSE cells with high levels of GULP were sensitive to TGF-β-mediated growth inhibition (Fig. 7C-E).

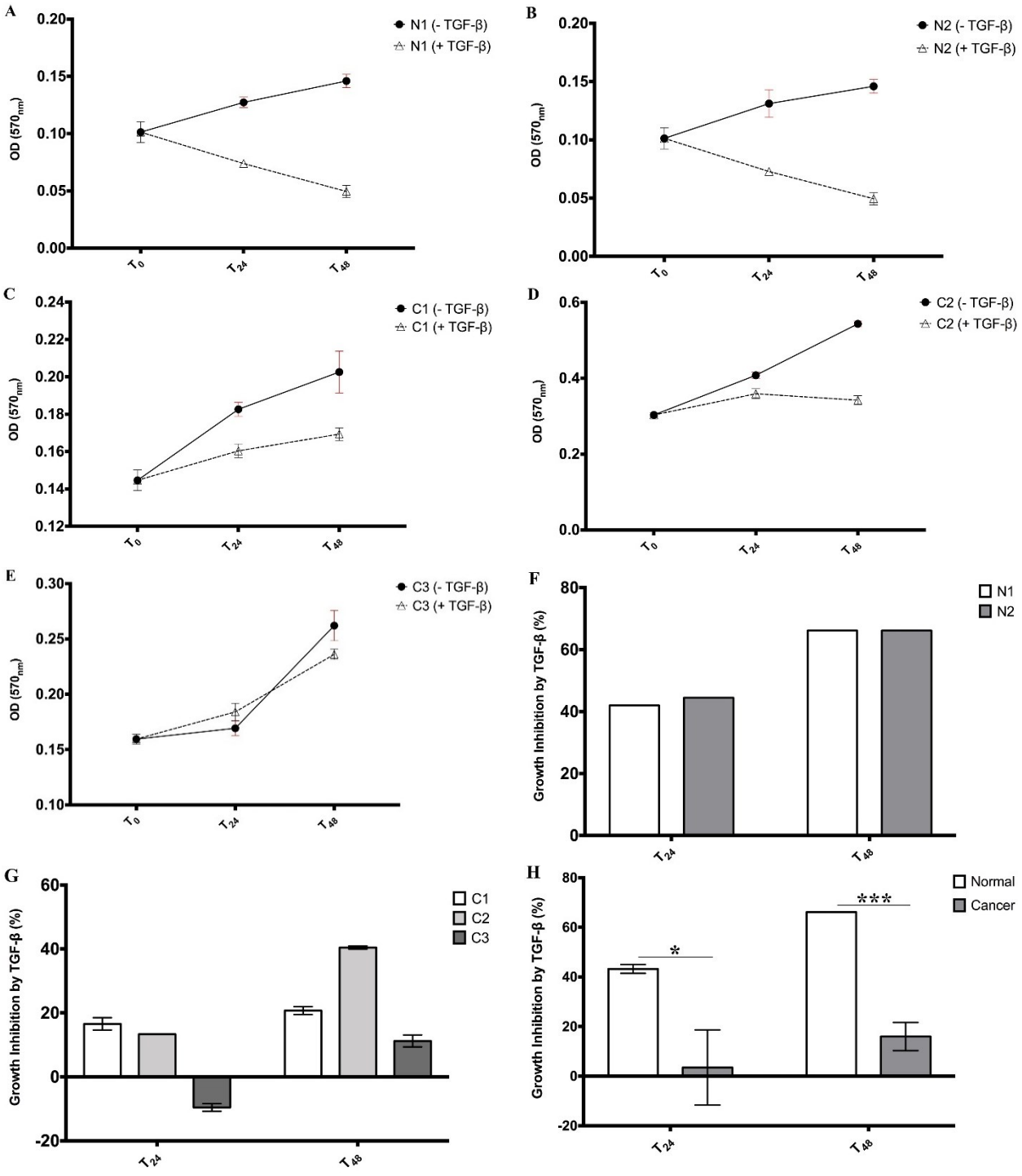

(Figure legend is on the next page.)

Figure 7. TGF-β mediated growth inhibition differentially affected in ovarian cancer

A-E. *Average absorbance at 570 nm following MTT assay in normal (Panel A, B) and cancerous (Panel C-E) primary OSE cells treated with or without TGF-β1 for 24 or 48 hours.* Both types of OSE cells were severely growth-inhibited by TGF-β and further associated with continued decreases in absorbance. Contrastingly, sensitivity towards TGF-β-mediated growth inhibition differed among cancerous OSE cells. TGF-β treatment was associated with decreased absorbance in cancerous samples 1 and 2 (Panels C and D), whereas absorbance was higher than non-treated cells at 24 hours for TGF-β-treated cancerous sample 3 (Panel E).

F-G. *Average percentage of growth inhibition by TGF-β.* The percentage of growth inhibition at 24 or 48 hours was calculated as: [1-((Average absorbance of control) - (Average absorbance upon TGF-β treatment)) *100]. Following significant and continuous decreases in absorbance, normal OSE cells were noticeably growth-inhibited by TGF-β (~40-60%) (Panel F). By contrast, while cancerous sample 2 was significantly growth inhibited at 48 hours (>40%), cancerous OSE cells were only moderately growth-inhibited or unresponsive to TGF-β (Panel G).

H. *Comparison of growth inhibition by TGF-β between normal and cancerous OSE cells.* The percentage of growth inhibition shown in panels F and G were averaged to represent the average degree of growth inhibition in normal and cancerous OSE cells. Both at 24 and 48 hours, cancerous OSE cells mainly were not growth-inhibited compared to normal, healthy OSE cells (two-tailed *t*-test, $p = 0.0251, 0.0003$).

According to the MTT assay, in agreement with the findings in ovarian cancer cell lines, high levels of GULP were associated with responsiveness to TGF-β-associated growth inhibition. More specifically, similar to PEO-14 cells, absorbance in normal primary OSE cells continued to decrease in response to TGF-β1 for up to 48 hours (Panels A, B). By contrast, cancerous OSE cells showed variable sensitivity towards TGF-β, and cancerous OSE cells with high levels of GULP – which was associated with rapid increases in Smad3 phosphorylation – were moderately growth-inhibited by TGF-β (Panels C, D). Similar to SKOV3 cells and in comparison to normal OSE cells, the absorbance of TGF-β-treated cancerous OSE cells continued to increase for up to 48 hours, although absorbance was lower than non-treated cells. Additionally, cancerous OSE cells with low levels of GULP showed significantly reduced levels of p-Smad3 at 30 minutes of TGF-β treatment and were mostly resistant against growth inhibition (Panel E). Finally, concerning the heterogeneric nature of cancer, which may influence the aggressiveness, individual results were combined and averaged. As shown, compared to normal OSE cells – which were universally and significantly growth-inhibited (>40-60%) – cancerous OSE cells were only weakly growth-inhibited by TGF-β despite differences in responsiveness (Panel H).

Knockout of GULP in SKOV3 ovarian adenocarcinoma cells

GULP's expression was positively correlated with the intensity and longevity of Smad3 phosphorylation in ovarian cancer cell lines and primary OSE cells. Although neither GULP expression nor the level of p-Smad3 were affected in several cancerous OSE cultures (Fig. 6), low or decreased GULP level always correlated with significant decrease in p-Smad3; this was most strongly pronounced in HEY ovarian adenocarcinoma cells. More importantly, high levels of GULP were associated with increased responsiveness towards the tumour-suppressive effects of TGF-β, including growth inhibition. GULP was largely unaffected – but remained high – in SKOV3 and PEO-14 cells and in cancerous primary OSE cells, with one exception (C3). In addition, while cancerous primary OSE cells with high levels of GULP were somewhat growth-inhibited (~20%), the degree of growth inhibition was significantly lower than in normal cells (Fig. 7H). However, considering GULP's primary role as a 'tumour-suppressor', it was unclear whether GULP expression would be downregulated with advances in ovarian cancer. Therefore, GULP

expression was knocked out using the CRISPR-Cas9 system in SKOV3 cells, which were originally weakly growth-inhibited by TGF-β yet significantly migratory in response to TGF-β (Fig. 4D). In a closely related issue, although GULP was reduced in several ovarian cancer cell lines (including HEY cells), knockout was further rationalized as a way to best recapitulate the physiological consequences of the decrease in GULP or its loss of function via secondary mutations.

Although GULP, which primarily regulated 'tumour-suppressive' TGF-β signaling, was knocked out, how significant decreases in GULP's expression affect Smad3 phosphorylation and Smad3-dependent TGF-β responses were unclear. As a matter of fact, changes in intracellular signaling might lead to the 'molecular switching' of TGF-β responses in favour of its tumour-promoting roles. Thus, SKOV3 cells targeted with 'scrambled' or the guide RNA specifically against GULP were lysed, and changes in GULP's levels and p-Smad3 were first assessed by Western blot (Fig. 8). 70-80% confluent cells were treated or not with TGF-β1 (0.2 nM) for variable durations (30 minutes or one, six, or 24 hours). Fifteen µg of each lysate was resolved in 4-15% gradient gels and GAPDH was used as loading control.

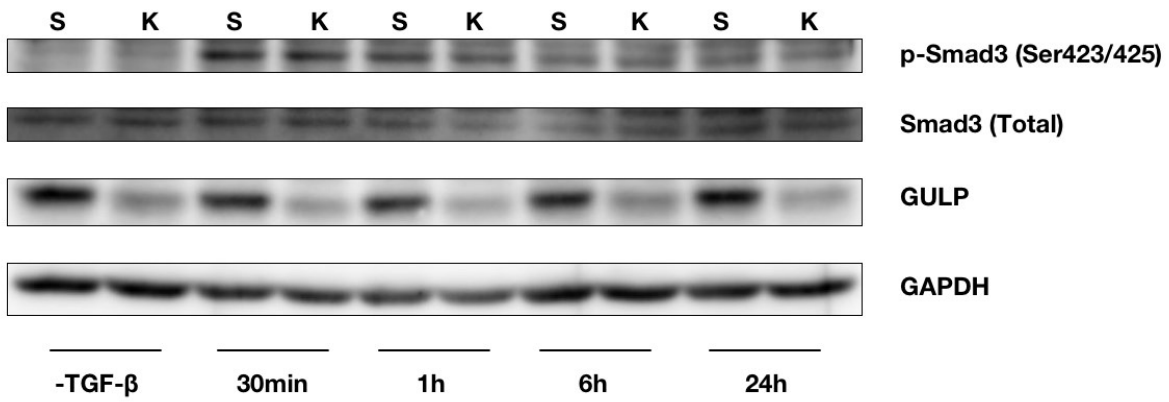

Figure 8. Association between decrease in GULP level and reduced Smad3 phosphorylation

Western blot analysis of Smad3 phosphorylation in SKOV3 (scrambled) or SKOV3 (GULP-KO). Although targeted knockout of GULP expression resulted in significant decreases in GULP levels, its effect on Smad3 phosphorylation was rather mild. Smad3 phosphorylation was reduced following short-term treatment (30 minutes or one hour) or long-term treatment (24 hours) with TGF-β1. *(S: SKOV3 scrambled, K: SKOV3 GULP-knockout)*

Surprisingly, while GULP level noticeably decreased in SKOV3 GULP-KO cells, levels of p-Smad3 were only moderately affected. More specifically, although decreases in Smad3's phosphorylation in response to TGF-β could be seen in short- and long-term treatment with TGF-β (i.e. one and 24 hours), rapid and significant phosphorylation of Smad3 in response to TGF-β could be observed within 30 minutes despite reduced levels of GULP. More importantly, despite the significant reduction in GULP's expression, the longevity of Smad3 phosphorylation in SKOV3 GULP-KO cells was nearly identical to SKOV3 cells targeted with the scrambled guide RNA.

Uncontrollable proliferation of GULP-KO ovarian cancer cells

Despite the lower impact, decreased expression of GULP in SKOV3 cells resulted in a moderate reduction in both short- and long-term Smad3 phosphorylation, which might be associated with functional consequences. More importantly, despite its relatively weak impact, the decreased level of p-Smad3 might be associated with increased resistance against growth inhibition, as seen in HEY cells. A growth assay was performed to address how reduced levels of GULP in SKOV3 cells (SKOV3 GULP-KO) initially with high levels of GULP affect the tumour-suppressive roles of TGF-β responses (Fig. 9). Scrambled and GULP-KO SKOV3 cells were seeded at 70,000 cells/mL in triplicate. Cells were serum-starved for 24 hours to deprive them of residual TGF-β present in FBS and synchronise the cell cycle. Cell number was counted after 24 hours of serum starvation (T_0), which was used for the normalization. Cells were then further incubated with or without TGF-β1 (0.2 nM) for 48 and 72 hours in a growth medium with 1% serum and counted.

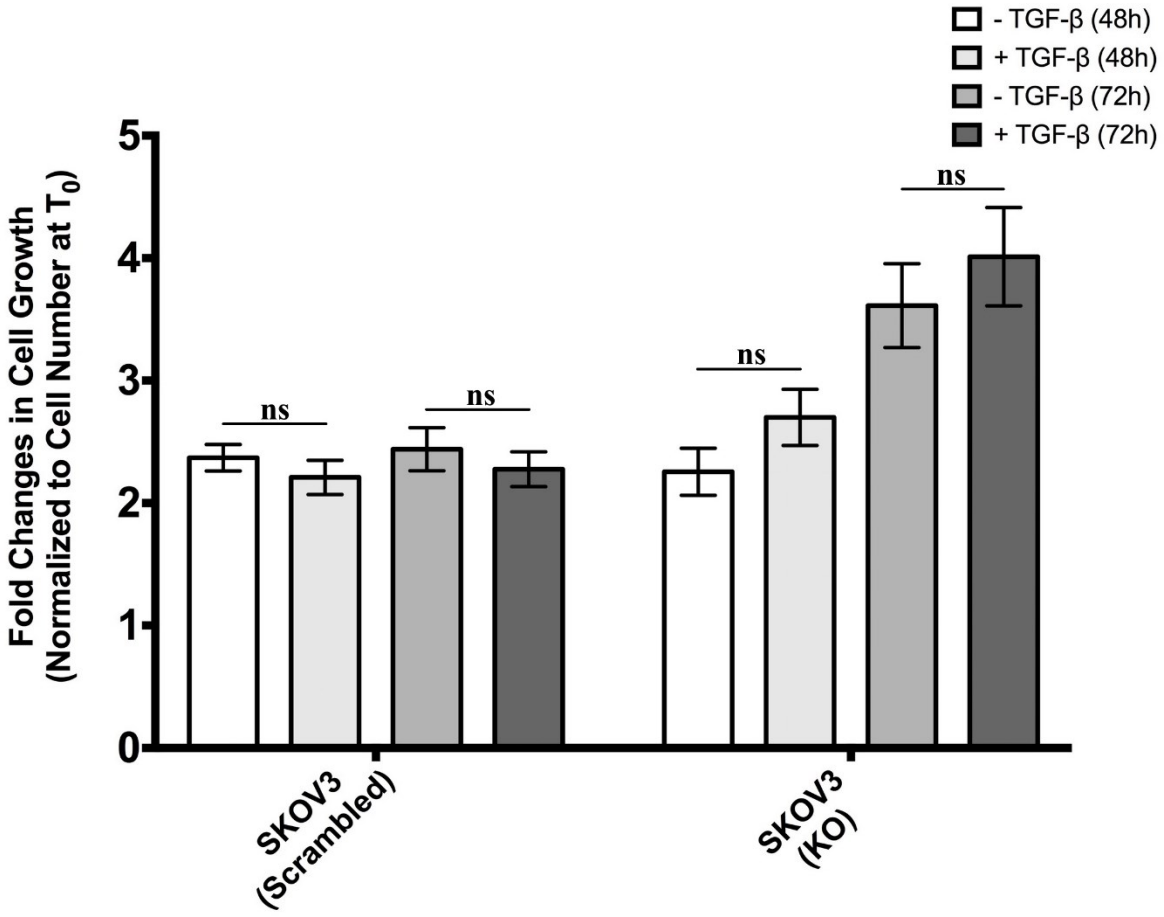

Figure 9. SKOV3 GULP-KO cells no longer growth inhibited by TGF-β

Comparison of average fold changes in cell growth. Fold changes in cell growth were calculated as: (Average Cell Number at T_{48} or T_{72})/(Average Cell Number at T_0). Although SKOV3 (scrambled) was moderately growth-inhibited at 48 and 72 hours in response to TGF-β1, there was not statistical significance (*t*-test 95% confidence, p = 0.1907, 0.2792). By contrast, decreased levels of GULP were associated with increased cell growth (*t*-test 95% confidence, p = 0.0615, 0.2596).

In strong contrast to the weak impact on Smad3 phosphorylation, knockout of GULP expression in SKOV3 cells resulted in a loss of responsiveness to growth inhibition and instead resulted in increased cellular proliferation. This effect, however, was strictly restricted to changes in GULP expression since SKOV3 cells targeted with the scrambled guide RNA were moderately growth-inhibited, similar to parental SKOV3 cells. Most importantly, both at 48 and 72 hours of TGF-β treatment, the growth of SKOV3 GULP-KO cells increased, which further indicated the 'molecular switching' of Smad3-dependent TGF-β responses towards its oncogenic roles, with high levels of regulatory Smads promoting either cancer cell proliferation or its migration and invasiveness (80,82,87).

SKOV3 GULP-KO cells no longer growth-inhibited by TGF-β1

A growth assay assessing changes in cell number indicated SKOV3 cells' increased resistance against the growth-inhibitory effects of TGF-β upon significant loss in GULP expression. However, despite the increased cell number at 48 and 72 hours in response to TGF-β1, it could not be determined if this increase was associated with significantly decreased cell death (i.e., evasion of apoptosis) or significantly increased proliferation. Better differentiating which aspect was severely impaired by GULP's knockout in SKOV3 cells may be crucial for GULP's therapeutic potential, and thus an MTT assay was performed to precisely assess the impact of GULP knockout on cellular proliferation (Fig. 10 A-B).

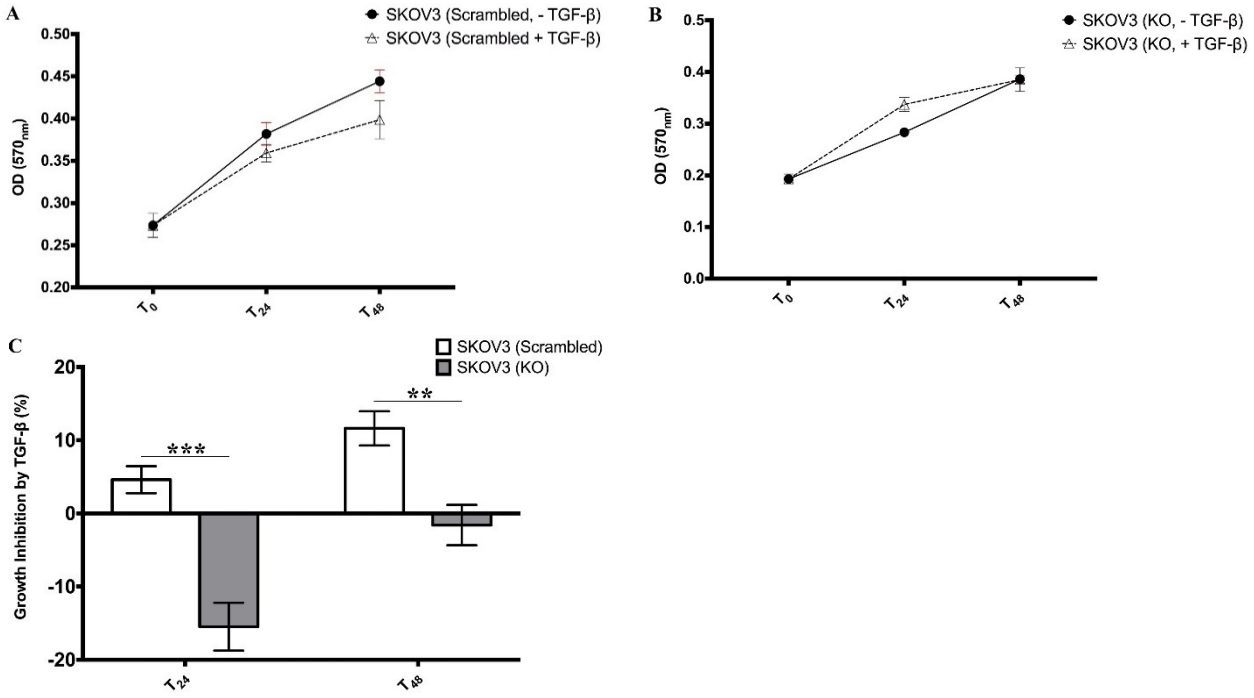

Figure 10. Knockout of GULP in SKOV3 results in loss of growth inhibition

A-B. *Average absorbance (O.D.) at 570 nm of SKOV3 scrambled and SKOV3 GULP KO cells*. An MTT assay was performed in replicates of six, with each cell treated with or without TGF-β1 (0.2 nM) for 24 or 48 hours. TGF-β associated growth inhibition was not affected in scrambled sgRNA-targeted SKOV3 cells (Panel A), whereas SKOV3 GULP-KO cells instead proliferated (Panel B).

C. *Comparison of average percentage growth inhibition by TGF-β.* The percentage of growth inhibition was calculated as: [1-((Average O.D. Control) - (Average O.D. TGF-β treated)) * 100]. Similar to parental SKOV3 cells, SKOV3 scrambled cells were moderately growth inhibited by TGF-β1 both at 24 and 48 hours (~10-20%). By contrast, SKOV3 GULP-KO cells were insensitive to TGF-β-mediated growth inhibition, instead continuing to proliferate at 24 and 48 hours (two-tailed *t*-test, p = 0.0008, 0.0032).

In agreement with the growth assay, the absorbance of TGF-β-treated SKOV3 scrambled cells was lower than for the matching non-treated cells at 24 and 48 hours, indicative of growth inhibition. More importantly and similar to parental SKOV3 cells, while absorbance was lower in SKOV3 scrambled cells, it continued to increase over time – indicative of cell growth (Panel A). By contrast, GULP knockout in SKOV3 cells resulted in higher absorbance compared to non-treated control cells in response to TGF-β at 24 hours (Panel B), further supporting the trend related to increased cell growth (Fig. 9). Although cell growth seemed to slow down at 48 hours of TGF-β treatment, SKOV3 GULP-KO cells were still not growth-inhibited (Panel E), further indicating GULP's primary role as a 'tumour-suppressor' in humans and the association between its loss and the increased risk of ovarian cancer onset.

Increase in cell migration in SKOV3 GULP-KO cells

Based on the growth and MTT assays, the results indicated that Smad3-dependent TGF-β responses elicit tumour-suppressive roles in SKOV3 ovarian cancer cells. However, despite moderate growth inhibition, parental SKOV3 cells were significantly migratory in response to TGF-β (Fig. 4). Increased migration in SKOV3 cells with high levels of GULP led to the question of whether reduced GULP levels might hamper cancer progression by reducing migratory potential – crucial for cancer metastasis to secondary organs in advanced cancers – despite the increased resistance against tumour-suppressive effects (i.e., growth-inhibition and cytotoxicity). To address this question, a scratch assay was performed at the same cell density using SKOV3 scrambled and SKOV3 GULP-KO ovarian adenocarcinoma cells (Fig. 11). Cells were grown to 80~90% confluence before the wound was created. After scratching the monolayer of cells, each well was gently rinsed with serum-free culture medium to remove excess cellular debris.

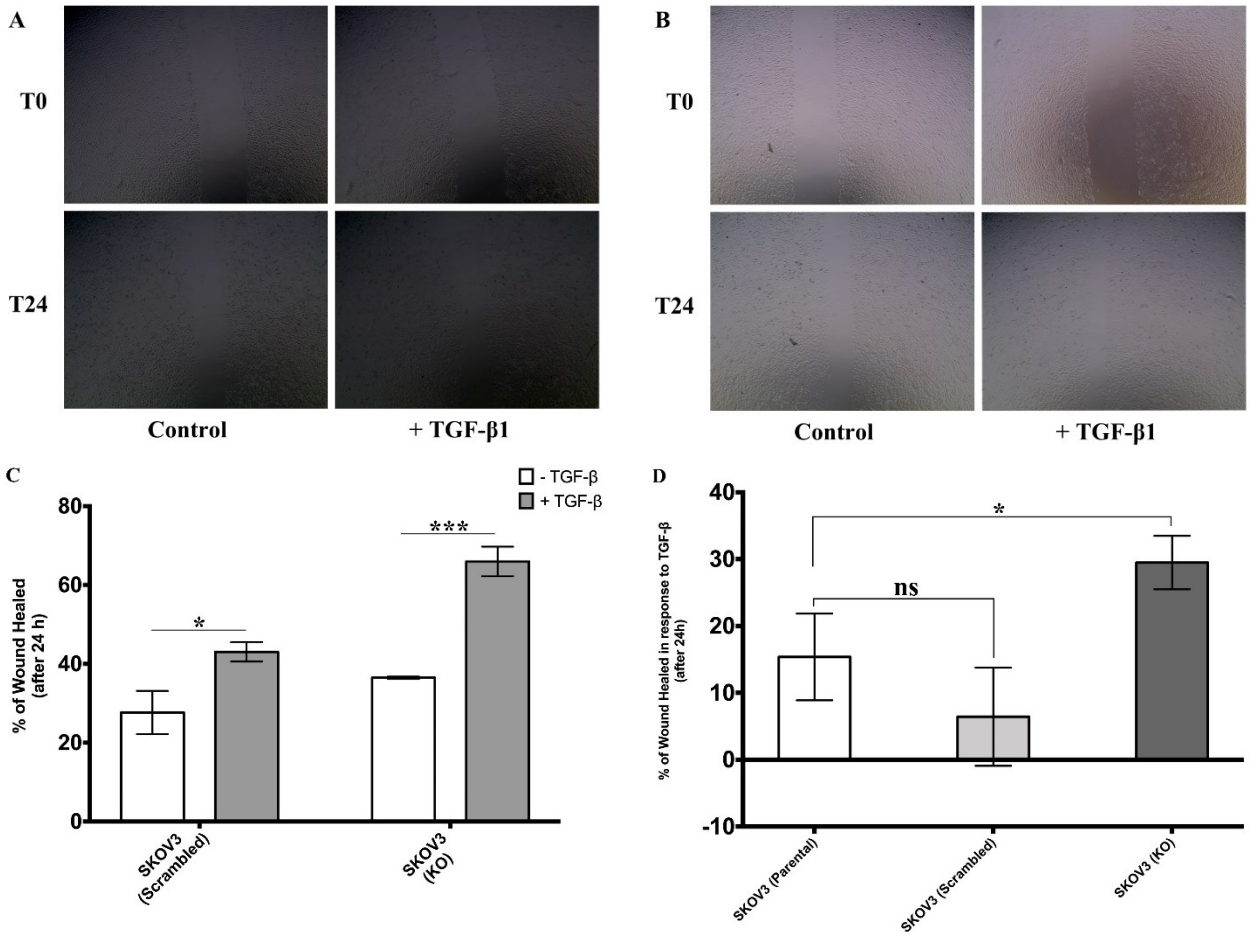

(Figure legend continues on the next page.)

Figure 11. Association between GULP knockout in SKOV3 cells and increased migration

A-B. *Representative images acquired immediately after the 'scratch' (T_0) or after 24 hours of treatment with TGF-β1 (0.2 nM) in SKOV3 scrambled (Panel A) or SKOV3 GULP-KO cells (Panel B).*

C. *Comparison of average percentage of wound healing.* The percentage of wound-healing, used to represent cell migration, was measured as: [(Average area of wound at T_0) - (Average area of the wound at T_{24})]/ (Average area of the wound at T_0) * 100. SKOV3 scrambled and SKOV3 GULP-KO cells were moderately migratory in the absence of TGF-β1. By contrast, migration was noticeably induced in response to TGF-β1 (two-tailed *t*-test, p = 0.0116, 0.0002). The Wound was significantly healed in TGF-β treated SKOV3 GULP-KO cells.

D. *Comparison of average percentage of wound healed in response to TGF-β1.* Similar to in parental SKOV3 cells, scrambled sgRNA did not affect TGF-β induced increases in cell migration in SKOV3 scrambled cells (two-tailed *t*-test, p = 0.1892). By contrast, knockout of GULP expression was associated with significantly increased cell migration, which was nearly double that of parental SKOV3 cells (two-tailed *t*-test, p = 0.0326).

Surprisingly, while the decrease in GULP – a specific adapter protein of LRP1 regulating TGF-β responses in the ovary surface epithelium (100,101) – was expected to reduce cell migration, migration instead significantly increased in response to TGF-β in SKOV3 GULP-KO cells. However, SKOV3 scrambled cells with unaffected, high levels of GULP showed a similar response to TGF-β as seen in parental SKOV3 cells, for which migration increased significantly (~15%). Most importantly, despite the significant reduction in GULP expression, migration nearly doubled (~30%) in SKOV3 GULP-KO cells (Panel D). These somewhat surprising findings align with our proposal that GULP is a 'tumour-suppressor' in humans, with a decrease in or loss of its expression associated with the promotion of oncogenic TGF-β responses (including induction of cell migration) and increased resistance against growth inhibition.

4. Discussions

Association between high levels of GULP and long-lasting Smad3 phosphorylation

Despite TGF-β's growth inhibitory effects, it is now widely accepted that TGF-β response is not only involved in a tumour-suppressive role (77,81) but also can be involved in cancer progression by promoting cell migration and invasion (80,82). Since GULP – an adapter protein of LRP1 (101,102) – might be essential for TGF-β signaling in the ovary (100), this study first addressed whether its expression is differentially affected in ovarian cancer cell lines. As shown in Figure 1A, significant differences in GULP level could be seen between HEY (low GULP) and SKOV3 (high GULP) ovarian adenocarcinoma cells. Furthermore, high levels of GULP were associated with significant induction of Smad3 phosphorylation following TGF-β1 treatment. Also, despite gradual decreases in Smad3 phosphorylation, its intensity at 24 hours was noticeably higher than for the untreated control. These observations were further confirmed in PEO-14 cells (Fig. 1B).

TGF-β-Smad signaling activities' effect on cancer progression

Different forms of cancer negatively affect the secretion of TGF-β or its components (83). Paradoxically, apart from the 'dual-edged sword' posed by TGF-β signaling (77,80-82), cancer cells have been shown to be capable of secreting TGF-β themselves, supporting cancer progression (104,130).

Smad3 previously has been found critical in regulating cell proliferation, differentiation, and apoptosis (131). Further supporting the tumour-suppressive role of Smad-dependent TGF-β responses, the loss of Samd3 was associated with the development of resistance against TGF-β-associated growth inhibition and apoptosis (131). However, in a strong argument against this claim, Smad2 was found to be highly phosphorylated in ovarian cancers independent of subtype (87). More specifically, TGF-β might function as the 'dual-edged sword' – promoting cancer progression through the accumulation of genetic aberrations that abrogate the growth-inhibitory effects of TGF-β, while maintaining its stimulatory effects on angiogenesis, EMT induction,

migration, and invasion (80,82). Nevertheless, high TGF-β-Smad activity was associated with poor prognosis in glioma patients, promoting cancer cell proliferation via the induction of PDGF (platelet-derived growth factor)-B. Similarly, it was recently found that TGF-β positively regulated the IGF (insulin growth factor) 1 receptor, which, when inhibited, interrupted tumour growth on the ovary *in vivo* (87).

Even though the intensity of p-Smad3 was correlated with GULP level, functional consequences of differences in the 'longevity' of Smad3-phosphorylation were unclear. Therefore, several functional assays were performed to assess changes in TGF-β's tumour-suppressive or tumour-promoting aspects. Specifically, a growth assay was performed to examine how changes in TGF-β response might affect cell proliferation. Furthermore, an MTT assay – which forms formazan crystals under the presence of active mitochondria in living cells – was performed as another measure of changes in cell proliferation (123). In comparison, a scratch (or 'wound-healing') assay was performed to examine changes in cell migration.

Association between high levels of GULP and TGF-β-mediated growth inhibition

Despite the correlation between the GULP level and Smad3 phosphorylation (Fig. 1), its functional consequences in ovarian cancer remained contentious. To address the functional consequence of increased Smad3-dependent TGF-β signaling, a growth assay was performed. Interestingly, HEY cells with low levels of GULP were not only resistant to growth inhibition but also seemed to proliferate in an uncontrolled fashion (Fig. 2). By contrast, PEO-14 and SKOV3 ovarian cancer cells with high levels of GULP were growth-inhibited by TGF-β1. Despite decreased cell number compared to the matching control, SKOV3 cells were only weakly growth-inhibited. More importantly, even with the presence of TGF-β, SKOV3 cells were able to moderately proliferate for up to 72 hours (Fig. 2). Although the growth assay indicated tumour-suppressive TGF-β responses were present in ovarian cancer cells with high levels of GULP, it was unclear whether growth inhibition was primarily due to cell death or lack of proliferation. An MTT assay was performed to examine the growth-inhibitory effects of TGF-β in ovarian cancer cells.

In the MTT assay in response to TGF-β1, HEY cells were non-responsive to growth-inhibitory effects of TGF-β. Absorbance (which correlates with cell viability) was higher than non-

TGF-β-treated HEY cells at 48 hours (Fig. 3A), signifying the failure of growth inhibition. By contrast, the absorbance of TGF-β1-treated SKOV3 and PEO-14 cells was lower (Fig. 3B, C). Despite high levels of GULP, the degree of growth inhibition was rather modest in SKOV3 cells (~20%) at 24 and 48 hours (Fig. 3D). Furthermore, while the absorbance of TGF-β-treated SKOV3 cells was lower compared to non-treated cells, it continued to increase for 24 and 48 hours of treatment, indicative of only moderate cell proliferation (Fig. 3B). It thus could be inferred that while growth inhibition by TGF-β1 is present in SKOV3 cells, sensitivities are reduced. In support of this idea, Zeinoun, *et al.* found weaker or a loss of TGF-β1-associated growth inhibition in several epithelial ovarian cancer cell lines, including in SKOV3, AZ224, and AZ547 cells (131).

By contrast, PEO-14 cells showed significant growth inhibition, approximately 20% at 24 hours and 50% at 48 hours (Fig. 3D). Additionally, absorbance continued to decrease, further indicative of cell death. The dramatic cytotoxic effects of TGF-β1 in PEO-14 cells may be due to decreased expression of TGF-β isoforms instead of aberrations in TGF-β signaling components. In fact, as Bartlett, *et al.* documented in 1992, while TGF-β2 and -β3 isoforms were present in PEO-14 cells, the TGF-β1 isoform was not; supporting this study's findings, PEO-14 cells were most sensitive to TGF-β1, with more than 50% of cells growth-inhibited (132). Therefore, one could infer that GULP plays a 'tumour-suppressive' role in the ovary and its loss might exacerbate ovarian cancer progression.

Potential of high GULP levels to exacerbate ovarian cancer progression

Increasing evidence suggests tumour-promoting roles for TGF-β, including the promotion of EMT allowing cells to become migratory (82). However, since ovarian cells are known to be less migratory (4), it was unclear in this study whether variation in GULP level is associated with ovarian cancer metastasis. Based on the wound-healing assay, SKOV3 cells became more migratory in response to TGF-β1; HEY ovarian cancer cells were by contrast largely unresponsive (Fig. 4A, B, D). By contrast, PEO-14 cells were completely unresponsive to TGF-β1 in migration, despite high levels of GULP (Fig. 4D).

However, as Guo, *et al.* insist, wound-healing – commonly used to assess cell migration *in vitro* – is an intricate and dynamic process involving the combined action of cellular proliferation and migration (133). Indeed, PEO-14 cells experienced the most extensive degree of TGF-β1-

medaited growth inhibition (~50%) (Fig. 3D). Taking this into account, the lack of change in cell migration for PEO-14 cells in response to TGF-β1 may be due to TGF-β1's dominant, tumour-suppressive effects. Therefore, both the lack of resistance against growth-inhibition and the increased death of PEO-14 cells might have limited the active supply of newly divided cells to be migrated to the wound area, further restricting wound closure in conjunction with the low migratory potential of cells in proximity to the wound.

GULP regulation of TGF-β responses in primary OSE cells

Research has made tremendous progress through *in vitro* studies using established cell lines to represent model systems. Nevertheless, the use of a specific cell line may cloud understanding of how the protein of interest genuinely behaves *in vivo*. In fact, despite the existence of several databases, classification of ovarian cancer cell lines is misleading (115). For instance, several (including A2008) have unknown or ambiguous tumour origin and have suspect classification (115). Most importantly, since precise classification standards are lacking for ovarian cancer (115), ambiguous classification of ovarian cancer cell lines is somewhat troublesome due to the heterogeneity of a tumour (62,63), as the subtypes vastly differ (62,63). Additionally, an established cell line may vastly differ from human physiology by acquiring numerous spontaneous mutations during cell line establishment, which may affect gene stability or cell metabolism (117). To address the current limitations of using established cell lines, human primary OSE cells were utilized. First, per the need for TGF-β signaling for normal ovary epithelium development (74,86,87), Smad3 was rapidly phosphorylated in response to TGF-β1 in normal OSE cells with high levels of GULP (Fig. 5). However, the longevity of Smad3 phosphorylation differed among normal OSE cells despite similarities in GULP expression (Fig. 5). As summarized in Figure 6, the degree of Smad3 phosphorylation was lower in one of the cancerous OSE cells (C3) compared to normal OSE cells. This difference was also associated with reduced levels of GULP. Interestingly, cancerous OSE cells for which GULP expression was similar to that of the normal OSE cells demonstrated a nearly identical degree of Smad3 phosphorylation induced in response to TGF-β1.

We performed an MTT assay in primary OSE cells to further assess the functional consequences of differences in GULP level *in vivo*. Interestingly, as shown in Figure 7F, normal

cells were significantly growth-inhibited in response to TGF-β1 (40-60%); as with PEO-14 ovarian cancer cells, the absorbance of TGF-β1-treated normal OSE cells continued to decrease, indicative of cytotoxic effects (Fig. 7A, B). To the contrary, as shown in Figures 7C-E, TGF-β1 associated growth inhibition differed among primary cancerous OSE cells. In fact, while two cancerous samples were moderately growth inhibited (~20% upon 24 hours), which had higher levels of GULP, cancerous OSE cells C3, with low levels of GULP, were not growth inhibited (Fig. 7G). Therefore, it could be summarized that that while TGF-β1 elicits significant growth inhibition in the normal primary OSE, it is dramatically weakened in primary cancerous OSE (Fig. 7H). Nevertheless, variability in TGF-β1-mediated growth inhibition among cancerous OSE cells further signifies the heterogeneous nature of ovarian cancer and provide reasons why ovarian cancer cell lines need to be fully investigated.

Effect of GULP knockout on TGF-β responses in ovarian cancer cells

As with the dramatic downregulation of GULP expression in ovarian cancer irrespective of subtype (101), GULP level was significantly lower in HEY cells than SKOV3 and PEO-14 cells (Fig. 1). As a result, HEY cells were unresponsive to TGF-β-mediated growth inhibition (Fig. 3D). Although several ovarian cancer cell lines with low levels of GULP exist (i.e., HEY cells), the functional consequences and changes in cell signaling upon GULP's loss *in vivo* may not be well appreciated. Thus, to recapitulate the physiological consequences of GULP's loss and further address whether it is associated with ovarian cancer progression, GULP expression was knocked out in SKOV3 cells using the CRISPR-Cas9 system (119).

Surprisingly, whereas GULP expression significantly decreased following its knockout, the longevity of Smad3 phosphorylation was only weakly affected (Fig. 8). However, the decrease in GULP level resulted in dramatic functional consequences. First of all, although parental SKOV3 cells were moderately growth-inhibited (~20%) in response to TGF-β1 (Fig. 2), SKOV3 GULP-KO cells were no longer inhibited and instead continued to grow in an uncontrolled manner (Fig. 10B). As a control, scrambled guide RNA did not affect TGF-β1-associated growth inhibition (Fig. 9). The impairment of GULP function or reduction of GULP level thus may exacerbate the tumour-suppressive effects of TGF-β (77,81).

As TGF-β may instead promote cancer progression (80,82), we subsequently assessed how knocking out GULP expression affects cell migration. Because cell migration increased by more than 15% in response to TGF-β1 in parental SKOV3 cells (Fig. 4D), GULP knockout was initially expected to render SKOV3 cells less migratory. Surprisingly, as shown in Figure 11, knockout of GULP rather resulted in a two-fold increase in migration from the parental SKOV3 cells in response to TGF-β1 (~30%). In fact, the wound dramatically healed after just 24 hours (Fig. 11B). However, the increase in SKOV3 cells' migratory potential was strictly restricted to GULP knockout. Considering the importance of cellular proliferation in wound-healing (133), it is important to reiterate that SKOV3 GULP-KO cells were no longer growth-inhibited (Fig. 10B); rather, growth increased in response to TGF-β1 (Fig. 9). Increased proliferation thus might have somewhat improved the wound-healing process. By contrast, if proliferation were to be severely hampered by TGF-β, the wound-healing process would be affected and cells would be mostly immobile, as in PEO-14 cells (Fig. 4D). Alternatively, the unexpected increase in cell migration for SKOV3 GULP-KO cells might have been due to GULP's predominant role in mediating tumour-suppressive TGF-β responses. TGF-β ligands are a 'dual-edged sword' with a function that may switch from tumour suppression to cancer promotion (77,81). If so, decreased levels or impaired function of GULP may facilitate the use of TGF-β signaling components (i.e., Smads) for cell migration and invasion (80,82), serving a role as a 'molecular switch' (Illustration 7). In further support of this claim, TGF-β1 did not induce cell migration for PEO-14 cells (which were most significantly growth-inhibited) (Fig. 4D). HEY cells with low levels of GULP were not noticeably migratory without TGF-β1; this was not further induced by TGF-β1 (Fig. 4D), which might be due to the lack of effective activation or assembly of the Smad complex (Illustration 7).

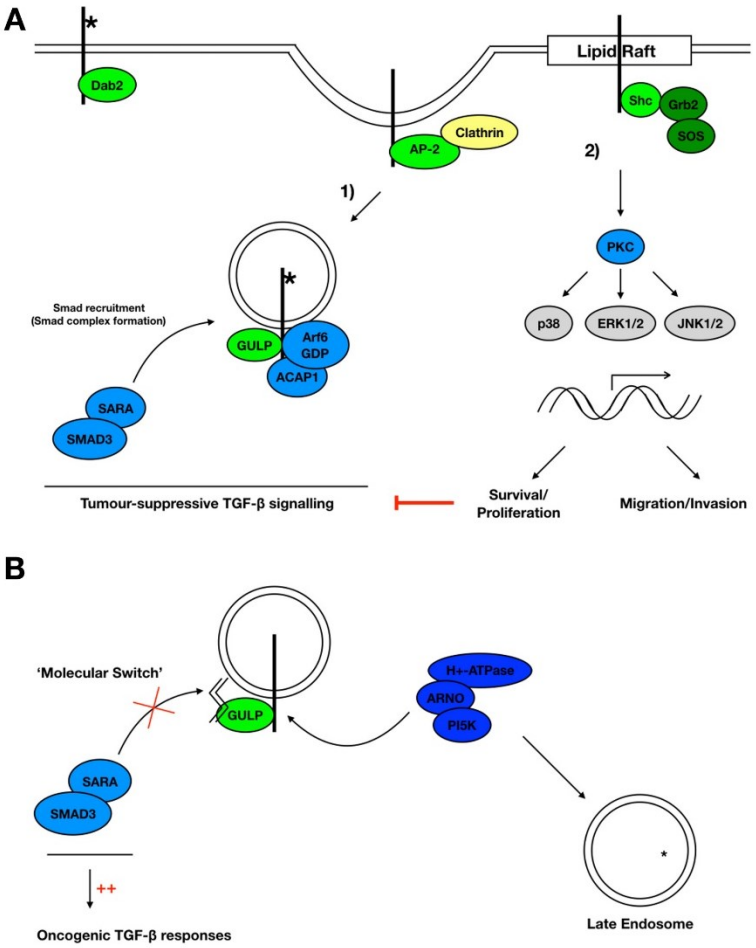

Illustration 7. Proposed role of GULP as the 'molecular switch'

A. *Schematic model illustrating GULP's primary role as a 'tumour-suppressor.* TGF-β (*asterisk*)-bound LRP1 (*bold line*) can be internalized by endocytosis, where GULP prolongs the tumour-suppressive TGF-β signaling by preventing the late endosome maturation. Alternatively, ligand-bound LRP1 can localize to lipid rafts, which may instead activate MAPK signaling, responsible for cell survival or migration. Despite high levels of GULP, alternative LRP1 signaling may inhibit GULP-mediated tumour-suppressive effects of TGF-β responses (i.e. inhibition of p15ink4b or p21cip1).

B. *GULP may function as the 'molecular switch'.* Following the decreased expression or impairment of GULP's function (i.e. knock-out), internalized TGF-β in early endosome is rather promptly degraded in late endosomes. Then, in cells with high levels of GULP initially, actively assembled Smad complex may instead promote oncogenic responses.

Thus, decreased expression of GULP regulating tumour-suppressive TGF-β responses in SKOV3 cells could have promoted oncogenic TGF-β responses instead, resulting in increased cell migration. By contrast, low GULP levels could have meant that while HEY cells might have been largely shielded from TGF-β1's growth-inhibitory effects compared to SKOV3 (or, more importantly, to PEO-14 cells), active Smad complex assembly might be absent in HEY cells. This indicates that HEY cells may require additional factors for migration. While contradicting observations exist between HEY and SKOV3 GULP-KO cells, despite similarly low levels of GULP (Fig. 4D, 11D), the results support our claim that knockout of GULP may only represent the functional consequence of GULP's loss. Further GULP knockout experiments in PEO-14 cells will enhance this discussion.

PI3K-Akt-mTOR pathway and ovarian cancer

Among numerous signaling pathways, the PI3K-Akt-mTOR (PAM) pathway is compromised in more than 80% of all cancers diagnosed (80,85), which may be largely due to Akt-mediated cell survival allowing the evasion of the programmed cell death or apoptosis (134). Similarly, mTOR – the master regulator of nutrient-sensing in eukaryotic cells (85) – may further enhance cellular proliferation and increase protein translation by phosphorylating and inhibiting eIF4E binding protein 1 (4EBP1) (85). In fact, PAM pathways drive cancer progression in several forms of cancer, including breast and ovarian (85). Additionally, TGF-β ligands have been shown to non-canonically activate different signaling pathways, including PI3K-AKT-mTOR, RHOA, and MAPK pathways (80).

Interestingly, rapid Akt phosphorylation has been observed in several ovarian cancer cell lines, including OVCAR-3 at Thr308 under serum starvation (134). More importantly, although cancer is known to be the result of accumulated aberrations in multiple genes (52,62,63), it might depend on a single or few oncogenes, referred to as oncogenic addiction (135), whose inactivation may severely impair the growth and progression of cancer. Akt activation may not only allow cancer cell survival but also rapid cell proliferation in association with mTOR (80,85,134). Therefore, 'Torin 1' – a specific mTORC1 inhibitor, which inhibited the phosphorylation of Akt (Ser473) at 100 nM, (136) – was used to examine whether ovarian cancer cells are oncogenically

addicted to Akt and whether its inhibition could restore the sensitivity to TGF-β's growth-inhibitory effects (Fig. 12).

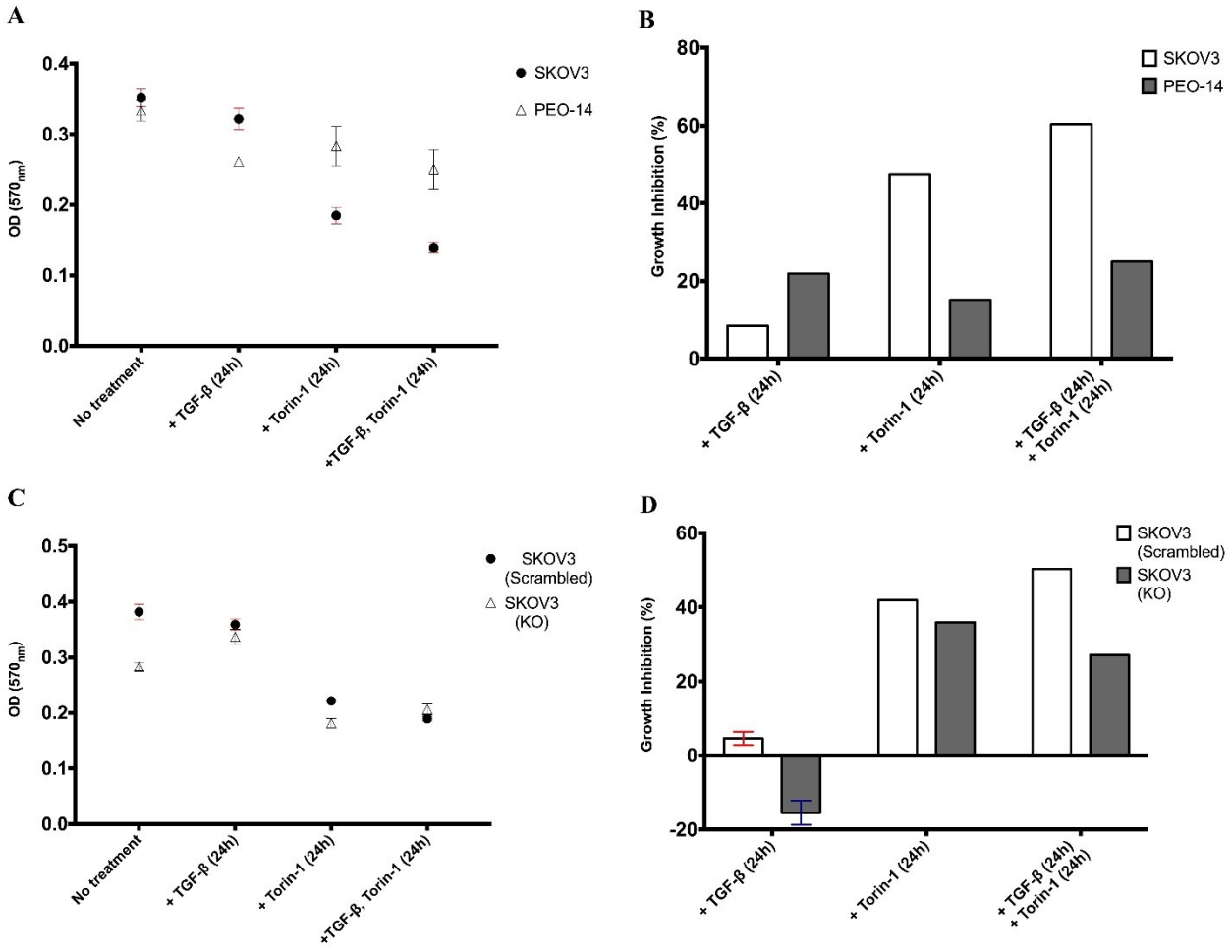

(Figure legend continues on the next page)

Figure 12. Akt inhibition by Torin-1 is associated with increased cell death

A. *Average absorbance measured at 570 nm following MTT assay.* Cells were seeded at a density of 2,000 cells/well and treated with the following for 24 hours: 1) TGF-β1 (0.2 nM), 2) Torin-1 (125 nM), and 3) TGF-β1 (0.2 nM) and Torin-1 (125 nM). Next day, cells were incubated at 37 °C with 25 µL of MTT solution (5mg/mL) for 2 hours before solubilization of formazan crystals.

B. *Percent growth inhibition (%) by each treatment.* Average absorbance from each treatment in each cell line was compared to the non-treated control. Growth inhibition was represented as: [(Absorbance of non-treated control) - (Absorbance of treated cells)/(Absorbance of non-treated control)]*100.
C. *Average absorbance measured at 570 nm.* 2,000 cells (SKOV3 scrambled or SKOV3 GULP-KO) were seeded to each well in replicates of six. Following overnight incubation at 37 ℃, cells were treated with: 1) TGF-β1 (0.2 nM), 2) Torin-1 (125 nM), and 3) TGF-β1 (0.2 nM) and Torin-1 (125 nM) for an additional 24 hours. Next day, cells were incubated at 37 ℃ with 25 µL MTT solution (5mg/mL) for 2 hours before solubilization of formazan crystals.
D. *Percent growth inhibition (%) by each treatment.* Average absorbance from each treatment was compared to the non-treated control. Growth inhibition was represented as: [(Absorbance of non-treated control) - (Absorbance of treated cells)/(Absorbance of non-treated control)]*100.

As shown in Figure 12B, SKOV3 cells were significantly growth-inhibited in response to Torin-1 (~50%), indicating the necessity of PAM pathways for their survival. But despite having equally high levels of GULP to SKOV3 cells, PEO-14 cells were moderately growth-inhibited. Similarly, while SKOV3 cells were also growth-inhibited by TGF-β1, additive growth inhibition was absent in PEO-14 cells following the inhibition of Akt by Torin-1. Therefore, while further experiments are required, one could infer that PEO-14 cells do not depend on Akt, explaining the significant growth inhibition observed in response to TGF-β1 (Fig. 3D). Subsequently, whether changes in GULP's expression or impairment of its function could affect increases in TGF-β sensitivity was tested in SKOV3 GULP-KO cells. As shown in Figure 12D, growth inhibition in response to Torin-1 was nearly identical between SKOV3 scrambled and SKOV3 GULP-KO cells (~40%). By contrast, SKOV3 GULP-KO cells lost sensitivity towards TGF-β's growth inhibition. Moreover, in association with moderately increased cell growth (Fig. 9), TGF-β1 reduced growth-inhibitory effects posed by Torin-1 by nearly 10%.

One common limitations in therapeutics is the occurrence of unforeseen detrimental side effects. For example, aromatase inhibitors (e.g., anastrozole) reducing estrogen levels in women can facilitate bone loss and increase the risk of osteoporosis (137). Therefore, this study examined

if a Torin-1 mediated increase in TGF-β sensitivity instead leads to oncogenic TGF-β responses by increasing cancer cell migration (Fig. 13).

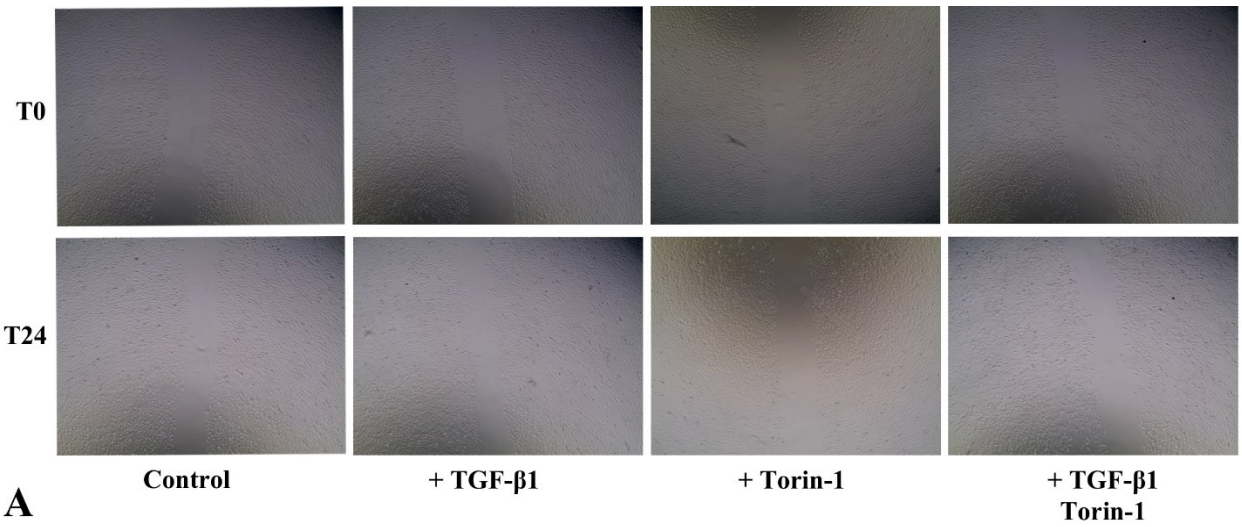

A

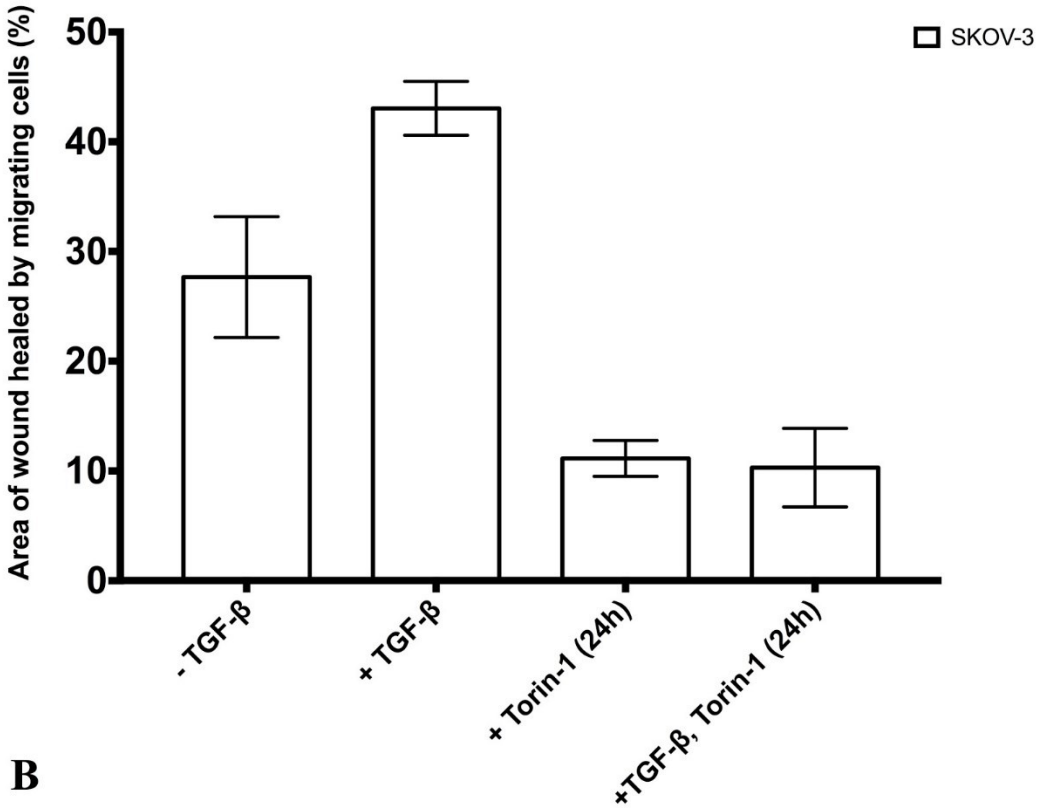

B

(Figure legend is on the next page.)

Figure 13. Migration is inhibited by Torin-1 and cannot be restored

A. *Images obtained upon initial 'scratch' (T_0) or after 24 hours (T_{24}) of treatment with Torin-1 (125 nM) or TGF-β1 (0.2 nM) and Torin-1 (125 nM).* The wound was manually created by scratching the confluent monolayer of SKOV3 cells with sterile, P200 pipette tips. An experiment was performed in triplicate.
B. *The average area of wound healed by migrating cells (%).* Area of wound healed by migratory cells was measured and averaged. The degree of cell migration was represented as: [(Average area at T_0) - (Average area at T_{24})/(Average area at T_0)]*100. Although migration was induced by TGF-β1 (0.2 nM) in SKOV3 cells, migration was severely suppressed by Torin-1 (125 nM) and could not be restored by TGF-β1.

As shown in Figure 13B, although Torin-1 enhanced TGF-β1-mediated growth inhibition in SKOV3 cells, cell migration was significantly hampered. More significantly, additional treatment of TGF-β1 could not restore cell migration. In support of this data, Gulhati, *et al.* demonstrated that mTOR was closely associated with the activation of RhoA and Rac1, governing cell motility and metastasis (138). One could thus infer that the blockade of Akt activation specifically correlates with the enhancement of TGF-β's tumour-suppressive effects. While further *in vitro* studies are required, this exciting possibility may help reduce ovarian cancer deaths.

Therapeutic potential of GULP

Despite the lack of a test on the association between GULP expression and angiogenesis, GULP expression was significantly lower for ovarian cancers compared to the normal ovary irrespective of subtype (Illustration 4). Hence, GULP might be a reliable biomarker, which may allow for each patient to receive better guidance on the most beneficial therapeutics and thus improve overall ovarian cancer survival. In fact, targeted, personalized therapy is emerging alongside advances in understanding aberrations in different types of cancer (139,140). Nonetheless, the effectiveness of a specific drug can be severely dampened by compensatory mechanisms, which may rescue blocked signaling pathways targeted by small molecule inhibitors (9). Additionally, effective delivery of drugs to the brain is restricted due to the blood-brain barrier (10).

With improvements in genetic sequencing and the emergence of databases, researchers quickly recognized the importance of small, noncoding RNAs collectively known as microRNAs (miRNAs) (141). Indeed, miRNAs may be either tumour-suppressive or oncogenic, with expression differentially affected among cancers (141,142). According to Chong, *et al.*, in 2015, four miRNAs (miR-551b, miR-19b, miR196b, and miR-3198) were shown to be significantly overexpressed in EOC, whereas four miRNAs were significantly downregulated (miR-8084, miR-3201, miR-3613, and miR-7515) (142). More importantly, expressions of miRNAs may be dependent on the GULP gene, or vice versa. In fact, although the physiological consequences of its downregulation are unclear, miR-561's (an intronic miRNA) expression was correlated with the expression of GULP (143), an additional finding supporting the close association between miRNAs and cancer progression. Although antisense oligonucleotides have been developed to block the function of oncogenic miRNAs (144), which might affect the expression or function of GULP, effectively delivering therapeutics across the body is still challenging. In 1983, however, Harding, *et al.* first identified cell-derived vesicles, or exosomes, in reticulocytes (145). Exosomes consist of numerous constituents, including proteins, RNAs, metabolites, and lipids (11); they were quickly explored as a drug-delivery carrier due to their small size (with a diameter of less than 100 nm), ease of transport, and prompt internalization into cells (11). Exosomes can now be bioengineered for targeted drug delivery into cancer cells (11). Therefore, antisense oligomers against oncogenic miRNAs in ovarian cancer or miRNAs downregulating GULP expression may be packaged into exosomes and delivered to ovarian adenocarcinomas no longer sensitive to TGF-β-mediated growth inhibition.

Limitations and future directions

Limitations in experimental design

although primary OSE cultures from normal and cancerous human ovary tissue samples were utilized, its numbers were largely limited, where only 3 primary cultures of ovarian cancer samples could be obtained. Similarly, while several ovarian cancer cell lines have been utilized, its extent should be increased to strengthen results obtained in this study. Lastly, although normal OSE cells were used as reference for the comparison against behaviors of primary cultures of

ovarian cancer samples, additional studies must be performed to further strengthen and justify the use of normal OSE cells as reference. For instance, expressions of characteristic 'epithelial markers' (82) may be monitored by Western blot or immunofluorescence.

Technical limitations

This study has made several improvements to existing laboratory protocols, including MTT assay, to address limitations that could have impacted the results. One major downside to MTT assays is the intensive washing steps, which might significantly impact loosely attached cells and thus lead to lower absorbance. Therefore, a medium containing twice the final desired concentration of each treatment (TGF-β1, Torin-1, or both) was prepared and added on top of the existing medium in each well. Moreover, since absorbance could be easily affected by pH and thus cloud results, Sorensen's glycine buffer was used to create a single absorbance maximum at 570 nm and to stop any residual MTT reactions (123).

Despite several improvements, MTT assay and its derivatives (MTS, XTT, and WST-1) continue to have limitations. For instance, Chakrabarti, *et al.* reported in 2000 that supplements in specific growth media might mask the understanding of cell proliferation (144). Among different factors, L-ascorbic acid – often found in several basal culture media – was capable of reducing MTT by itself. More importantly, increases in absorbance did not correlate with changes in cell number, which subtracting absorbance from growth medium alone (control) could not correct; subtracting absorbance due to L-ascorbic acid alone could (146).

Thus, as an alternative to MTT assay, DNA synthesis should be monitored to assess changes in cell proliferation in the future. For example, 5-bromo-2'-deoxyuridine (BrdU) may be used (147). BrdU serves as substitute for the nucleotide thymidine and is only incorporated into the newly synthesized DNA of dividing cells (147), and thus it may offer the most accurate estimate of the responsiveness towards TGF-β1-associated growth inhibition in each cell line.

Conceptual limitations

This study addresses whether GULP, an adapter protein specific to LRP1 (102), regulates TGF-β responses in human ovarian cancer. Although several of its results indicate that high levels of GULP are associated with the growth-inhibitory effects of TGF-β1 (Fig. 3D, Fig. 9), this study – like many others – has focused on genetic aberrations in cancer cells themselves. However,

carcinomas consist of cancer cells and stromal cells surrounding a tumour (148). While cancer-associated stromal cells were believed to not play malignant roles, tumour-surrounding cells such as tumour-infiltrating immune cells and cancer-associated fibroblasts (CAFs) have been shown in recent years to interact with and influence cancer cells (148,149). Although CAFs are morphologically and functionally similar to myofibroblasts (150), CAFs remain constitutively active and are not eliminated by apoptosis (150). Moreover, CAFs account for the majority of cancer stroma, and they have been shown to be the important source of interleukin-6 (IL-6), a type of cytokine essential for the cancer proliferation, migration, and angiogenesis (151). Most significantly, while HEY cells were unresponsive to TGF-β-mediated induction of cell migration (Fig. 4D), 'co-culture' of HEY cells with fibroblasts was shown to result in noticeable cell migration, whereas HEY cells cultured alone were mostly immobile (152).

Additionally, while GULP has been found to be a highly specific adapter protein for LRP1 (102), it has not been examined if the internalization and prolonged half-life of TGF-β-bound LRP1 in early endosomes are sufficient for TGF-β responses. While directly binding ligands to LRP1 has been shown to be sufficient for activation and downstream signaling in several cells, other cells might require LRP1 co-receptors for their activation (91). In fact, N-methyl-D aspartate and Trk receptors have been described as LRP1 co-receptors mediating the activation of Src and Akt (91). Furthermore, while LRP1 is activated by its agonist-mediated phosphorylation of tyrosine residue within the NPxY motif (91,93,94), it remains unclear if tyrosine-phosphorylated active LRP1's level is affected by changes in GULP expression. More importantly, since various adapter proteins exist for LRP1 (including Shc) (102), the functional consequences of LRP1 signaling within cells may vastly differ. In fact, while clathrin-coat-mediated internalization of TGF-β receptors to EEA1-positive endosomes is more likely to promote R-Smad activation and Smad complex formation (153), caveolin-1-mediated internalization has been shown to degrade and inhibit TGF-β receptors where CD109 (a GPI-anchored protein) serves as a co-receptor (153). Moreover, TGF-β receptors localized in lipid rafts or caveolae were necessary for MAPK activation (154). Future examination should thus investigate how changes in GULP level affect LRP1's phosphorylation on its tyrosine residue within the NPxY motif and hence its activation.

Future direction

Although cancer poses a health risk at its primary site, most mortality due to cancer results from metastasis, which commonly spreads cancer to neighbouring organs and rapidly worsening patient outcomes (1,155). However, metastasis is not only the result of the migration of cells from the tumour of origin to different organs through lymph nodes and blood vessels; it also requires 'invasion'. Invasion is essential for allowing disseminated tumour cells to migrate out of the blood vessel (extravasation) and conquering secondary organs (invagination) (155).

Among other factors, matrix metalloproteases (including MMP-2 and MMP-9) are crucial for invasion by allowing the digestion of extracellular matrix and helping cancer cells to survive by recruiting tumour-associated macrophages that supply nutrients to cancer cells (90,149). Future research should thus investigate if differences in GULP expression affect cancer cell invasion by comparing MMP2/9 levels in response to TGF-β1 in each ovarian cancer cell line. More importantly, although Wang, *et al.* report that ovarian cells are less migratory (4), this might have been due to ignoring the contribution of stromal cells. CAFs have been shown to actually remodel the extracellular matrix by expressing matrix metalloproteinases, including MMP-9 (130), which may substantially increase the invasiveness of disseminated ovarian cancer cells. Of concern here, TGF-β secreted from breast cancer cells has been shown to induce the expression of MMP-9 in cancer-associated fibroblasts (130). Co-culture of primary OSE cells with surrounding stromal cells (fibroblasts) therefore should be performed in the future to understand how changes in GULP level or function affects tumour-stromal, heterotypic interactions, which may be associated with ovarian cancer progression via the regulation of angiogenesis, cell migration, and invasion.

Lastly, *in vivo* animal studies may be performed to strengthen the role of GULP as the tumour-suppressor. More specifically, mice may be injected with different ovarian cancer cell lines with unaffected, high levels of GULP or GULP-knocked out cells (ie. SKOV3 GULP-KO) to monitor how the decreased expression of GULP increases the risk of cancer with respects to several 'hallmarks of cancer' (106).

5. General conclusion

In addition to decreased levels of GULP among different subtypes of epithelial ovarian cancers (101), epigenetic silencing of the GULP gene was recently reported in humans (*personal communication*). These collectively indicate GULP is the primary regulator of tumour-suppressive TGF-β signaling *in vivo*. Nonetheless, the functional consequences of GULP loss in human were absent from the literature. To address current limitations, we used ovarian cancer cell lines that included HEY, PEO-14, and SKOV3 cells, which were representative of cells with significantly reduced levels of GULP (HEY) or with unaltered, high levels of GULP (PEO-14 and SKOV3). Most importantly, this study's value and innovation are derived from its use of primary OSE cells isolated from surgically removed normal or cancerous ovary tissues, which best recapitulate changes in intracellular events in ovarian cancer. High levels of GULP were positively correlated with the intensity of p-Smad3 and resulted in growth inhibition. Nevertheless, its magnitude differed, and high levels of GULP allowed for increased cell migration, which might be associated with the risk of ovarian cancer metastasis in SKOV3 cells. More importantly, whereas GULP was highly expressed in primary normal OSE cells (resulting in significant growth inhibition of 40-60%), its expression was differentially affected among cancerous samples. Finally, the knockout of GULP expression in SKOV3 cells resulted in the loss of growth inhibition and increased cell migration despite decreased levels of GULP.

Thus, one could infer that GULP functions as the primary regulator of tumour-suppressive TGF-β responses, further serving as the 'molecular switch' associated with ovarian cancer advancement. In fact, while growth-inhibitory effects of TGF-β1 was significantly reduced in SKOV3 cells (high levels of GULP), its migration noticeably increased in response to TGF-β1. Hence, it could also be inferred that ovarian cancer may rapidly build resistance against tumour-suppressors such as p15ink4b or p21cip1 produced by TGF-β, allowing them to benefit from the oncogenic TGF-β responses exclusively, despite the high expression of GULP. If so, GULP expression may be further repressed secondarily with mutation, allowing common components (i.e., regulatory Smads) to be preferentially utilized in oncogenic TGF-β responses. Indeed, GULP-knockout in SKOV3 cells (which were not growth inhibited) supported this hypothesis, where migration was further enhanced despite reduced levels of GULP.

7. References

1. Weir, H.K., Thompson, T.D., Soman, A., Møller, B., Leadbetter, S. (2015) The past, present, and future of cancer incidence in the United States: 1975 through 2020. *Cancer*, *121*, 1827–1837. https://doi.org/10.1002/cncr.29258
2. Reid, B.M., Permuth, J.B., Sellers, T.A. (2017) Epidemiology of ovarian cancer: a review. *Cancer Biol. Med*. 14, 9-32. https://doi.org/10.20892/j.issn.2095-3941.2016.0084.
3. Karakasis, K., Burnier, J.V., Bowering, V., Oza, A.M., Lheureux, S. (2016) Ovarian cancer and BRCA1/2 testing: opportunities to improve clinical care and disease prevention. *Front. Oncol*. 6, 119. https://doi.org/10.3389/fonc.2016.00119.
4. Wang, H., Quah, S.Y., Jing, M.D., Manser, E., Jing, P.T., Zeng, Q. (2007) PRL-3 down-regulates PTEN expression and signals through PI3K to promote epithelial-mesenchymal transition. *Cancer Res.* 67, 2922–2926. https://doi.org/10.1158/008-5472.CAN-06-3598.
5. Erekson, E.A., Martin, D.K., Ratner, E.S. (2013) Oophorectomy: the debate between ovarian conservation and elective oophorectomy. *Menopause* 20, 110–114. https://doi.org/10.1097/gme.0b013e31825a27ab.
6. Neff, R.T., Senter, L., Salani, R. (2017) BRCA mutation in ovarian cancer: Testing, implications and treatment considerations. *Ther. Adv. Med. Oncol*. 9, 519-531. https://doi.org/10.1177/1758834017714993.
7. Doufekas, K., Olaitan, A. (2014) Clinical epidemiology of epithelial ovarian cancer in the UK. *Int. J. Womens Health* 6, 537–545. https://doi.org/10.2147/IJWH.S40894.
8. Chen, W., Zheng, R., Baade, P.D., Zhang, S., Zeng, H., Bray, F. et al. (2016) Cancer statistics in China, 2015. *CA Cancer J. Clin*. 66, 115-132. https://doi.org/10.3322/caac.21338.
9. Lokadasan, R., James, F.V., Narayanan, G., Prabhakaran, P.K. (2016) Targeted agents in epithelial ovarian cancer: review on emerging therapies and future developments. *Ecancermedicalscience* 10, 626. https://doi.org/10.3332/ecancer.2016.626.
10. Wang, Y., Zhang, L., Xu, Z., Miao, L., Huang, L. (2018) mRNA vaccine with antigen-specific checkpoint blockade induces an enhanced immune response against established melanoma. *Mol. Ther*. 26, 420-434. https://doi.org/10.1016/j.ymthe.2017.11.009.

11. Syn, N.L., Wang, L., Chow, E.K.H., Lim, C.T., Goh, B.C. (2017) Exosomes in cancer nanomedicine and immunotherapy: prospects and challenges. *Trends Biotechnol*. 35, 665-676. https://doi.org/10.1016/j.tibtech.2017.03.004.
12. Markman, M., Rothman, R., Hakes, T., Reichman, B., Hoskins, W., et al. (1991) Second-line platinum therapy in patients with ovarian cancer previously treated with cisplatin. *J. Clin. Oncol.* 9, 389-393. https://doi.org/10.1200/jco.1991.9.3.389.
13. Casagrande, J.T., Pike, M.C., Ross, R.K., Louie, E.W., Roy, S., Henderson, B.E. (1979) "Incessant ovulation" and ovarian cancer. *Lancet*. 314, 170-173. https://doi.org/10.1016/S0140-6736(79)91435-1.
14. Risch, H.A. (1998) Hormonal etiology of epithelial ovarian cancer, with a hypothesis concerning the role of androgens and progesterone. *J. Natl. Cancer Inst*. 90, 1774-1786. https://doi.org/10.1093/jnci/90.23.1774.
15. Cramer, D.W., Welch, W.R. (1983) Determinants of ovarian cancer risk. II. Inferences regarding pathogenesis. *J. Natl. Cancer Inst*. 71, 717-721. https://doi.org/10.1093/jnci/71.4.717.
16. Gong, T.T., Wu, Q.J., Vogtmann, E., Lin, B., Wang, Y.L. (2012) Age at menarche and risk of ovarian cancer: a meta-analysis of epidemiological studies. *Int. J. Cance*. 132, 2894-2900. https://doi.org/10.1002/ijc.27952.
17. Gates, M.A., Rosner, B.A., Hecht, J.L., Tworoger, S.S. (2010) Risk factors for epithelial ovarian cancer by histologic subtype. *Am. J. Epidemiol*. 171, 45-53. https://doi.org/10.1093/aje/kwp314.
18. Booth, M., Beral, V., Smith, P. (1989) Risk factors for ovarian cancer: a case-control study. *Br. J. Cancer*. 60, 592-598. https://doi.org/10.1038/bjc.1989.320.
19. Parazzini, F., La Vecchia, C., Negri, E., Gentile, A. (1989) Menstrual factors and the risk of epithelial ovarian cancer. *J. Clin. Epidemiol*. 42, 443-448. https://doi.org/10.1016/0895-4356(89)90134-0.
20. Shu, X.O., Brinton, L.A., Gao, Y.T., Yuan, J.M. (1989) Population-based case-control study of ovarian cancer in Shanghai. *Cancer Res*. 49, 3670-3674.
21. Shook, L.L. (2011) An update on hormone replacement therapy: health and medicine for women: a multidisciplinary, evidence-based review of mid-life health concerns. *Yale J. Biol. Med*. 84, 39-42.

22. Sood, R., Faubion, S.S., Kuhle, C.L., Thielen, J.M., Shuster, L.T. (2014) Prescribing menopausal hormone therapy: An evidence-based approach. *Int. J. Womens Health* 6, 47-57. https://doi.org/10.2147/IJWH.S38342.
23. Hildebrand, J.S., Gapstur, S.M., Feigelson, H.S., Teras, L.R., Thun, M.J., Patel, A.V. (2010) Postmenopausal hormone use and incident ovarian cancer: associations differ by regimen. *Int. J. Cancer*. 127, 2928-2935. https://doi.org/10.1002/ijc.25515.
24. Pearce, C.L., Chung, K., Pike, M.C., Wu, A.H. (2009) Increased ovarian cancer risk associated with menopausal estrogen therapy is reduced by adding a progestin. *Cancer* 115, 531-539. https://doi.org/10.1002/cncr.23956.
25. Danforth, K.N., Tworoger, S.S., Hecht, J.L., Rosner, B.A., Colditz, G.A., Hankinson, S.E. (2007) A prospective study of postmenopausal hormone use and ovarian cancer risk. *Br. J. Cancer* 96, 151-156. https://doi.org/10.1038/sj.bjc.6603527.
26. Chlebowski, R.T., Hendrix, S.L., Langer, R.D., Stefanick, M.L., Gass, M., Lane, D., et al. (2003) Influence of estrogen plus progestin on breast cancer and mammography in healthy postmenopausal women: the Women's Health Initiative randomized trial. *JAMA* 289, 3243-3253. https://doi.org/10.1001/jama.289.24.3243.
27. Coombs, N.J., Cronin, K.A., Taylor, R.J., Freedman, A.N., Boyages, J. (2010) The impact of changes in hormone therapy on breast cancer incidence in the US population. *Cancer Causes Control* 21, 83-90. https://doi.org/10.1007/s10552-009-9437-5.
28. Ness, J., Aronow, W.S. (2006) Prevalence and causes of persistent use of hormone replacement therapy among postmenopausal women: a follow-up study. *Am. J. Ther*. 13, 109-112. https://doi.org/10.1097/00045391-200603000-00004.
29. Collaborative Group on Epidemiological Studies of Ovarian Cancer (2015) Menopausal hormone use and ovarian cancer risk: individual participant meta-analysis of 52 epidemiological studies. *Lancet* 385, 1835-1842. https://doi.org/10.1016/S0140-6736(14)61687-1.
30. Tung, K.H., Goodman, M.T., Wu, A.H., McDuffie, K., Wilkens, L.R., et al. (2003) Reproductive factors and epithelial ovarian cancer risk by histologic type: a multiethnic case-control study. *Am. J Epidemiol*. 158, 629-638. https://doi.org/10.1093/aje/kwg177.
31. Wentzensen, N., Poole, E.M., Trabert, B., White, E., Arslan, A.A., Patel, A.V., et al. (2016) Ovarian cancer risk factors by histologic subtype: an analysis from the Ovarian Cancer

Cohort Consortium. *J. Clin. Oncol*. 34, 2888-2898. https://doi.org/10.1200/JCO.2016.66.8178.

32. Whittmore, A.S., Harris, R., Itnyre, J. (1992) Characteristics relating to ovarian cancer risk: collaborative analysis of 12 US case-control studies: II. invasive epithelial ovarian cancers in white women. Collaborative Ovarian Cancer Group. *Am. J. Epidemiol*. 136, 1184-1203. https://doi.org/10.1093/oxfordjournals.aje.a116427.
33. Kvåle, G., Heuch, I., Nilssen, S., Beral, V. (1988) Reproductive factors and risk of ovarian cancer: a prospective study. *Int. J. Cancer* 42, 246-251. https://doi.org/10.1002/ijc.2910420217.
34. Mosgaard, B.J., Schou, G., Lidegaard, Ø., Andersen, A.N., Kjaer, S.K. (1997) Infertility, fertility drugs, and invasive ovarian cancer: a case-control study. *Fertil. Steril*. 67, 1005-1012. https://doi.org/10.1016/S0015-0282(97)81431-8.
35. Ron, E., Lunenfeld, B., Menczer, J., Blumstein, T., Katz, L., Oelsner, G., Serr, D. (1987) Cancer incidence in a cohort of infertile women. *Am. J. Epidemiol*. 125, 780-790. https://doi.org/10.1093/oxfordjournals.aje.a114595.
36. Wu, M.L., Whittemore, A.S., Paffenbarger Jr., R.S., Sarles, D.L., Kampert, J.B., Grosser, S., et al. (1988) Personal and environmental characteristics related to epithelial ovarian cancer. I. reproductive and menstrual events and oral contraceptive use. *Am. J. Epidemiol*. 128, 1216-1227. https://doi.org/10.1093/oxfordjournals.aje.a115076.
37. Li, D.P., Du, C., Zhang, Z.M., Li, G.X., Yu, Z.F., Wang, X., et al. (2014) Breastfeeding and ovarian cancer risk: a systematic review and meta-analysis of 40 epidemiological studies. *Asian Pac. J. Cancer Prev*. 15, 4829-4837. https://doi.org/10.7314/APJCP.2014.15.12.4829.
38. Patel, A.V., Hildebrand, J.S., Campbell, P.T., Teras, L.R., Craft, L L., McCullough, M.L., Gapstur, S.M. (2015) Leisure-time spent sitting and site-specific cancer incidence in a large U.S. cohort. *Cancer Epidemiol. Biomarkers Prev*. 24, 1350-1359. https://doi.org/10.1158/1055-9965.EPI-15-0237.
39. Hildebrand, J., Gapstur, S., Gaudet, M., Campbell, P., Patel, A., Hildebrand, J.S., et al. (2015) Moderate-to-vigorous physical activity and leisure-time sitting in relation to ovarian cancer risk in a large prospective US cohort. *Cancer Causes Control* 26, 1691-1697. https://doi.org/10.1007/s10552-015-0656-7.

40. Olsen, C.M., Bain, C.J., Jordan, S.J., Nagle, C.M., Green, A.C., Whiteman, D.C., Webb, P.M. (2007) Recreational physical activity and epithelial ovarian cancer: a case-control study, systematic review, and meta-analysis. *Cancer Epidemiol. Biomarkers Prev.*16, 2321-2330. https://doi.org/10.1158/1055-9965.EPI-07-0566.
41. Olsen, C.M., Nagle, C.M., Whiteman, D.C., Ness, R., Pearce, C.L., Pike, M.C., et al. (2013) Obesity and risk of ovarian cancer subtypes: evidence from the Ovarian Cancer Association Consortium. *Endocr. Relat. Cancer* 20, 251-262. https://doi.org/10.1530/ERC-12-0395.
42. Collaborative Group on Epidemiological Studies of Ovarian Cancer (2012) Ovarian cancer and body size: individual participant meta-analysis including 25,157 women with ovarian cancer from 47 epidemiological studies. *PLoS Med*. 9(4): e1001200. https://doi.org/10.1371/journal.pmed.1001200.
43. Rodriguez, C., Calle, E.E., Fakhrabadi-Shokoohi, D., Jacobs, E.J., Thun, M.J. (2002) Body mass index, height, and the risk of ovarian cancer mortality in a prospective cohort of postmenopausal women. *Cancer Epidemiol. Biomarkers Prev.* 11, 822-828.
44. Hruby, A., Hu, F.B. (2015) The epidemiology of obesity: a big picture. *PharmacoEconomics 33*, 673–689. https://doi.org/10.1007/s40273-014-0243-x.
45. Gilsing, A.M.J., Weijenberg, M.P., Goldbohm, R.A., Van Den Brandt, P.A., Schouten, L.J. (2011) Consumption of dietary fat and meat and risk of ovarian cancer in the Netherlands cohort study. *Am. J. Clin. Nutr*. 93, 118-126. https://doi.org/10.3945/ajcn.2010.29888.
46. Inoue-Choi, M., Jones, R.R., Anderson, K.E., Cantor, K.P., Cerhan, J.R., Krasner, S., Robien, K., Weyer, P.J., Ward, M.H. (2015) Nitrate and nitrite ingestion and risk of ovarian cancer among postmenopausal women in Iowa. *Int. J. Cancer* 137, 173–182. https://doi.org/10.1002/ijc.29365.
47. Rinaldi, S., Peeters, P.H.M., Bezemer, I.D., Dossus, L., Biessy, C., Sacerdote, C., et al. (2006) Relationship of alcohol intake and sex steroid concentrations in blood in pre- and post-menopausal women: the European prospective investigation into cancer and nutrition. *Cancer Causes Control* 17, 1033-1043. https://doi.org/10.1007/s10552-006-0041-7.
48. Peterson, N.B., Trentham-Dietz, A., Newcomb, P.A., Chen, Z., Hampton, J.M., Willett, W.C., Egan, K.M. (2006) Alcohol consumption and ovarian cancer risk in a population-based case-control study. *Int. J. Cancer* 119, 2423-2427. https://doi.org/10.1002/ijc.22137.

49. Collaborative Group on Epidemiological Studies of Ovarian Cancer (2012) Ovarian cancer and smoking: individual participant meta-analysis including 28 114 women with ovarian cancer from 51 epidemiological studies. *Lancet Oncol*. 13, 946-956. https://doi.org/10.1016/S1470-2045(12)70322-4.
50. Friend, S.H., Bernards, R., Rogelj, S., Weinberg, R.A., Rapaport, J.M., Albert, D.M., Dryja T.P. (1986) A human DNA segment with properties of the gene that predisposes to retinoblastoma and osteosarcoma. *Nature* 323, 643-646. https://doi.org/10.1038/323643a0.
51. Nguyen, H.N., Averette, H.E., Janicek, M. (1994) Ovarian carcinoma. a review of the significance of familial risk factors and the role of prophylactic oophorectomy in cancer prevention. *Cancer* 74, 545-555. https://doi.org/10.1002/1097-0142(19940715)74:2<545::AID-CNCR2820740204>3.0.CO;2-Q.
52. Liliac, L., Amălinei, C., Balan, R., Grigoraş, A., Căruntu, I.D. (2012) Ovarian cancer: insights into genetics and pathogeny. *Histol. Histopathol* 27, 707-719. https://doi.org/10.14670/HH-27.707.
53. Walsh, T., Casadei, S., Lee, M.K., Pennil, C.C., Nord, A.S., Thornton, A.M., et al. (2011) Mutations in 12 genes for inherited ovarian, fallopian tube, and peritoneal carcinoma identified by massively parallel sequencing. *Proc. Natl. Acad. Sci* 108, 18032-18037. https://doi.org/10.1073/pnas.1115052108.
54. Lynch, H.T., Shaw, M.W., Magnuson, C.W., Larsen, A.L., Krush, A.J. (1966) Hereditary factors in cancer: study of two large midwestern kindreds. *Arch. Intern. Med*. 117, 206-212. https://doi.org/10.1001/archinte.1966.03870080050009.
55. Lynch, H.T., Boland, C.R., Gong, G., Shaw, T.G., Lynch, P.M., Fodde, R., et al. (2006) Phenotypic and genotypic heterogeneity in the Lynch syndrome: diagnostic, surveillance and management implications. *Eur. J. Hum. Genet.* 14, 390-402. https://doi.org/10.1038/sj.ejhg.5201584.
56. Lynch, H.T., Lynch, P.M. (1979) The cancer-family syndrome: a pragmatic basis for syndrome identification. *Dis. Colon Rectum*. 22, 106-110. https://doi.org/10.1007/BF02586773.
57. Lynch, H.T., Casey, M.J., Snyder, C.L., Bewtra, C., Lynch, J.F., Butts, M., Godwin, A.K. (2009) Hereditary ovarian carcinoma: heterogeneity, molecular genetics, pathology, and management. *Mo.r Oncol*. 3, 97-137. https://doi.org/10.1016/j.molonc.2009.02.004.

58. Moreira, L., Balaguer, F., Lindor, N., de la Chapelle, A., Hampel, H., Aaltonen, L.A., et al. (2012) Identification of Lynch syndrome among patients with colorectal cancer. *JAMA* 308, 1555-1565. https://doi.org/10.1001/jama.2012.13088.
59. Carethers, J.M. (2014) Differentiating Lynch-like from Lynch syndrome. *Gastroenterology* 146, 602–604. https://doi.org/10.1053/j.gastro.2014.01.041.
60. Malkin, D. (2011) Li-Fraumeni syndrome. *Genes Cancer* 2, 475–484. https://doi.org/10.1177/1947601911413466.
61. Olivier, M., Goldgar, D.E., Sodha, N., Ohgaki, H., Kleihues, P., Hainaut, P., Eeles, R.A. (2003) Li-Fraumeni and related syndromes: correlation between tumor type, family structure, and TP53 genotype. *Cancer Res*. 63, 6643-6650.
62. Kurman, R.J. (2013) Origin and molecular pathogenesis of ovarian high-grade serous carcinoma. *Ann. Oncol*. Suppl. 10, 16-21. https://doi.org/10.1093/annonc/mdt463.
63. Kurman, R.J., Shih, I.M. (2008) Pathogenesis of ovarian cancer: lessons from morphology and molecular biology and their clinical implications. *Int. J. Gynecol. Pathol.* 27, 151-160. https://doi.org/10.1097/PGP.0b013e318161e4f5.
64. Toss, A., Laura, C. (2013) Molecular mechanisms of PARP inhibitors In BRCA-related ovarian cancer. *J. Cancer Sci. Ther.* 5, 409-416. https://doi.org/10.4172/1948-5956.1000234.
65. Venkitaraman, A.R. (2003) A growing network of cancer-susceptibility genes. *N. Engl. J. Med*. 348, 1917-1919. https://doi.org/10.1056/NEJMcibr023150.
66. Lieber, M.R., Gu, J., Lu, H., Shimazaki, N., Tsai, A.G. (2014) Nonhomologous DNA end joining (NHEJ) and chromosomal translocations in humans. *Subcell. Biochem*. 50, 279-296. https://doi.org/10.1007/978-90-481-3471-7_14.
67. Kwong, A., Chen, J., Shin, V.Y., Ho, J.C.W., Law, F.B.F., Au, C.H., et al. (2015) The importance of analysis of long-range rearrangement of BRCA1 and BRCA2 in genetic diagnosis of familial breast cancer. *Cancer Genet*. 208, 448-454. https://doi.org/10.1016/j.cancergen.2015.05.031.
68. King, M.C., Marks, J.H., Mandell, J.B., New York Breast Cancer Study Group (2003) Breast and ovarian cancer risks due to inherited mutations in BRCA1 and BRCA2. *Science* 302, 643-646. https://doi.org/10.1126/science.1088759.

69. Levy-Lahad, E., Catane, R., Eisenberg, S., Kaufman, B., Hornreich, G., Lishinsky, E., et al. (1997) Founder BRCA1 and BRCA2 mutations in Ashkenazi Jews in Israel: frequency and differential penetrance in ovarian cancer and in breast-ovarian cancer families. *Am. J. Human Genet.* 60, 1059–1067.
70. Rebbeck, T.R., Mitra, N., Domchek, S.M., Wan, F., Chuai, S., Friebel, T. M., et al. (2009) Modification of ovarian cancer risk by *BRCA1/2* interacting genes in a multicenter cohort of *BRCA1/2* mutation carriers. *Cancer Res.* 69, 5801–5810. https://doi.org/10.1158/0008-5472.CAN-09-0625.
71. Alnegheimish, N.A., Alshatwi, R.A., Alhefdhi, R.M., Arafah, M.M., AlRikabi, A.C., Husain, S. (2016) Molecular subtypes of breast carcinoma in Saudi Arabia: a retrospective study. *Saudi Med. J.* 37, 506–512. https://doi.org/10.15537/smj.2016.5.15000.
72. Sankaranarayanan, R., Ferlay, J. (2006) Worldwide burden of gynaecological cancer: the size of the problem. *Best Pract. Res. Clin. Obstet. Gynaecol*. 20, 207-225. https://doi.org/10.1016/j.bpobgyn.2005.10.007.
73. McCluggage, W.G. (2011) Morphological subtypes of ovarian carcinoma: A review with emphasis on new developments and pathogenesis. *Pathology* 43, 420-432. https://doi.org/10.1097/PAT.0b013e328348a6e7.
74. Alsina-Sanchís, E., Figueras, A., Lahiguera, A., Gil-Martín, M., Pardo, B., Piulats, J. M., et al. (2017) TGFβ controls ovarian cancer cell proliferation. *Int. J. Mol. Sci*. 18, 1658. https://doi.org/10.3390/ijms18081658.
75. Tavani, A., Negri, E., Franceschi, S., Parazzini, F., La Vecchia, C. (1993) Risk factors for epithelial ovarian cancer in women under age 45. *Eur. J. Cancer* 29A, 1297-1301. https://doi.org/10.1016/0959-8049(93)90077-S.
76. Rifkin, D.B. (2005) Latent transforming growth factor-beta (TGF-beta) binding proteins: orchestrators of TGF-beta availability. *J. Biol. Chem*. 280, 7409-7412. https://doi.org/10.1074/jbc.R400029200.
77. Shi, Y., Massagué, J. (2003) Mechanisms of TGF-beta signaling from cell membrane to the nucleus. *Cell* 113, 685-700. https://doi.org/10.1016/S0092-8674(03)00432-X.
78. Derynck, R., Zhang, Y.E. (2003) Smad-dependent and Smad-independent pathways in TGF-β family signalling. *Nature* 425, 577-584. https://doi.org/10.1038/nature02006.

79. Schmierer, B., Hill, C.S. (2005) Kinetic analysis of Smad nucleocytoplasmic shuttling reveals a mechanism for transforming growth factor β-dependent nuclear accumulation of Smads. *Mol. Cell. Biol.* 25, 9845–9858. https://doi.org/10.1128/MCB.25.22.9845-9858.2005.
80. Zhang, Y.E. (2009) Non-Smad pathways in TGF-β signaling. *Cell Res.* 19, 128–139. https://doi.org/10.1038/cr.2008.328.
81. Ewen, M.E., Oliver, C.J., Sluss, H.K., Miller, S.J., Peeper, D.S. (1995) p53-dependent repression of CDK4 translation in TGF-beta-induced G1 cell-cycle arrest. *Genes Dev*. 9, 204-217. https://doi.org/10.1101/gad.9.2.204.
82. Huber, M.A., Kraut, N., Beug, H. (2005) Molecular requirements for epithelial-mesenchymal transition during tumor progression. *Curr. Opin. Cell Biol.* 17, 548-558. https://doi.org/10.1016/j.ceb.2005.08.001.
83. Böttinger, E.P., Jakubczak, J.L., Roberts, I.S., Mumy, M., Hemmati, P., Bagnall, K., et al. (1997) Expression of a dominant-negative mutant TGF-beta type II receptor in transgenic mice reveals essential roles for TGF-beta in regulation of growth and differentiation in the exocrine pancreas. *EMBO J.* 16, 2621–2633. https://doi.org/10.1093/emboj/16.10.2621.
84. Pardali, K., Moustakas, A. (2007) Actions of TGF-beta as tumor suppressor and pro-metastatic factor in human cancer. *Biochem. Biophys. Acta* 1775, 21-62. https://doi.org/10.1016/j.bbcan.2006.06.004.
85. Mabuchi, S., Kuroda, H., Takahashi, R., Sasano, T. (2015) The PI3K/AKT/mTOR pathway as a therapeutic target in ovarian cancer. *Gynecol. Oncol*. 137, 173-179. https://doi.org/10.1016/j.ygyno.2015.02.003.
86. Nilsson, E., Doraiswamy, V., Parrott, J.A., Skinner, M.K. (2001) Expression and action of transforming growth factor beta (TGFbeta1, TGFbeta2, TGFbeta3) in normal bovine ovarian surface epithelium and implications for human ovarian cancer. *Mol.d Cell. Endocrinol*. 182, 145-155. https://doi.org/10.1016/S0303-7207(01)00584-6.
87. Alsina-Sanchis, E., Figueras, A., Lahiguera, Á., Vidal, A., Casanovas, O., Graupera, M., et al. (2016) The TGFβ pathway stimulates ovarian cancer cell proliferation by increasing IGF1R levels. *Int. J. Cancer* 139, 1894-1903. https://doi.org/10.1002/ijc.30233.
88. Jozan, S., Guerrin, M., Mazars, P., Dutaur, M., Monsarrat, B., Cheutin, F., et al. (1992) Transforming growth factor beta 1 (TGF-beta 1) inhibits growth of a human ovarian

carcinoma cell line (OVCCR1) and is expressed in human ovarian tumors. *Int. J. Cancer* 52, 766-770. https://doi.org/10.1002/ijc.2910520516.

89. Steffensen, K.D., Waldstrom, M., Grove, A., Lund, B., Pallisgard, N., Jakobsen, A. (2011) Improved classification of epithelial ovarian cancer: results of 3 Danish cohorts. *Int. J. Gynecol. Cancer* 21, 1592-1600. https://doi.org/10.1097/IGC.0b013e31822a0f6b.
90. Do, T.V., Kubba, L.A., Du, H., Sturgis, C.D., Woodruff, T.K. (2008) Transforming growth factor-β1, transforming growth factor-β2, and transforming growth factor-β3 enhance ovarian cancer metastatic potential by inducing a Smad3-dependent epithelial-to-mesenchymal transition. *Mol. Cancer Res*. 6, 695-705. https://doi.org/10.1158/1541-7786.MCR-07-0294.
91. Gonias, S.L., Campana, W.M. (2014) LDL receptor-related protein-1: a regulator of inflammation in atherosclerosis, cancer, and injury to the nervous system. *Am. J. Pathol*. 184, 18-27. https://doi.org/10.1016/j.ajpath.2013.08.029.
92. Neels, J.G., Van Den Berg, B.M.M., Lookene, A., Olivecrona, G., Pannekoekt, H., Van Zonneveld, A.J. (1999) The second and fourth cluster of class A cysteine-rich repeats of the low density lipoprotein receptor-related protein share ligand-binding properties. *J. Biol. Chem*. 274, 31305-31311. https://doi.org/10.1074/jbc.274.44.31305.
93. Li, Y., Marzolo, M.P., Van Kerkhof, P., Strous, G.J., Bu, G. (2000) The YXXL motif, but not the two NPXY motifs, serves as the dominant endocytosis signal for low density lipoprotein receptor-related protein. *J. Biol Chem*. 275, 17187-17194. https://doi.org/10.1074/jbc.M000490200.
94. Trommsdorff, M., Borg, J.P., Margolis, B., Herz, J. (1998) Interaction of cytosolic adaptor proteins with neuronal apolipoprotein E receptors and the amyloid precursor protein. *J. Biol. Chem*. 273, 33556-33560. https://doi.org/10.1074/jbc.273.50.33556.
95. Kowal, R.C., Herz, J., Goldstein, J.L., Esser, V., Brown, M.S. (1989) Low density lipoprotein receptor-related protein mediates uptake of cholesteryl esters derived from apoprotein E-enriched lipoproteins. *Proc. Natl. Acad. Sci. U. S. A*. 86, 5810-5814. https://doi.org/10.1073/pnas.86.15.5810.
96. Strickland, D.K., Ashcom, J.D., Williams, S., Burgess, W.H., Migliorini, M., Scott Argraves, W. (1990) Sequence identity between the alpha 2-macroglobulin receptor and

low density lipoprotein receptor-related protein suggests that this molecule is a multifunctional receptor. *J. Biol. Chem.* 265, 17401-17404.

97. Van Leuven, F., Cassiman, J.J., Van Den Berghe, H. (1980) Primary amines inhibit recycling of α2M receptors in fibroblasts. *Cell* 20, 37-43. https://doi.org/10.1016/0092-8674(80)90232-9.
98. Herz, J., Kowal, R.C., Ho, Y.K., Brown, M.S., Goldstein, J.L. (1990) Low density lipoprotein receptor-related protein mediates endocytosis of monoclonal antibodies in cultured cells and rabbit liver. *J. Biol. Chem*. 265, 21355-21362.
99. Huang, S.S., Ling, T.Y., Tseng, W.F., Huang, Y.H., Tang, F.M., Leal, S.M., Huang, J.S. (2003) Cellular growth inhibition by IGFBP-3 and TGF-beta1 requires LRP-1. *FASEB J.* 17, 2068-2081. https://doi.org/10.1096/fj.03-0256com.
100. Tseng, W.F., Huang, S.S., Huang, J.S. (2004) LRP-1/TbetaR-V mediates TGF-beta1-induced growth inhibition in CHO cells. *FEBS Lett*. 562, 71-78. https://doi.org/10.1016/S0014-5793(04)00185-1.
101. Ma, C.I., Martin, C., Ma, Z., Hafiane, A., Dai, M., Lebrun, J.J., Kiss, R.S. (2012) Engulfment protein GULP is regulator of transforming growth factor-β response in ovarian cells. *J. Biol. Chem*. 287, 20636-20651. https://doi.org/10.1074/jbc.M111.314997.
102. Su, H.P., Nakada-Tsukui, K., Tosello-Trampont, A.C., Li, Y., Bu, G., Henson, P.M., Ravichandran, K.S. (2002) Interaction of CED-6/GULP, an adapter protein involved in engulfment of apoptotic cells with CED-1 and CD91/low density lipoprotein receptor-related protein (LRP). *J. Biol. Chem*. 277, 11772-11779. https://doi.org/10.1074/jbc.M109336200.
103. Ma, Z., Nie, Z., Luo, R., Casanova, J.E.E., Ravichandran, K.S. (2007. Regulation of Arf6 and ACAP1 signaling by the PTB-domain-containing adaptor protein GULP. *Curr. Biol.* 17, 722-727. https://doi.org/10.1016/j.cub.2007.03.014.
104. Pickup, M., Novitskiy, S., Moses, H. (2013) The roles of TGFb in the tumour microenvironment. *Nat. Rev. Cancer* 13, 788-799. https://doi.org/10.1038/nrc3603.
105. Saad, A.F., Hu, W., Sood, A.K. (2010) Microenvironment and pathogenesis of epithelial ovarian cancer. *Hormones Cancer* 1, 277–290. https://doi.org/10.1007/s12672-010-0054-2.

106. Hanahan, D., Weinberg, R.A. (2011) Hallmarks of cancer: the next generation. *Cell* 144, 646-674. https://doi.org/10.1016/j.cell.2011.02.013.

107. Abu-Jawdeh, G.M., Faix, J.D., Niloff, J., Tognazzi, K., Manseau, E., Dvorak, H.F., Brown, L.F. (1996) Strong expression of vascular permeability factor (vascular endothelial growth factor) and its receptors in ovarian borderline and malignant neoplasms. *Lab. Invest*. 74, 1105-1115.

108. Ferrara, N., Gerber, H.P., LeCouter, J. (2003) The biology of VEGF and its receptors. *Nat. Med.* 9, 669-676. https://doi.org/10.1038/nm0603-669.

109. Biagi, J.J., Oza, A.M. ChalChal, H.I., Grimshaw, R., Ellard, S.L., Lee, U., Hirte, H., Sederias, J., Ivy, S.P., Eisenhauer, E.A. (2011) A phase II study of sunitinib in patients with recurrent epithelial ovarian and primary peritoneal carcinoma: an NCIC clinical trials group study. *Ann. Oncol.* 22, 335-340. https://doi.org/10.1093/annonc/mdq357.

110. Matulonis, U.A., Berlin, S., Ivy, P., Tyburski, K., Krasner, C., Zarwan, C., et al. (2009) Cediranib, an oral inhibitor of vascular endothelial growth factor receptor kinases, is an active drug in recurrent epithelial ovarian, fallopian tube, and peritoneal cancer. *J. Clin. Oncol.* 27, 5601–5606. https://doi.org/10.1200/JCO.2009.23.2777.

111. Cohn, D.E., Kim, K.H., Resnick, K.E., O'Malley, D.M., Straughn, J.M. (2011) At what cost does a potential survival advantage of bevacizumab make sense for the primary treatment of ovarian cancer? a cost-effectiveness analysis. *J. Clin. Oncol.* 29, 1247-1251. https://doi.org/10.1200/JCO.2010.32.1075.

112. Evans, T., Matulonis, U. (2017) PARP inhibitors in ovarian cancer: evidence, experience and clinical potential. *Ther. Adv. Med. Oncol.* 9, 253–267. https://doi.org/10.1177/1758834016687254.

113. O'Neil, N.J., Bailey, M.L., Hieter, P. (2017) Synthetic lethality and cancer. *Nat. Rev. Genet.* 18, 613-623. https://doi.org/10.1038/nrg.2017.47.

114. Kaufman, B., Shapira-Frommer, R., Schmutzler, R.K., Audeh, M.W., et al. (2015) Olaparib monotherapy in patients with advanced cancer and a germline BRCA1/2 mutation. *J. Clin. Oncol.* 33, 244-350. https://doi.org/10.1200/JCO.2014.56.2728.

115. Korch, C., Spillman, M.A., Jackson, T.A., Jacobsen, B.M., Murphy, S.K., Lessey, B.A., et al. (2012) DNA profiling analysis of endometrial and ovarian cell lines reveals

misidentification, redundancy and contamination. *Gynecol. Oncol.* 127, 241–248. https://doi.org/10.1016/j.ygyno.2012.06.017.

116. Puck, T.T., Cieciura, S.J., Robinson, A. (1958) Genetics of somatic mammalian cells: III. Long-term cultivation of euploid cells from human and animal subjects. *J. Exp. Med.* 108, 945–956. https://doi.org/10.1084/jem.108.6.945.

117. Wurm, F., Wurm, M. (2017) Cloning of CHO cells, productivity and genetic stability—a discussion. *Processes* 5, 20. https://doi.org/10.3390/pr50200020.

118. Cadigan, K.M., Chang, C.C., Chang, T.Y. (1989) Isolation of Chinese hamster ovary cell lines expressing human acyl-coenzyme A/cholesterol acyltransferase activity. *J. Cell Biol.* 108, 2201-2210. https://doi.org/10.1083/jcb.108.6.2201.

119. Sanjana, N.E., Shalem, O., Zhang, F. (2014) Improved vectors and genome-wide libraries for CRISPR screening. *Nature Methods* 11, 783–784. https://doi.org/10.1038/nmeth.3047.

120. Shepherd, T.G., Thériault, B.L., Campbell, E.J., Nachtigal, M.W. (2006) Primary culture of ovarian surface epithelial cells and ascites-derived ovarian cancer cells from patients. *Nat. Protoc.* 1, 2643-2649. https://doi.org/10.1038/nprot.2006.328.

121. Dairkee, S.H., Paulo, E.C., Traquina, P., Moore, D.H., Ljung, B.M., Smith, H.S. (1997) Partial enzymatic degradation of stroma allows enrichment and expansion of primary breast tumor cells. *Cancer Res.* 57, 1590-1596.

122. O′Donnell, R.L., McCormick, A., Mukhopadhyay, A., Woodhouse, L.C., Moat, M., Grundy, A., et al. (2014) The use of ovarian cancer cells from patients undergoing surgery to generate primary cultures capable of undergoing functional analysis. *PLoS One* 9(6): e90604. https://doi.org/10.1371/journal.pone.0090604.

123. Plumb, J.A., Milroy, R., Kaye, S.B. (1989) Effects of the pH dependence of 3-(4,5-Dimethylthiazol-2-yl)-2,5-diphenyltetrazolium bromide-formazan absorption on chemosensitivity determined by a novel tetrazolium-based assay. *Cancer Res.* 49, 4435-4440.

124. Kyhse-Andersen, J. (1984) Electroblotting of multiple gels: a simple apparatus without buffer tank for rapid transfer of proteins from polyacrylamide to nitrocellulose. *J. Biochem. Biophys. Methods* 10, 203-209. https://doi.org/10.1016/0165-022X(84)90040-X.

125. Cell Signaling Technology. Western blotting protocol. https://www.cellsignal.com/contents/resources-protocols/western-blotting-protocol/western.
126. Sharma, S.K., Carew, T.J. (2002) Inclusion of phosphatase inhibitors during Western blotting enhances signal detection with phospho-specific antibodies. *Anal. Biochem.* 307, 187-189. https://doi.org/10.1016/S0003-2697(02)00008-8.
127. Yeung, Y.G., Stanley, E.R. (2009) A solution for stripping antibodies from PVDF immunoblots for multiple reprobing. *Anal. Biochem*. 389, 89–91. https://doi.org/10.1016/j.ab.2009.03.017.
128. Huang, R.Y., Chung, V.Y., Thiery, J.P. (2012) Targeting pathways contributing to epithelial-mesenchymal transition (EMT) in epithelial ovarian cancer. *Curr Drug Targets.* 13, 1649-1653.
129. Yoshida, S., Furukawa, N., Haruta, S., Tanase, Y., Kanayama, S., Noguchi, T., Sakata, M., Yamada, Y., Oi, H., Kobayashi, H. (2009) Expression profiles of genes involved in poor prognosis of epithelial ovarian carcinoma: a review. *Int J Gynecol Cancer.* 19, 992-997.
130. Stuelten, C.H., DaCosta Byfield, S., Arany, P.R., Karpova, T.S., Stetler-Stevenson, W.G., Roberts, A.B. (2005) Breast cancer cells induce stromal fibroblasts to express MMP-9 via secretion of TNF-alpha and TGF-beta. *J. Cell Sci*. 118, 2143-2153. https://doi.org/10.1242/jcs.02334.
131. Zeinoun, Z., Teugels, E., De Bleser, P.J., Neyns, B., Geerts, A., De Greve J. (1999) Insufficient TGF-beta 1 production inactivates the autocrine growth suppressive circuit in human ovarian cancer cell lines. *Anticancer Res.* 19, 413-420.
132. Bartlett, J.M., Rabiasz, G.J., Scott, W.N., Langdon, S.P., Smyth, J.F., Miller, W.R. (1992) Transforming growth factor-beta mRNA expression and growth control of human ovarian carcinoma cells. *Br. J. Cancer* 65, 655–660. https://doi.org/10.1038/bjc.1992.140.
133. Guo, S., DiPietro, L.A. (2010) Factors affecting wound healing. *J. Dental Res.* 89, 219–229. https://doi.org/10.1177/0022034509359125.
134. Dai, S., Gocher, A., Euscher, L., Edelman, A. (2016) Serum starvation induces a rapid increase of Akt phosphorylation in ovarian cancer cells (Abstract). *FASEB J.* 30(1) Suppl. 714.9.

135. Vivanco, I. (2014) Targeting molecular addictions in cancer. *Br. J. Cancer* 111, 2033–2038. https://doi.org/10.1038/bjc.2014.461.

136. Giubellino, A., Bullova, P., Nölting, S., Turkova, H., Powers, J.F., Liu, Q., et al. (2013) Combined inhibition of mTORC1 and mTORC2 signaling pathways is a promising therapeutic option in inhibiting pheochromocytoma tumor growth: in vitro and in vivo studies in female athymic nude mice. *Endocrinology* 154, 646–655. https://doi.org/10.1210/en.2012-1854.

137. Perez, E.A., Weilbaecher, K. (2006) Aromatase inhibitors and bone loss. *Oncology (Williston Park)*, 20, 1029–1048.

138. Gulhati, P., Bowen, K. A., Liu, J., Stevens, P. D., Rychahou, P. G., Chen, M., … Evers, B. M. (2011). mTORC1 and mTORC2 regulate EMT, motility and metastasis of colorectal cancer via RhoA and Rac1 signaling pathways. *Cancer Research*, 71, 3246–3256. http://doi.org/10.1158/0008-5472.

139. Lambrechts, D., Lenz, H.J., De Haas, S., Carmeliet, P., Scherer, S.J. (2013) Markers of response for the antiangiogenic agent bevacizumab. *J. Clin. Oncol.* 31, 1219-1230. https://doi.org/10.1200/JCO.2012.46.2762.

140. Steffensen, K.D., Madsen, C.V., Andersen, R.F., Waldstrøm, M., Adimi, P., Jakobsen, A. (2014) Prognostic importance of cell-free DNA in chemotherapy resistant ovarian cancer treated with bevacizumab. *Eur. J. Cancer* 50, 2611-2618. https://doi.org/10.1016/j.ejca.2014.06.022.

141. He, L., Hannon, G.J. (2004) MicroRNAs: small RNAs with a big role in gene regulation. *Nat. Rev. Genet.* 5, 522-531. https://doi.org/10.1038/nrg1379.

142. Chong, G.O., Jeon, H.S., Han, H.S., Son, J.W., Lee, Y.H., Hong, D.G., Lee, Y.S., Cho, Y.L. (2015) Differential microRNA expression profiles in primary and recurrent epithelial ovarian cancer. *Anticancer Res*. 35, 2611-2617.

143. Ronchetti, D., Lionetti, M., Mosca, L., Agnelli, L., Andronache, A., Fabris, S., et al. (2008) An integrative genomic approach reveals coordinated expression of intronic miR-335, miR-342, and miR-561 with deregulated host genes in multiple myeloma. *BMC Med. Genomics* 1, 37. https://doi.org/10.1186/1755-8794-1-37.

144. Christopher, A.F., Kaur, R.P., Kaur, G., Kaur, A., Gupta, V., Bansal, P. (2016) MicroRNA therapeutics: Discovering novel targets and developing specific therapy. *Perspect. Clin. Res*. 7, 68–74. https://doi.org/10.4103/2229-3485.179431.

145. Harding, C.V., Heuser, J.E., Stahl, P.D. (2013) Exosomes: looking back three decades and into the future. *J. Cell Biol*. 200, 367–371. https://doi.org/10.1083/jcb.201212113.

146. Chakrabarti, R., Kundu, S., Kumar, S., Chakrabarti, R. (2000) Vitamin A as an enzyme that catalyzes the reduction of MTT to formazan by vitamin C. *J. Cell. Biochem*. 80, 133-138. https://doi.org/10.1002/1097-4644(20010101)80:1<133::AID-JCB120>3.0.CO;2-T.

147. Rothaeusler, K., Baumgarth, N. (2007) Assessment of cell proliferation by 5-bromodeoxyuridine (BrdU) labeling for multicolor flow cytometry. *Curr. Protoc. Cytom*. Chapter 7: Unit 7.31. https://doi.org/10.1002/0471142956.cy0731s40.

148. Regier, M.C., Alarid, E.T., Beebe, D.J. (2016) Progress towards understanding heterotypic interactions in multi-culture models of breast cancer. *Integr. Biol. (Camb.)* 8, 684–692. https://doi.org/10.1039/c6ib00001k.

149. Holliday, D.L., Brouilette, K.T., Markert, A., Gordon, L.A., Jones, J.L. (2009) Novel multicellular organotypic models of normal and malignant breast: tools for dissecting the role of the microenvironment in breast cancer progression. *Breast Cancer Res*. 11, R3. https://doi.org/10.1186/bcr2218.

150. Shiga, K., Hara, M., Nagasaki, T., Sato, T., Takahashi, H., Takeyama, H. (2015) Cancer-associated fibroblasts: their characteristics and their roles in tumor growth. *Cancers* 7, 2443–2458. https://doi.org/10.3390/cancers7040902.

151. Nagasaki, T., Hara, M., Nakanishi, H., Takahashi, H., Sato, M., Takeyama, H. (2014) Interleukin-6 released by colon cancer-associated fibroblasts is critical for tumour angiogenesis: anti-interleukin-6 receptor antibody suppressed angiogenesis and inhibited tumour–stroma interaction. *Br. J. Cancer* 110, 469–478. https://doi.org/10.1038/bjc.2013.748.

152. Yeung, T.L., Leung, C.S., Wong, K.K., Samimi, G., Thompson, M.S., Liu, J., Zaid, T.M., Ghosh, S., Birrer, M.J., Mok, S.C. (2013) TGF-β modulates ovarian cancer invasion by upregulating CAF-derived versican in the tumor microenvironment. *Cancer Res*. 73, 5016-5028. https://doi.org/10.1158/0008-5472.CAN-13-0023.

153. Huang, F., Chen, Y.G. (2012) Regulation of TGF-β receptor activity. *Cell Biosci*. 2, 9. https://doi.org/10.1186/2045-3701-2-9.

154. Zuo, W., Chen, Y.G. (2009) Specific activation of mitogen-activated protein kinase by transforming growth factor-β receptors in lipid rafts is required for epithelial cell plasticity. *Mol. Biol. Cell* 20, 1020–1029. https://doi.org/10.1091/mbc.E08-09-0898.

155. Kalluri, R., Weinberg, R.A. (2009) The basics of epithelial-mesenchymal transition. *J. Clin. Invest.* 119, 1420–1428. https://doi.org/10.1172/JCI39104.